Grant Agreement No.: 226479

SafeLand

Living with landslide risk in Europe: Assessment, effects of global change, and risk management strategies

7th Framework Programme
Cooperation Theme 6 Environment (including climate change)
Sub-Activity 6.1.3 Natural Hazards

Deliverable 4.2

Short-term weather forecasting for shallow landslide prediction – Methodology, evaluation of technologies and validation at selected test sites

Work Package WP 4.1 - **Short-term weather forecasting for shallow landslide prediction**

Deliverable/Work Package Leader: CMCC Revision: 2 – Final

November, 2011

Rev.	Deliverable Responsible	Controlled by	Date
0	Paola Mercogliano	UNIFI, AMRA, CMCC	05-05-2011
1	Paola Mercogliano	NGI,UNIFI,AMRA,CMCC	03-10-2011
2	Paola Mercogliano	NGI	14-11-2011

SUMMARY

This deliverable describes the activities developed within the work package 4.1 of the UE/FP7 SAFELAND Project. Meteorological hazards as severe rain and convective outbreaks can trigger rapid shallow landslides; usually these phenomena give rise to severe soil impacts as life and properties loss in the most vulnerable areas. Some expected effects of the climate changes: as the modification in the precipitation patterns (more extreme rain events), in the amount of snow cover and in the ground temperatures, can alter the soil stability and can trigger in the future more landslides and, in general, decrease the slope stability supporting the vulnerability growth. The first scope of this research activity is firs of all to define a warning system for shallow landslide prediction, at large and slope scale, based on the forecast precipitation. Different components contribute to the definition of the simulation chain adopted for the definition of the early warning system: numerical weather prediction (NWP) models, tools implementing downscaling techniques to realize the connection between NWP models and stability analysis models and, therefore, software codes for the production of safety maps on very large area or detailed analysis at slope level. The second scope of the research is to test this new system producing a high number of test cases permitting to make an evaluation of the performances of the system and to capture advantages and deficiencies. For this reason the "hydrometeorological simulation chain" has been tested on the instrumented Cervinara site (from 6 to 10 February 2007, from 6 to 7 March 2007, from 3 to 4 April 2007) and on the Tuscan region (from 20 December 2009 to 6 January 2010, from 30 October 2003 to 1st November 2003) and on the Ischia isle (from 29 April 2006 to 1st May 2006). The test cases regard different meteorological situations: advection rain events, with a long time period, convective rainfall happening in a short time periods and also days in which the rainfall is not intense. About the stability models the test cases study very large areas or very small and soil with different properties.

Note about contributors

The following organisations contributed to the work described in this deliverable:

CMCC
AMRA
UNIFI

Lead partner responsible for the deliverable:

CMCC
Deliverable prepared by:
P.Mercogliano, P.Schiano, N.Casagli, L.Picarelli, V.Tofani, S.Segoni, F. Catani, G. Rossi, L.Comegna, E.Damiano, L. Olivares , B.Sikorski.

Partner responsible for quality control:

NGI
Deliverable reviewed by:
José Mauricio Cepeda, Christian Jaedicke

CONTENTS

1 Introduction 6

2 State of art 8
2.1 Numerical weather prediction models 8
2.2 High resolution weather forecast models for prediction of extreme events in the short time range 13
2.3 Models for prediction of the extreme events in the nowcasting range 13
2.3.1 Model Based on NWP models 14
2.3.2 Persistence 14
2.3.3 Extrapolation/Advection 15
2.3.4 Statistical 15
2.3.5 Satellite cloud-tops monitoring 15
2.3.6 Future development 15
2.4 State of art of landslide prediction models 16
2.4.1 Introduction 16
2.4.2 Regional scale 18
2.4.3 Slope Scale 21

3 Description of the developed simulation chains for shallow landslide prediction 24
3.1 Description of the models 24
3.1.1 The COSMO-LM model 24
3.1.2 The numerical model for stability analysis at regional scale .. 27
3.1.3 Numerical model for infiltration and stability analysis at slope scale 30
3.1.4 The downscaling algorithms for precipitation (RMI module) 31

4 Test case description and results 38
4.1 Cervinara 38
4.2 Ischia 55
4.2.1 Meteorological event description and forecasting simulation 57
4.2.2 Measured rainfall intensity data 61
4.2.3 Geotechnical input data preparation 62
4.2.4 Slope stability analysis 64
4.2.5 Discussion of results 69
4.3 Apennine area: Tuscany region 70
4.3.1 Geotechnical input data preparation 71
4.3.2 First test case: from 20th December 2009 to 6th January 201074
4.3.3 Meteorological event description and forecasting simulation 75
4.3.4 Slope stability analysis 80
4.3.5 Discussion of results 85
4.3.6 Second test case: from 30th October 2003 to 1st November 2003 85
4.3.7 Meteorological event description and forecasting simulation 86

4.3.8 Slope stability analysis 87
4.3.9 Discussion of results 92

5 Implementation of the simulation chain within early warning systems 93

6 Acknowledgement 95

7 References 96

1 INTRODUCTION

The activities under development within the WP 4.1 have the goal to design and to develop simulation models able to produce regional warning maps for shallow landslides triggered by meteorological events. Meteorological hazards such as severe rain or convective outbreaks can cause shallow landslides with a rapid velocity. Usually these phenomena create severe soil impacts with life and property loss in vulnerable areas. Some expected effects of the climate change such as the modification in the precipitation patterns, changes in the amount of snow cover and in ground temperatures, can modify the soil's stability and can trigger more landslides in the future. In general, such processes may decrease slope stability and lead to an increase of vulnerability.

In this WP a real time warning system for shallow landslides will be defined at large scale or basin scale. The system is based on forecasted meteorological variables as precipitation (rain and snow) and also atmospherical parameters at the soil level. The goal will be obtained by developing a set of connected numerical simulations able to realize an early warning procedure for the prevention of hydrological instability phenomena (landslides) caused by meteorological events.

The first simulation models of the set are represented by the Numerical Weather Prediction (NWP). Two different kind of NWP models are used: the IFS global (by ECMWF), for global forecast at 20 km of horizontal resolution and the regional model COSMO-LM model developed by the European COSMO Consortium, an operative code for many national European weather services.

Task 1 of this WP deals with the improvement of the COSMO-LM mesoscale meteorological model. The model provides precipitation forecasts taking also into account orographic effects, an important factor in triggering mass movements. It contains parameterization providing reliable estimates of convective cell dynamics, which are the cause of the most extreme rainfall events. The COSMO-LM model will be used in two configurations: a) with 7km of horizontal resolution (providing 72 hour forecasts) and b) with the higher horizontal resolution of 2.8 km (providing 24 hour forecasts), nested on the operative one with 7 km of horizontal resolution.

Landslides are generally circumscribed (basin and/or slope scale) therefore the models for the evaluation of stability work at very high resolution. The different resolutions between these models and the meteorological one can produce some inconsistencies during their coupling. In order to avoid inconsistencies, due to the different order of magnitude of resolution between the atmospherical models and the soil stability analysis models in task 2 some downscaling (e.g. dynamical and statistical downscaling) techniques for precipitation and other atmospherical variables are developed. The two different versions of COSMO-LM will provide, after downscaling, the precipitation used by basin-scale soil depth estimation method that takes into consideration: the local soil characteristic, relative position on the slope, profile slope curvature, slope gradient and local lithological parameters. In task three a basin scale model will be developed by integration soil moisture monitoring data at different scales (from slope parcels, using in situ monitoring instrumentation, to large area using remote sensing

data), the improvement of the soil saturation component, statistical treatment of the input parameters to reduce uncertainty and revision of the infinite slope approach. Finally, in the last task of the WP (task 4) a prototype procedure of the early warning system will be presented. It produces basin-scale raster maps containing the spatial distribution of the factor of safety (FS). The FS provides an indication of the relative stability of the slope. The prototype will produce the forecasts of FS at short time range and at nowcasting range. The two different versions of COSMO-LM, 7 km and 2.8 km, will provide respectively the input for a first and a second estimate of relative slope stability. The second estimate will be more precise but will need more computing time and only be available some hours after the first estimate.

2 STATE OF ART

2.1 NUMERICAL WEATHER PREDICTION MODELS

The numerical models used for weather forecasts are a simplified schematic representation of physical reality, described through a set of equations that simulate the behaviour of nature.
These equations are nonlinear and are impossible to solve exactly. Therefore, numerical methods can obtain only approximate solutions.
In general the numerical models, in a mixed initial and boundary value problem, are defined by 3 steps:

- initialization by input data,
- solving of 3D spatial-temporal partial differential equation
- evaluation of the atmospherical variables forecasted on a spatial grid.

Being a fluid, the dynamics of the atmosphere is part of that branch of physics that goes by the name of fluid dynamics and its evolution can be described mathematically by the following equations:

- mass conservation (or continuity equation), which ensures that in a given volume of air the entering amount is equal to that which goes out;
- Navier Stokes equations to define the components of the wind (also called fluid momentum balance equation);
- equation of thermodynamics (also known as the energy conservation equation);
- the equation of state of gas linking pressure, density and temperature and volume of air mass;
- the equation of water vapour taking into account all the processes involving water cycles and its state changes, as evaporation, condensation, melting, solidification and sublimation.

The solution of these partial differential equations requires knowledge of the initial condition that is given by complex processes of observations assimilation (as radiosondes, surface stations, aircraft, satellite) on a background state represented by the forecasted data of the previous model simulation. The determination of the initial state can be made only in a very approximate way, mainly because observations are sparse and have error; in particular the worldwide network of observation (GTS) accounts very well the northern continents, less good or almost absent from the southern oceans. This integration produces an estimate of the state of the atmosphere called analysis (the initial three-dimensional atmospheric state).
So there are 3 principal motivations for the uncertainty of the numerical weather forecast:

- Analysis error: errors in the background fields, observation data and data assimilation techniques used.
- Model uncertainty: inadequacy of physical model processes
- Atmosphere chaotic nature: the atmospheric motions follow non-linear dynamic, small errors in the analysis may quickly be amplified. This last is called "butterfly effect".

In order to quantify the uncertainty are defined the probabilistic forecast generating more prediction beginning from very similar initial states. The generated predictions are usually sorted into groups (clusters); depending from the number of prediction that fall in the same clusters it is possible to associate a probability of occurrence to a certain forecast (Ensemble Prediction System).

Therefore different approaches exist to the NWP problems:

- Deterministic approach: it postulates that, at least over a certain time period, the laws of physics, as applied to the atmosphere, can be solved (integrated forward in time) to find the forecast fields given initial data describing the current conditions.
- Probabilistic approach: it is based on the idea of starting a set of forecast integrations from slightly different initial conditions, reflecting the range of uncertainty in the estimated initial state. This ensemble approach allows a probability to be assigned to the likelihood of rainfall (for example).

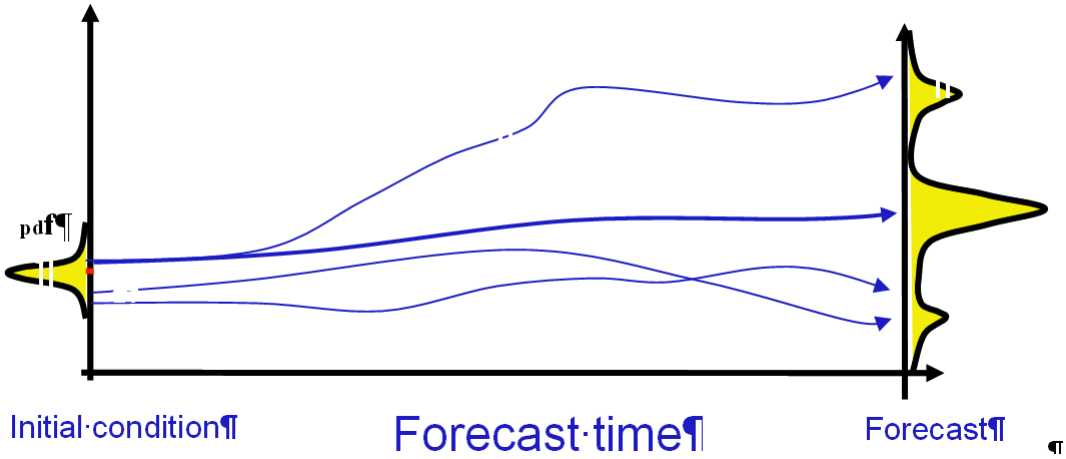

Figure 1: Numerical weather prediction models as well as the atmosphere itself can be viewed as nonlinear dynamical systems in which the evolution depends sensitively on the initial conditions. The fact that estimates of the current state are inaccurate and that numerical models have inadequacies, leads to forecast errors that grow with increasing forecast lead time. The growth of errors depends on the flow itself [http://www.elsevierscitech.com/emails/physics/climate/Ensemble_forecasting.pdf]. Ensemble forecasting aims at quantifying this flow-dependent forecast uncertainty; the picture represents the probabilistic approach to the forecast problem. The ensemble forecast permits a complete description of weather prediction in terms of a Probability Density Function (PDF). At the initial state the variable is represented by its mean value and a Gaussian distribution for the error. Due to the model error after a certain time a spread if the initial error is obtained.

Different types of numerical weather forecasts, made in relation to time, exist:

- short-range forecast: weather forecast made for a time period up to 48 hours. Due to the chaotic nature of the atmosphere in this range the forecasts are generally more accurate than the other types of forecasts
- medium range forecasts are for a period extending from about three days to seven days in advance
- long-range forecasts are for a period greater than seven days in advance but there are no absolute limits to the period.

Different types of numerical weather forecasts, made in relation to the area on which weather forecast are performed exist:

- Global circulation models: producing atmospherical forecast on the whole globe. Their spatial and temporal resolution is adapt to simulate the synoptic weather phenomena and to provide medium range forecast. Synoptic meteorology concerning the atmospheric processes that unfold over vast areas and are of sufficiently large scale as to be regarded as links in the general atmospheric circulation (circulation systems).

Typical synoptic weather phenomena are cyclones, anticyclones, jet streams and fronts.

- Limited area models (LAM): producing atmospherical forecast only on a specific region of the earth. Therefore, they require not only initial condition but also time dependent boundary conditions; these are obtained by interpolating on the model grid a meteorological analysis which results from a data assimilation scheme combining data from global model and observations. They provide a physical downscaling of the global model in certain areas. They are characterized by a higher spatial-temporal resolution than the global model. LAM models in operational use usually simulation for forecast lead times of up to two to three days. Integrations beyond this limit are of little value for weather prediction, but may be beneficial for various operative and research purposes. Due to the higher resolution they are able to simulate the mesoscale phenomena that range in size from a few km to about 100 km. It includes local winds, thunderstorms, and tornadoes and, more in general, phenomena orographically forced and/or due to atmospheric convection. Meteorologists sometimes differentiate between the meso-β-scale and meso-γ-scale, where the former discriminates phenomena ranging from 20 to 100 kilometres in the horizontal and the latter discriminates phenomena ranging from 2 to 20 km.

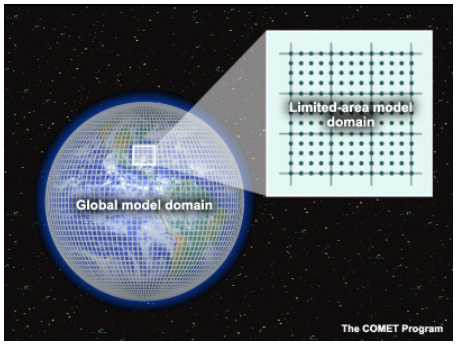

Figure 2: the concept of global and limited area model domain

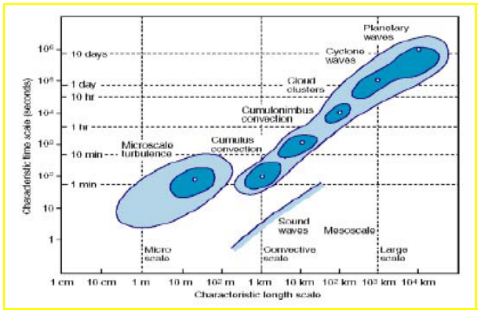

Figure 3: typical spatial and temporal scale of the main atmospherical phenomena

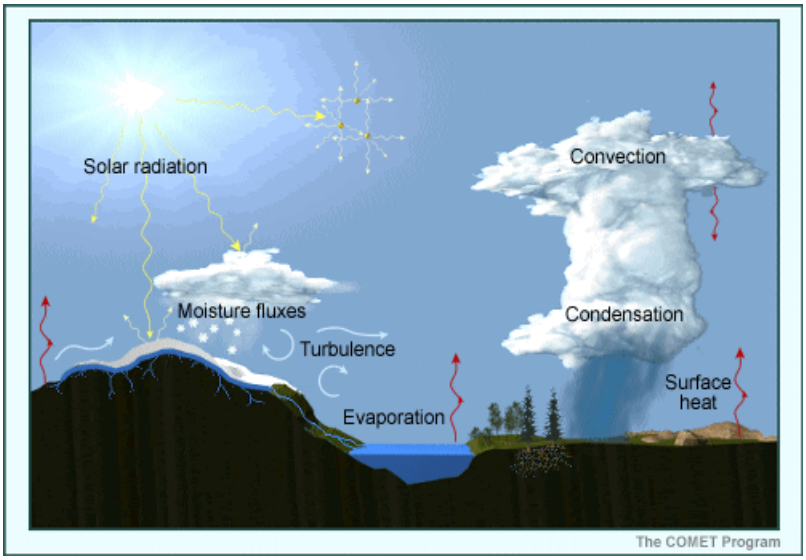

Figure 4: This Figure illustrates many of the atmospheric processes that have non-hydrostatic effects. These include surface and atmospheric heat and moisture fluxes, turbulence, convection, evaporation, and condensation. For features less than 10-20 km, meteorological models must incorporate these non hydrostatic processes

Table 1: main global models developed in Europe and America

GLOBAL MODEL	DEVELOPED BY
Integrated Forecast System (IFS) *(http://www.ecmwf.int/research/)*	European Centre for Medium-Range Weather Forecasts (based in England)
Unified Model (UM) *(http://www.metoffice.gov.uk/science/creating/daysahead/nwp/um.html)*	UK Met Office
German Global Meteorological Model (GME) *http://www.dwd.de*	Deutscher Wetterdienst (DWD), the German Weather Service
Arpege *http://www.cnrm.meteo.fr/gmgec/spip.php?article83&lang=fr*	French Weather Service, Météo-France
Intermediate General Circulation Model (IGCM) *(http://www.met.rdg.ac.uk/~mike/dyn_models/igcm/)*	University of Reading, Department of Meteorology (England)
The Navy Operational Global Atmospheric Prediction System (NOGAPS)	National Oceanic and Atmospheric Administration (NOAA) (U.S.A.)

Table 2: main regional model developed in Europe and America

REGIONAL MODEL	DEVELOPED BY
COSMO LM	Consortium European COSMO
Weather Research and Forecasting Model (WRF) *(http://www.wrf-model.org/index.php)*	A partnership that includes the NOAA, NCAR, and more than 150 other organizations and universities
Regional Atmospheric Modeling System (RAMS) (*http://rams.atmos.colostate.edu/*)	Colorado State University
Fifth Generation Penn State/NCAR Mesoscale Model (MM5) *(http://www.mmm.ucar.edu/mm5/)*	Mesoscale Prediction Group in the Mesoscale and Microscale Meteorology Division, NCAR
Advanced Region Prediction System (ARPS) *(http://www.caps.ou.edu/ARPS/)*	University of Oklahoma
High Resolution Limited Area Model (HIRLAM) *(http://hirlam.org/)*	International HIRLAM programme
Global Environmental Multiscale Limited Area Model (GEM-LAM)	Meteorological Service of Canada (MSC)

Limited Area, dynamical Adaptation, International Development (ALADIN) *(http://www.cnrm.meteo.fr/aladin/)*	16 national meteorological services
Skiron/Eta (*http://forecast.uoa.gr/forecastnew.php*)	Institute of Accelerating Systems and Applications - University of Athens (IASA)
Méso-NH (*http://mesonh.aero.obs-mip.fr/mesonh/*)	Laboratoire d'Aérologie (UMR 5560 UPS/CNRS) and CNRM-GAME (URA 1357 CNRS/Météo-France)
Rapid Update Cycle (RUC) *(http://ruc.noaa.gov/*	NOAA (U.S.A)

Shorter time scales (up to a few hours) can be predicted using time series techniques, advanced statistics methods like Kalman filters, neural networks or even simpler models; these models have a little better performance than persistence for the first few hours, but for longer ranges, the use of a NWP model helps cut the error dramatically. There is also another motivation to justify the importance of the development of a very high resolution model in this time range: the prediction possibility of severe weather events. This is possible because the very high resolution permits:

- the explicit representation of deep moist convection (Convection: vertical motion of molecules driven by buoyancy forces arising from static instability leading to cloud formation) leading e.g. to super- and multi-cell thunderstorms or squall lines[1]
- the most correct evaluation of the interaction between the dynamics forcing and the fine scale topography which can induce e.g. severe down slope wind, fog, flash flooding.

Looking at the Figure 3 and at the NWP model's state it is quite clear that the explicit representation of deep moist convention is possible only with a model resolution higher than 1-2 km. High resolution models produce usually forecast in the time range of 18-24 hours. Lower resolution models do not produce satisfactory results either with any convective parameterisation or with the standard one included. With no convective parameterisation the large grid length (relative to the typical cloud size) means that the model tends to produce too few, too heavy and too widely spaced showers in strongly forced situations and nothing at all in weakly forced ones. With the standard convective parameterisation the model misses organisation of showers which sometimes means roughly underestimating the amount of rain.
Unfortunately at the moment even if deep convection is resolved, remain in strong uncertainties in cloud microphysics parameterization that still lead to substantial uncertainty in the model's forecast.
In the short time range model this is also another important problem to be taken into account: NWP models need some time to settle into optimal performance. If model is not forced by the data acquisition (warm start) but only initialized by model data interpolation (cold start) for the first six hours or so on the model is in a "unnatural" state, and the model performances are very bad (spin up problems) while in the warm start after few steps (initial relaxation period) the model is in a state more compatible with the model equations and the error does not increase very much with the horizon. This is why there are significant efforts underway in the meteorological community to improve the data acquisition schemes and number of

[1] The shall line is a line of active thunderstorms, either continuous or with breaks, including contiguous precipitation areas resulting from the existence of the thunderstorms. The squall line is a type of mesoscale convective system distinguished from other types by a larger length-to-width ratio. For more details see http://www.theweatherprediction.com/habyhints/150/

assimilated data that have to be of appropriate scale: a similar spatial and temporal resolution of the model. Weather radar could play an important role in this respect as other high resolution observing system such as satellite data. It is hoped, in particular that, increasing data assimilation in the model will be possible to reduce the over prediction of rain. Short range ensembles are also a road to pursue in the next future. Different experiments are in testing phases at the moment with multi-model, multi-analysis, multi boundary and targeted ensembles. All these methods aim at producing ensemble forecasts with reliable probabilities even if they are computationally very expensive.

2.2 HIGH RESOLUTION WEATHER FORECAST MODELS FOR PREDICTION OF EXTREME EVENTS IN THE SHORT TIME RANGE

There are two main motivations to justify the importance of the development of very high resolution models in this time range; the first is that the other methods as, time series techniques, advanced statistics methods like Kalman filters, neural networks or even simpler models; have bad performances in this time range and, the second one, is that these particular models have the possibility to predict severe weather events. This is possible because the very high resolution permits:

- the explicit representation of deep moist convection (Convection: vertical motion of molecules driven by buoyancy forces arising from static instability leading to cloud formation) leading e.g. to super- and multi-cell thunderstorms or squall lines
- the most correct evaluation of the interaction between the dynamics forcing and the fine scale topography which can induce e.g. severe down slope wind, fog flash flooding.

Looking at Figure 2 and at the NWP model's state it is quite clear that the explicit representation of deep moist convention is possible only with a model resolution higher than 1-2 km. High resolution models produce usually forecasts in the time range of 18-24 hours. Lower resolution models do not produce satisfactory results; either with no convective parameterisation or with the standard one included. With no convective parameterisation the large grid length (relative to the typical cloud size) means that the model tends to produce too few, too heavy and too widely spaced showers in strongly forced situations and nothing at all in weakly forced ones. With the standard convective parameterisation the model misses organisation of showers which sometimes means roughly underestimating the amount of rain. Unfortunately at the moment also if deep convection is resolved, remaining strong uncertainties in cloud microphysics parameterization that still lead to substantial uncertainty in the model forecast.

2.3 MODELS FOR PREDICTION OF THE EXTREME EVENTS IN THE NOWCASTING RANGE

Precipitation nowcasting is a very short-term forecasting of the location and intensity of rainfall. Short-term refers to a time period of up to 6 hours of lead time. Such forecasting already has been of high interest for over 50 years and it turns to be one of the most difficult earth system problems. Numerous models designed specifically to forecast rainfall have been

created and analyzed, but each and every one of them imprecise, the reason being the chaotic and transient nature of the precipitation phenomenon.
The forecasting models can be categorized basing on their main method:

- numerical weather prediction (NWP)
- persistence
- extrapolation/advection
- statistical
- satellite cloud-tops monitoring

Of course hybrid techniques have been proposed and utilized as well

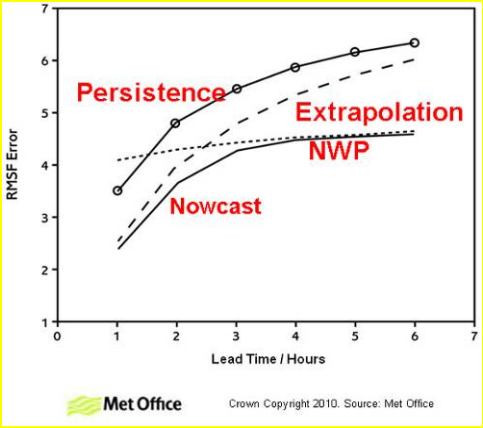

Figure 5: Relative skill and RMSF error statistics comparing the performance of the different methods available for the prediction in the nowcasting range (http://www.metoffice.gov.uk/research/areas/joint-centres/precipitation-nowcasting)

2.3.1 Model Based on NWP models

Numerical Weather Prediction (NWP) suffers from a number of shortcomings:

- coarser space/time resolution
- needs wide area initial conditions
- timely computations
- spin-up effect for precipitation or relaxation initial time if assimilation cycle is present

Nonetheless NWPs are being used for short-term forecasting. Recent developments in accelerating the numerical computations allowed the use of this model at the required for nowcasting higher resolutions in both space and time. The numerical modelling techniques are more and more assimilated with external data like radar and/or satellite data and coming directly from ground weather monitoring station networks.
Cluckie and Xuan (2006) present a high resolution mesoscale weather model to improve lead time and accuracy for prediction which takes into account more detailed information such as microphysical data, the relations between weather variables as well as structure of the atmosphere and its dynamic characteristics.

2.3.2 Persistence

The persistence model is the simplest possible precipitation nowcasting method. It simply assumes that the precipitation will remain unchanged during the nowcast duration. The rainfall data of each future time snapshot that is required is made equal to the last actual

precipitation data observed, independent how the data was acquired (rain gauges, radar, satellite etc). Examples of use can be found in Ciccione and Pircher (2984), Bell and Moore (2000).

2.3.3 Extrapolation/Advection

This forecasting model assumes that the precipitation data will not change in local intensities and the domain features will "move" with a constant and uniform velocity, if not already stationary. A singular velocity is computed from the whole domain data using data from the last two observed time-steps. The nearest future precipitation is estimated by applying the calculated translation velocity to the last observed data preserving the intensities. The single-velocity nowcasting is called uniform advection.
This model has received many further extensions. One of such is the rain cell identification and tracking where the precipitation data is not treated like a singular identity, but local features (rain cells) are identified and handled individually. Each rain cell gets its own predicted path and velocity. Algorithms for elaboration of the temporal evolution of rain cells have been developed and they allow their variation in time - strengthening, decaying, shrinking, and growth, merging and splitting.
A description of various threshold-based approaches to define rain cells can be found in Burton and O'Connell (2003a) and the estimation of their properties in Burton and O'Connell (2003b).
Optical flow models from the computer vision area that work directly on radar images has also been used with some success to predict short-term precipitation.

2.3.4 Statistical

Another area used by quantitative precipitation prediction is time-series analysis techniques, such as linear stochastic auto-regressive models, artificial neural networks and nearest-neighbour methods. In Toth and Montanari (2000) the three methods are compared.

2.3.5 Satellite cloud-tops monitoring

The ability to monitor cloud-top (and infer incloud) microphysics is important to the precipitation-generation process. Satellite observations provide an enhanced ability to monitor atmospheric stability and inversions that subsequently offer signs of pending convective initiations (CIs). Description of such a model can be found in Mecikalski (2007).

2.3.6 Future development

The recent trend in data systems gave birth to data fusion nowcasting where artificial intelligence combines data coming from a vast number of techniques to provide a single precipitation forecast.

2.4 STATE OF ART OF LANDSLIDE PREDICTION MODELS

2.4.1 Introduction

Slope stability is usually analyzed evaluating the equilibrium conditions of a potential landslide body, whose mechanism of failure develops by shearing along a failure surface (Figure 6). Landslide thus occurs if the shear strength τ_{lim} is attained along every point of the failure surface. In particular, according to the assumptions of the frequently used limit equilibrium method, which considers the landslide body as a rigid mass, failure occurs at the same time along each point of the principal shear surface. In a natural slope, while the shear stress τ along a potential failure surface remains practically constant with time, the shear strength τ_{lim} is subjected to continuous changes, which are often governed by weather conditions.

The formulation to be used in order to express the shear strength τ_{lim} depends first of all on the degree of saturation of soils. Before being subjected to unfavourable weather conditions, most of slopes are characterised by negative and positive pore-water pressures that develop respectively above and below the groundwater table (Figure 6). In particular, the soil is saturated below the groundwater table and within that portion located immediately above it, known as capillary fringe, with a thickness strongly governed by grain size(larger than 10 m for clays and less than 2 m for sands).

Therefore, natural slopes in fine-grained soils are essentially saturated. For such soils, the shear strength takes the expression known as the classical Mohr-Coulomb failure criterion:

$$\tau_{lim} = c' + (\sigma - u_w) \cdot tg\ \varphi' \qquad \textbf{Eq 1}$$

where c' andφ' are the saturated effective shear strength parameters (cohesion and friction angle); u_w is the pore-water pressure, σ is the total normal stress. In particular, pore-water pressure is positive or negative, respectively if the soil is below or above the groundwater table. As a matter of fact, negative pore-water pressures significantly contribute to the shear strength of the soil and consequently to slope stability.

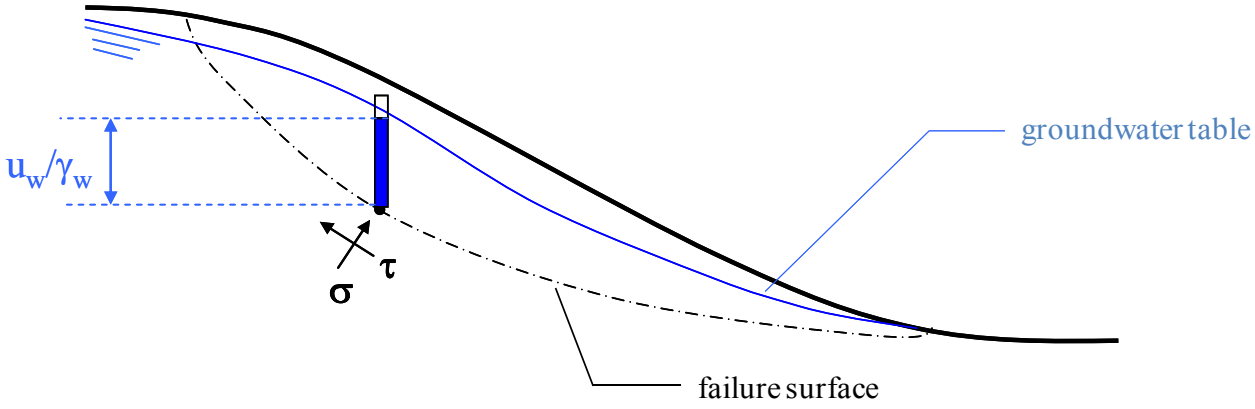

Figure 6: State of stress along a potential failure surface:
σ is the normal stress, τ is the shear stress, u_w is the pore-water pressure, γ_w is the water unit weight

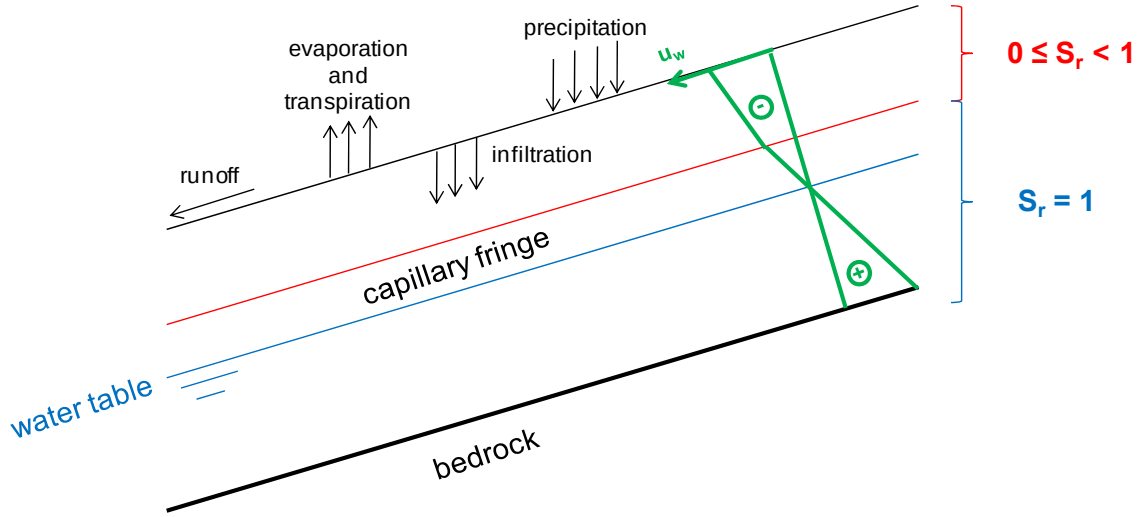

Figure 7: Scheme of typical pore water pressure conditions of a slope

On the other side, significant portions of deposits in granular soils are initially unsaturated, being located above the capillary fringe. An expression of the shear strength τ_{lim} which can be associated to such a zone is furnished by the formulation proposed by Fredlund (1979)

$$\tau_{lim} = [c' + (u_a - u_w) \cdot \chi \cdot tg\,\varphi'] + (\sigma - u_a) \cdot tg\,\varphi' \qquad \textbf{Eq 2}$$

where u_a is the relative air pressure; $u_a - u_w$ is the matric suction, χ is a coefficient function of various factors (as confining total stress, suction, degree of saturation, void ratio, etc.). In turn, the coefficient χ, which is less than one, can be expressed through the equation proposed by Vanapalli et al. (1996)

$$\chi = \Theta^{k} \qquad \textbf{Eq 3}$$

where

$$\Theta = \frac{\theta - \theta_r}{\theta_s - \theta_r}$$

θ is the volumetric water content; θ_s is the saturated volumetric water content; θ_r is the residual volumetric water content; k is a fitting parameter.

Combining equations [2] and [3], the shear strength takes the following expression

$$\tau_{lim} = [c' + (u_a - u_w) \cdot \Theta^{k} \cdot tg\,\varphi'] + (\sigma - u_a) \cdot tg\,\varphi' \qquad \textbf{Eq 4}$$

where the term $(u_a - u_w) \cdot \Theta^{k} \cdot tg\,\varphi'$ is also known as "apparent cohesion". In the saturated portion of the deposit within and below the capillary fringe, which is featured by a relative volumetric water content Θ equal to 1, the shear strength takes again the expression [1].

The knowledge of the piezometric regime is in turn related to the solution of the seepage problem within the slope, which is generally subjected to non isothermal conditions established by seasonal weather changes. It is necessary to couple the analysis of stability with the solution of the equations relative to the hydraulic flow (for both water and vapour

phases), the heat flow and the gas flow. In addition, the presence of vegetation requires accounting for the effects of evapotranspiration [see Deliverable 1.4 for further details].

Equations [1] and [4] point out that the wetting-drying cycles affecting seasonally the piezometric regime, can strongly influence the soil strength. During rainfall events, the hydrological response is strictly related to the geotechnical response of the deposit. In particular, the rates of rain water infiltration, runoff and pore-water pressure increase (or suction decrease) affect the rates of shear strength reduction and so the stability conditions of the slope.

The slope response is affected by several factors such as soil properties, geometrical aspects, rainfall characteristics, initial conditions and boundary conditions. Different combinations of these factors lead to completely different consequences in terms of time and location of failure. For example, as a consequence of the low permeability (less than 10^{-6} m/s), typical of natural slopes consisting of fine grained soils, precipitation has general delayed effects on pore pressures, which is consistent with seasonal rainfalls cumulated over long-lasting time periods (usually some months) and generally decrease with depth (Kenney and Lau, 1977). For such a reason, short and intense rainfalls rarely control the piezometric regime of slopes in fine-grained soils; such precipitations produce important effects on the behaviour of slopes in granular soils. Regarding granular soils, experience shows that if the impervious boundary is not so far from the ground surface, failure occurs under saturated or unsaturated conditions for high or moderate rainfall intensities, respectively. Otherwise, the failure is typically shallow if the impervious bottom is very deep or the deposit includes intermediate strata of low permeability.

2.4.2 Regional scale

Shallow slips and flow-type failures are without any doubt the most frequently triggered types of landslides. They are most often triggered during heavy rainfalls of short duration and are commonly encountered in steep slopes with angles higher than 25° (Iverson et al. 1997).

Other than natural causes, anthropogenic factors play an important role in the triggering process as well. Failure takes often place in 1 to 2 meters depth soil deposits as a direct consequence of rainfall infiltration in initially partially saturated soils. Their volumes and kinematic features are however high, depending on site conditions, material type and their morphological history.

The relationship between rainfall, water table fluctuations and landslide movement is often difficult to establish and the prediction of place and time of landslide occurrence is still a challenging issue, because the properties of materials and slope conditions may vary greatly over short distances, and the timing, location and intensity of triggering events are generally difficult to forecast. In particular, for the case of shallow landslides, the relationship between landslide occurrence and meteorological events encouraged the investigation of the relationship between rainfall and geotechnical hazards by means of two different approaches: empirical approaches and physically-based approaches.

The empirical approaches relate rainstorm characteristics (storm mean and maximum hourly intensity, storm duration, rainfall amount, and antecedent rainfall) to landslide occurrence (Caine, 1980; Sidle and Swanston, 1982; Sidle 1984a, 1986; Wieczorek, 1987; Dhakal, 1995; Crosta and Frattini, 2001; Wieczorek and Glade, 2005). This approach relies on plotting storm

intensity-duration versus cumulative rainfall for observed events. The definition of the most critical rainfall conditions depends on the soil characteristics and initial state (soil moisture content). In particular, shallow landslides and debris flows often occur during, or suddenly after, short intense rainfall. This approach presents many limitations due to the empirical nature of the assumption that past-rainfall conditions associated with failures are likely to trigger landslides in the future.

The physically-based approaches integrate hydrological models for the description of the dynamics of infiltration and saturation phenomena, together with geotechnical approaches for stability analysis. In particular, the slope stability is investigated as a function of the effects of hydrological conditions and rainfall characteristics on groundwater conditions. These models rely on several simplifying assumptions that limit their applicability. Particularly, steady or quasi-steady models (e.g. Montgomery and Dietrich 1994; Wu and Sidle 1995) are limited to few unrealistic situations related to both rainfall characteristics and in situ conditions (Iverson 2000). Transient models, used either for saturated or unsaturated conditions, are able to improve the effectiveness of the analysis, accounting for the transient effects of varying rainfall on slope stability conditions (e.g. Baum et al. 2002, 2008; Crosta and Frattini 2003; Iverson 2000; Savage et al. 2004), but they generally need abundant and accurate spatial information. Moreover, they are sensitive to some of the required input data such as hydraulic properties of soils, initial steady-state groundwater conditions and soil depths, whose correct evaluation is often possible only using empirical models or inverse deterministic analyses (Godt et al. 2008; Salciarini et al. 2006; Sorbino et al. 2007).

In order to achieve significant results, the application of physically based models requires a deep understanding of the conceptual assumptions, the accurate definition over broad regions of the in situ conditions of soils, of the pore pressure regime characteristics, as well as of the different triggering mechanisms. Moreover, a critical interpretation of results needs a methodology based on the use of quantitative indexes (Crosta and Frattini 2003; Godt et al. 2008; Salciarini et al. 2006; Sorbino et al. 2007).

Physically based models usually attempt to account for infiltration and vertical movement of water into the ground surface in some simplified way (infiltration through unsaturated zone and into the saturated zone, below the rising phreatic surface), modelling the longitudinal movement of groundwater by downslope seepage (seepage flow within the phreatic zone).

Most of the authors consider the pore pressure as deriving uniquely from the rising of a saturated layer above a fixed slip surface. Others have proposed models that instead consider the pore pressure as generated by the advance of a wetting front coming from the top. The most common approach is based on two main models that combine simplicity with high reliability: the Green-Ampt infiltration model (Green, 1911), which infers the movements of the wetting front and finds the critical depth of triggering within the soil (Pradel, 1993), and Richards equation based models. Many authors use different solutions to the Richards equation (Richards, 1931) to represent the movement of water in unsaturated soils and to assess the effect of transient rainfall on the timing and location of landslides (Iverson, 2000; Crosta, 2003; Simoni, 2008).

Distributed physically-based models apply algorithms and equations to every cell of an extended area: usually the analyzed area is divided into a regular square grid from a few to thousands of meters. Sometimes it is required to apply the model equations at different depths

for each pixel which means the computation can be extremely time-consuming depending on the thickness of the soil, the extension of the study area, the spatial and temporal resolution and the complexity of the equation. Many software have been developed to handle this large amount of computations to apply stability models on a large scale and to visualize the results in various ways; all these software manage simpler versions of general forms of physical model equations introducing some approximations. It is usually possible to find two different software approaches: plug-in oriented and stand-alone. The plug-in oriented codes are routine or add-ons that work on an existent software that provides a platform; this approach usually discharges all the file management and logical operations on the platform software and in some cases even part or all calculations are entrusted to the host software computational engine. These codes are simpler to use because they are supported by known software that is familiar to use and easier to program due to the use of host platform computational framework. Stand-alone software has a file management, dedicated and optimized computing routine which is developed in universal programming language (C++, FORTRAN, Basic...etc).

SHALSTAB, SHAllow Landslide STABility model, is a popular software for distributed slope stability analysis (Montgomery & Dietrich, 1994). It has a physical core based on a distributed steady state description of the hydrological fluxes coupled with an infinite slope analysis. The basic tool is a grid-based model, a combination of C++ programs and ARC/INFO AML scripts intended to be used within an ESRI-ArcGIS software environment (http://www.esri.com/software/arcgis/index.html). Since topography plays an important role in driving surface and groundwater flows, Montgomery & Dietrich (1994) proposed a model that explicitly considers the topographic influence on soil saturation and slope stability. The hydrologic model TOPOG (O'Loughlin, 1986) is used to predict the degree of soil saturation in response to a steady state rainfall for topographic elements defined by the intersection of contours and flow tube boundaries. The flow tube approach used by TOPOG basically permits to include the topographic control on the pore pressure that is used to estimate the slope stability with the infinite slope model while treating the subsurface flow in the steady state. This topographic approach proves to be very efficient in capturing the spatial variability of shallow landslide hazards even though there is an over-predicted instability, depending on the topographic data quality. The SHALSTAB model has been classified as spatially predictive because it is not suited to forecast the timing of landslide triggering (Simoni et al., 2008).

SINMAP, Stability Index MAPping, and SINMAP 2 are two other add-on tools for the ESRI-ArcGIS software. These have their theoretical basis in the infinite slope stability model with groundwater pore pressures obtained from a topographically based steady state model of hydrology (Pack, 1998, 2001). The input information (slope and specific catchment area) is obtained from the analysis of Digital elevation models (DEM). These parameters can be adjusted and calibrated with an interactive visual procedure that adjusts them based on observed landslide observations. SINMAP allows uncertainty of the variables through the specification of lower and upper bounds that define uniform probability distributions. Between these bounds, the parameters are assumed to vary randomly in respect to the probability distribution.

The model dSLAM by Wu and Sidle (1996), based on an infinite slope model and a kinematic wave groundwater model, is designed to analyse shallow landslides in steep forested areas

and accommodates vegetation root strength and soil characterization, but it does not account for a vadose zone hydrology

TRIGRS, Transient Rainfall Infiltration and Grid based Regional Slope stability model, is a software developed in FORTRAN language, for computing the transient pore pressure distribution due to rainfall infiltration using the method proposed by Iverson (Baum et al., 2002). The results are stored in a distributed map of the factor of safety. TRIGRS, freely distributed both as source code and executable files, is widely used by many authors for regional landslide hazard assessment (Baum et al., 2005; Salciarini et al., 2006) and analysis under the approximation of nearly saturated soil, presence of flow field and isotropic, and homogeneous hydrologic properties (Baum et al., 2002). TRIGRS is very sensitive to initial conditions, therefore, if the initial water table depth is poorly constrained, it may produce questionable results.

GEOtop-FS is one of the most advanced models for distributed slope stability and was recently proposed by Rigon et al (2006) and Simoni et al (2008). This model uses the hydrological distributed model GEOtop (Rigon et al., 2006) to compute pore pressure distribution by an approximate solution of the Richards equations and an infinite slope stability analysis to compute the distributed factor of safety. The approximate solution of Richards equation used by the software works in saturated soil conditions. The factor of safety of GEOtop-FS is computed in a probabilistic approach assigning statistical distributions to soil parameters instead of a single deterministic value and analyzing the error propagation.

All these software use different models, approximations and programming languages but they have one common characteristic: all are suitable only for research purposes or for non-real time studies. In all these cases, computational speed is not the main objective. Even using a modern computational hardware, workstation or personal computer, the computational time can be longer than days for a relatively small area at high spatial and temporal resolution. It is impossible to use this software, even if they are state of art, in real time and for warning system purposes.

2.4.3 Slope Scale

Numerical codes modelling at the slope scale are generally characterized by a more complex approach compared to those working at the regional scale. This is essentially due to a more detailed discretization of the numerical domain, to more accurate assumed boundary conditions and to the large number of available constitutive soil models (often particularly sophisticated) to reproduce the physical mechanisms affecting slope behaviour. As a matter of fact, such intrinsic more complicated models involve more complex analyses requiring long computational time and advance knowledge of soil properties. At the same time, these software work very well for the stability analysis of single slopes (Casagli et al, 2005, Tofani et al., 2006) but are not appropriate to be applied over large areas (as typical of physically-based distributed models). In the follow, features, constraints and potentialities of some selected commercial codes will be reported.

GEO-SLOPE (Krahn, 2004) is doubtless one of the most widely distributed 2D numerical codes. It is a package that couples different stand-alone software components, which are featured by a user-friendly and well structured interface, offering solutions for complex

multiphysics problems, including slope stability under rain infiltration. Among the components, it is worth mentioning SEEP/W, VADOSE/W and SLOPE/W. SEEP/W is a FEM software that solves the Richards equations to simulate the steady state or transient groundwater flow within unsaturated or saturated soils. VADOSE/W is intended for solving seepage problems within soils subjected to non-isothermal conditions, taking into account the equations solving hydraulic flow (both water and vapour phases), heat flow and gas flow. Both software allow defining variable rainfall input over time. Results in terms of pore water pressures obtained in SEEP/W or in VADOSE/W can be in turn imported into the software SLOPE/W, which analyses slope stability based on the limit equilibrium method, i.e. evaluating the equilibrium conditions of a potential landslide body, considered as a rigid medium, which develops a mechanism of failure by shearing along a predetermined failure surface. A landslide occurs when equilibrium conditions require mobilisation of the shear strength along the entire failure surface. SLOPE/W can analyze natural as well as engineered and reinforced slopes, with the possibility to take into account heterogeneous soil types, complex stratigraphy and slip surface geometry using either deterministic or probabilistic approaches.

Another well-known 2D finite difference program for the simulation of the behaviour of geomaterials under different loading conditions is constituted by the code FLAC (Itasca, 2008), that is the acronym of “Fast Lagrangian Analysis of Continua”. A library of constitutive models for soils and rocks undergoing yield and plastic flow is provided. At the same time, user-defined constitutive models can also be implemented. The fluid flow in a partially saturated medium can be simulated using either a single-phase or two-phase flow. The single-phase flow module uses a predefined cubic law to link the hydraulic permeability and the degree of saturation. The two-phase flow module uses the relationship of Van Genuchten (1980) for the water/air permeability curves. The motion of the fluids in the porous medium is described by the groundwater flow equation and generalized Darcy law. In order to capture the capillary effects, the use of the two-phase flow is necessary, since the single-phase flow sets pore pressures to zero above the free surface. The influence of volumetric deformations on permeability and retention curve parameters is not automatically taken into account, but can be implemented by the user. The stability analysis is performed through the strength-reduction method. In particular, while the material undergoes plastic flow and collapse, the explicit Lagrangian formulation and the mixed-discretization zoning technique allows running accurate large strain step-by-step calculations without any excessive memory requirements (since no matrices are formed). In particular, the program offers also an automatic re-meshing tool for large strain simulations.

Z_SOIL (Zace Ltd., 2003) is a 2D/3D finite element code that offers a large number of constitutive models for soils and rocks to solve user-defined boundary value problems. It is characterized by an integrated pre-processor to define geometry, initial and boundary conditions and also by an integrated post-processor which allows the graphical display of the results. The hydro-mechanical features allow a transient analysis of the stress-deformation behaviour of a natural, partially or fully saturated slope subjected to rainfall infiltration. The three-phase medium air-fluid-solid is modelled by a two-phase liquid-solid medium, where the air is considered formed by bubbles that are trapped in the liquid phase. The air-fluid mixture forms a compressible fluid obeying Darcy’s law. Concerning the stability analysis, it is performed through the strength-reduction method, i.e. the strength parameters are reduced

until failure of the domain occurs, and then the safety factor is calculated as the ratio between the available strength and the one calculated at failure.

Another widespread 2D/3D finite element program used to simulate deformation and stability problems in geotechnical engineering is PLAXIS. The code, developed at the Technical University of Delft, contains a library providing simple and more advanced elasto-plastic constitutive models for soils and rocks. The program offers a user-friendly interface enabling to easily control the pre-processing, calculation and post-processing phases. The definition of boundary and initial conditions is easily accomplished. In particular, hydrostatic as well as non-hydrostatic pore-water pressure fields can be defined by the user through the pre-processor. The stress field is also calculated directly in the pre-processor or in a first gravity loading simulation phase. Every simulation can be easily divided into a series of sequences defined directly by the user. The stability analysis is performed through the strength-reduction method. In order to launch transient seepage analyses in saturated or partially saturated soils, isotropic or anisotropic, with different boundary conditions, it is necessary to use the additional module PLAXFLOW. The basic version offers only the possibility to run hydromechanically coupled analyses taken into account by the classical consolidation theory. Inflow and outflow of water due to infiltration and/or evaporation can be modelled and the particular flow characteristics in partially saturated soils can be considered by means of the permeability curve of linear or Van Genuchten type (1980). No solid matrix deformations are considered by PLAXFLOW for the two-phase porous medium, thus the corresponding results (in terms of time-dependent pore-water pressure) have to be imported into the basic version for deformation analysis. On the other hand, the code does not comprise the effect of suction on soil strength, but only on the unsaturated flow, thus uncoupled hydraulic and mechanical calculations can be exclusively run.

3 DESCRIPTION OF THE DEVELOPED SIMULATION CHAINS FOR SHALLOW LANDSLIDE PREDICTION

3.1 DESCRIPTION OF THE MODELS

The following chapter describes in details the models and the algorithms used to realize the simulation chain for shallow landslide prediction. A flow chart of the simulation chain is reproduced in the figure 8.

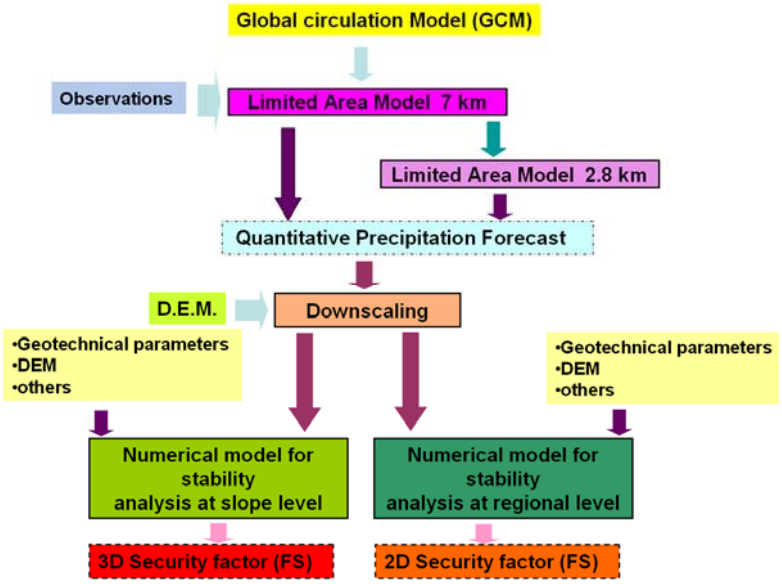

Figure 8: Numerical simulations chain: the time range is from 3 to 1 days before the event

3.1.1 The COSMO-LM model

The COSMO LM model, is a limited-area non hydrostatic computational model for weather prediction developed within the framework of the European Consortium for Small-Scale Modelling (Germany, Switzerland, Italy, Poland and Greece, Romania and Russia). This consortium was formed in October 1998. Its general goal is to develop, improve and maintain this non-hydrostatic limited-area atmospheric model, to be used both for operational and for research applications by the members of the consortium. COSMO is initially based on the "Lokal-Modell" (LM) of DWD (Germany National Weather Service). This model is used to solve the physical phenomena in the meso-β-scale and meso-γ-scale (see paragraph 2.1) The present operational application of the model uses a grid spacing of 7 km and 2.8 km.

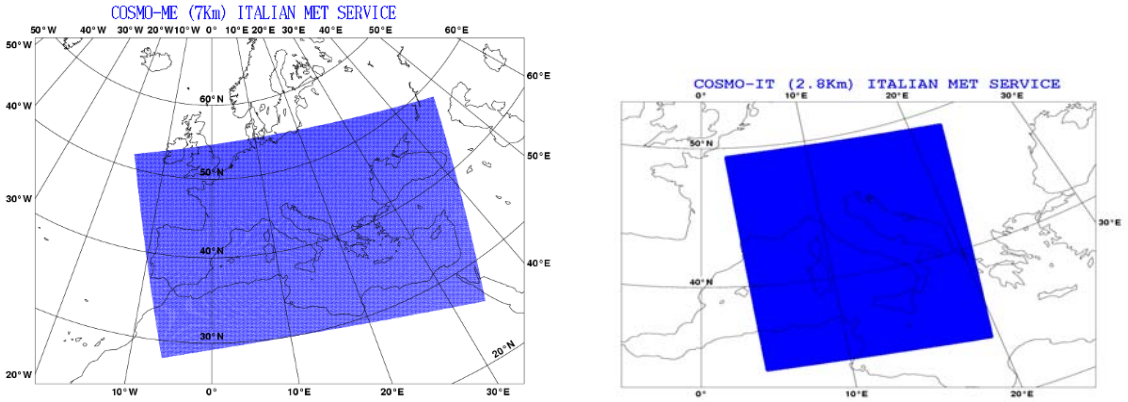

Figure 9: COSMO spatial domain for the 2 configuration running at the Italian meteorological service (picture available thanks to CNMCA): on the left the configuration with 7 km (with 40 vertical levels); on the right the configuration with 2.8 km of horizontal resolution (with 50 vertical levels). In the higher resolution configuration a direct simulation of the coarser parts of deep convention is performed (no parameterizations) and the lowest layer is 10 m above ground level.

The key issue of the configuration with 7 km is an accurate numerical prediction of near-surface weather conditions, focusing on clouds, fog, frontal precipitation, and orographically and thermally forced local wind systems. The model with 2.8 km resolution is expected to obtain a direct simulation of severe weather events triggered by deep moist convection, such as supercell thunderstorms, intense mesoscale convective complexes, prefrontal squall-line storms and heavy snowfall from wintertime mesocyclones.

Besides the operational application, LM provides a non hydrostatic modelling framework for various scientific and technical purposes. Examples are applications of the model to large eddy simulations, cloud resolving simulations, studies on orographic flow systems and storm dynamics, development and validation of large scale parameterization schemes by fine-scale modelling, and tests of computational strategies and numerical techniques. For these types of studies, the model should accommodate both real data cases and artificial cases using idealized initial data.

The wide range of applications imposes a number of requirements for the physical, numerical and technical design of the model. The main design requirements are:

- use of non hydrostatic, compressible dynamical equations to avoid restrictions on the spatial scales and the domain size, and application of an efficient numerical method of solution;
- provision of a comprehensive physics package to cover adequately the spatial scales of application, and provision of high-resolution data sets for all external parameters required by the parameterization schemes;
- flexible choice of initial and boundary conditions to accommodate both real data cases and idealized initial states, and use of a mesh-refinement technique to focus on regions of interest and to handle multi-scale phenomena;
- use of a high-resolution analysis method capable to assimilate high-frequency asynoptic data and remote sensing data;

- use of pure Fortran-90 constructs to render the code portable among a variety of computer systems, and application of the standard MPI-software for message passing on distributed memory machines to accommodate broad classes of parallel computers.

The COSMO LM is based on the primitive thermo-hydrodynamical equations describing compressible flow in a moist atmosphere. The model solves equation for the following prognostic variables:

- horizontal and vertical Cartesian wind components,
- pressure perturbation,
- temperature,
- specific humidity,
- cloud water content.
- optionally: cloud ice content,
- turbulent kinetic energy,
- specific water content of rain and snow.

Total air density and precipitation fluxes of rain and snow are, therefore computed (diagnostic variables).

The model equations are formulated in rotated geographical coordinates and generalized terrain following height coordinate. A variety of physical processes are taken into account by parameterization schemes, the main are:

- Surface Layer Parameterization
- Grid-Scale Clouds and Precipitation
- Radiation
- Soil Model
- Terrain and Surface Data
- Moist convection

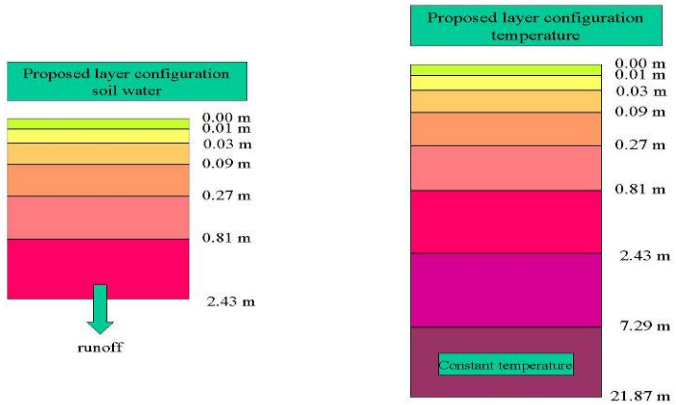

Figure 10: In the soil scheme the heat and water fluxes in the soil are described. The equations are solved for different vertical levels (the structure of the soil model is reported in the picture). The soil model is still strictly one-dimensional, i.e., all horizontal transports of water and energy in the soil are neglected. The effect of freezing/melting of soil water/ice is taken into account. The formulation accounts for the capability of the soil to retain a certain amount of liquid water at temperatures well below the freezing point. A single layer snow module complements the soil model. The top layer thickness of 1 cm, is prone to following significant instantaneous changes in variables like snow water content or near surface wind or abrupt changes in the solar forcing caused by large variations in cloud cover. For details of the soil model formulation the reader should refer to the extended documentation of the soil model (Doms et al., 2005).

Initial conditions for the model can be obtained by interpolating initial data from various coarse-grid driving models (GME, ECMWF, LM at a lower resolution) or from the continuous LM data assimilation stream. In more general way the initial state of the fluid obtained putting together interpolated data by global model and observation data through data assimilation scheme. The requirements for the data assimilation scheme for the operational LM are mainly determined by the very high resolution of the model and by the task to employ it also for nowcasting purposes in the future. Hence, detailed high-resolution analyses have to be able to be produced frequently, and this requires a thorough use of asynoptic and high-frequency observations such as aircraft data and remote sensing data.

Different method of data assimilation exist, the one selected in the COSMO-LM model is the nudging scheme. The nudging or Newtonian relaxation consists of relaxing the model's prognostic variables to wards prescribed values within a predetermined time window. Detailed description if the technique can be found e.g. in Anthes (1974), Davies and Turner (1977), and Stauffer and Seaman (1990). The main instruments and variables assimilated in the model are radiosonde (wind, temperature, and humidity), aircraft (wind, temperature), and surface-level data (SYNOP, SHIP, BUOY: pressure, wind, humidity). Optionally wind profiler and RASS data (wind, temperature). Surface-level temperature is used for the soil moisture analysis only. Experimental versions exist for the use of radar reflectivity by latent heat nudging, and for the use of GPS-derived precipitable water.

3.1.2 The numerical model for stability analysis at regional scale

HIRESSS is a stability simulator software, developed at UNIFI, capable of real time distributed analysis on a large scale area at high spatial and temporal resolution (Rossi, 2010). It is developed with the goal of being the analysis core of a real time landslide warning system. Therefore, the computational time is a key feature of the software code that is written to use parallel computing hardware from multicore workstations to high performance computing (HPC) hardware like supercomputers. The physical model implemented in HIRESSS uses solutions that permit to achieve a balanced runtime-reliability ratio, computing a probability distribution of factor of safety based on a Monte Carlo simulation. The result is a distributed map of failure probability, performing the evaluation for each cell or pixel in which the analysed area is divided (cell by cell computation).

The physical model implemented in HIRESSS is composed of two parts (Figure 11): hydrological and geotechnical.

The hydrological model receives the rainfall data as a dynamical input and provides the pressure head as a perturbation to the geotechnical stability model, which provides results in terms of factor of safety (FS).

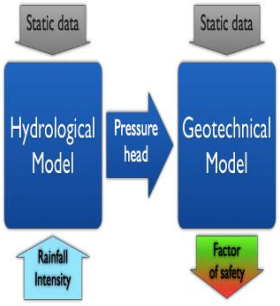

Figure 11: The physical model organization diagram.

The hydrological model is based on an analytical solution of an approximated form of the Richards equation under the wet condition hypothesis and coupled with a modelled form of hydraulic diffusivity that is introduced to improve the hydrological response.
The Richards equation is simplified assuming a wet initial condition and neglecting the gravity flux that mainly affects the long term behaviour of soil infiltration. The Richards equation can be rewritten as:

$$\frac{\partial h}{\partial t} = \left(D_0 \cos^2 \alpha\right) \frac{\partial^2 h}{\partial Z^2} \qquad \textbf{Eq 5}$$

where h is the pressure head, D_0 is soil saturated diffusivity, α is the slope angle and Z is the depth value. This is a linear equation and has an analytical solution (Iverson, 2000) throughout the duration T of a rainfall event:

$$\mathrm{h}(\mathrm{Z},\mathrm{t}) = \mathrm{h}(\mathrm{Z},\mathrm{t}_0) + \mathrm{Z}\frac{\mathrm{I}}{\mathrm{K}_\mathrm{Z}}\left[\mathrm{R}(\mathrm{t})\right] \qquad \textbf{Eq 6}$$

After a duration T, the rainfall stops and the solution is:

$$h(Z,t) = h(Z,t_0) + Z\frac{I}{K_Z}\left[R(t) - R(t-T)\right] \qquad \textbf{Eq 7}$$

where I is the rainfall intensity and K_Z is the soil saturated hydraulic conductivity and $R(t)$ is a response function (Iverson, 2000).

The geotechnical stability model is based on an infinite slope model that takes into account the unsaturated soil properties. During the slope stability analysis the model takes into account the increase in strength and cohesion due to matric suction in unsaturated soil, where the pressure head is negative. Moreover, the soil mass variation on partial saturated soil caused by the water infiltration is modelled (Rossi, 2010). The general form of the factor of safety is:

$$FS = \frac{\tan\phi'}{\tan\alpha} + \frac{c_a(h)}{\gamma_s Z \sin\alpha\cos\alpha} + \frac{h(Z,t)\tan\phi'}{\gamma_s Z \sin\alpha\cos\alpha} \qquad \textbf{Eq 8}$$

where φ' is the friction angle, $c_a(u)$ is the apparent cohesion function of pressure head, γ_s and γ_w are respectively the soil unit weight and the water unit weight.

The slope stability is evaluated at different soil depths, between the bedrock and the surface, avoiding the limiting assumption that shallow landslide triggering occurs only at bedrock soil contact.

The model is then inserted into a Monte Carlo simulation, to overcome the exact computation problems. This technique is introduced to manage the typical uncertainty in geotechnical parameters, which is the common weak point of the deterministic models. The Monte Carlo simulation reads the probability distributions of the input parameters and produces as a result probability of slope failure (Rossi, 2010).

HIRESSS uses distributed maps of topographic and geotechnical properties to simulate the water infiltration within the soil and to compute the slope stability using the geometrically simplified representation of the slope.

The most important topographic data is the slope angle obtained from a digital elevation model (DEM)The maximum change in elevation over the distance between each cell and its neighbours (steepest downhill descent) is also calculated. Other minor DEM-derived topographic features that play an indirect role in the HIRESSS model are the orientation of the slope, its length and curvature. These parameters are used in the soil thickness model, GIST (Catani et al., 2010), that compute the bedrock depth used in the HIRESSS physical model.
A robust dataset of geotechnical data is collected in order to describe the best spatial variations of soil properties. After a pre analysis of geotechnical data map, the values of soil properties are extended to an entire area that is expected to have similar features.

The input data necessary to apply HIRESSS on a study area are:

- Cohesion;
- Friction angle;
- Slope;
- Dry soil unit weight;
- Soil depth;
- Hydraulic conductivity;
- Initial soil saturation (can be calculated also from antecedent rainfall database);
- Pore size index distribution;
- Bubbling pressure;
- Porosity;
- Residual water content;
- Rainfall intensity;

Summarizing, the main characteristics of the physical model are:

- The capability of computing the factor of safety at each time step and not only at the end of the rainfall event;
- The variable-depth computation of slope stability;
- The introduction of the contribution of soil suction in unsaturated conditions;
- The probabilistic treatment of the uncertainties in the main hydrological and mechanical parameters and, thus, of the factor of safety.

The software code of the stability simulator HIRESSS has these main characteristics:

- High temporal and spatial resolutions physically based analysis.
- Operating on a large scale area.
- Probabilistic failure results.
- Fast computational time.

3.1.3 Numerical model for infiltration and stability analysis at slope scale

I-MOD 3D is a 3D Finite Volume Code for infiltration and stability analyses developed at the Geotechnical Laboratory of the Second University of Naples (Olivares & Tommasi 2008; Damiano & Olivares 2010; Olivares et al. 2010). The code was developed as a Visual Basic Application for ARC-GIS 9.2.

The goal of I-MOD 3D code is the geotechnical definition of a warning map at the basin scale in loose unsaturated pyroclastic soils less then 48 hours forecasted rain from the downscaling module (RMI). Such a code represents the "last ring" of a "simulation chain". This component of the chain consists of a finite volume model for infiltration analyses (I-MOD3D) and a stability module which have respectively the goal of analyzing the infiltration process induced by rainfall and assessing the stability conditions of shallow deposits (definition of a stability map). These two parts are integrated through an interface able to automatically define a finite volume discretization of soil starting from a Digital Terrain Model (DTM), and to capture the forecasted rain from the downscaling module (RMI).

The 3D finite volume module for infiltration analysis is developed in an uncoupled formulation for unsaturated porous medium in isothermal condition and neglecting the flux of the gas phase. The mesh-generation automatically starts from the Digital Terrain Model The general governing differential equation for 3D seepage are expressed as:

$$\vec{q}\,(x,\,y,\,z,\,t) = -K\,(\theta\,(x,\,y,\,z,\,t))\cdot\nabla\,(\psi\,(\theta\,(x,\,y,\,z,\,t)) + z) \qquad \textbf{Eq 9}$$

$$\frac{\partial\theta(x,y,z,t)}{\partial t} = -\nabla\cdot\vec{v}(x,y,z,t) \qquad \textbf{Eq 10}$$

where

$\theta(x,y,z,t)$ = volumetric water content;
$\vec{v}$ (x,y,z,t) = Darcy velocity x, y, z;
$K(\theta(x,y,z,t))$ = hydraulic conductivity;

$\psi(\theta)$ = relationship between capillary pressure head (fluid pressure potential) and volumetric water content (WRC water retention curves).

The water retention curves ($\psi(\theta)$) are described by the Van Genuchten expression (1980). The permeability functions of soil, depending on the volumetric water content or suction, are expressed by the Van Genuchten (1980) or Brooks & Corey (1964) relationships.

The stability module computes for each point of the subsoil the local safety factor under the assumption of infinite slope using the following expression:

$$FS = \frac{\tau_{\lim}}{\tau} = \frac{[c' + (\psi(\theta)/\gamma_{\varpi}) \cdot \chi \mathrm{tg}\phi'] + (\sigma_{\beta} - u_a) \cdot \mathrm{tg}\varphi'}{\tau_{\beta}} \quad \textbf{Eq 11}$$

where:

c' = effective cohesion;
γ_w = water specific weight;
τ_β = shear stresses;
$(\sigma_\beta - u_a)$ = normal net stresses;
ϕ' = effective frictional angle.

In this expression the shear strength of soil along planes parallel to the ground surface is calculated by means of the extension of the Mohr-Coulomb criterion for unsaturated soils (Fredlund and Rahardjo 1993) which is supplied by the values of suction which are calculated by I-MOD3D.

The code contains an integrated post processor displaying, for each integration time and for different depths, contour maps of the volumetric water content, matric suction and local safety factor.

3.1.4 The downscaling algorithms for precipitation (RMI module)

The simulation chain for landslides triggered by intense rainfall requires the use of weather computational models which can satisfactorily anticipate the evolution of the synoptic and mesoscale weather and, in particular, the rainfall pattern, especially for very intense events. However, it is also important to be able to “concatenate” the results of the weather forecasts models with the ones evaluating the stability of slopes subject to extreme rainfall. Therefore, the solution of these issues requires the development and the optimization of numerical codes, in such a way that they become more accurate, robust and efficient, but also the definition of an interface between the different models. The realization of this "in-chain" represents a high priority issue because landslides usually occur on very limited areas, while the weather forecast, even if using very high resolution models are defined on much larger scales. The whole simulation chain must also be designed to generate results in appropriate computational time, in order to be used operatively by the agencies responsible of population protection. This means short computational time and immediate interpretation output.

As described in the previous paragraph two different version of COSMO LM, with different resolution 7 km and 2.8 km are available. In order to obtain the higher spatial temporal resolution possible both are used in this simulation chain. The version with 2.8 km of resolution is "nested" in the version with resolution 7 km, which covers a greater domain simulation. This model is then nested on the global model. This configuration permits to decrease the space gap between the meteorological models and the impact models. This procedure, called "two-step nesting" is necessary to ensure an adequate quality of the produced results (in fact, a resolution of 2.8 km is better in taking into account the effects produced by a complex orography), but also enables a smaller resolution jump between the weather computational limited area model and the other simulation models placed “in cascade” in atmospherical computational model. This configuration needs a quite long computational time and powerful computing machines. If enough resources are available it is possible to produce results in less than half a day. The requirement, for models performing stability assessment, is to have an input of rain at very high resolution. NWP models can not provide forecast at this resolution; therefore it is necessary to define algorithms for downscaling of rain. The downscaled forecast rain provides the input for stability analysis model realizing the simulation models coupling.

Different Statistical Downscaling (SD) techniques have been studied (Antofie, 2009). SD techniques are a method of obtaining high-resolution climate/meteorological information from relatively coarse-resolution models. SD methods establish statistical relations among large-scale variables (predictors) and the variables on a finer-grid scale (predictands).

It is important to underline that the implemented downscaling algorithms, concern, at least at present, the field of foreseen precipitation; in the future in order to have more consistency among the models it is desirable to join to the precipitation the downscaling of wind, temperature and humidity at soil level. The precipitation represents the most important input for the stability model. It is also the most complicated variable to downscale because it is a very discontinuous meteorological variable, whose distribution strongly depends on the orography and more in general by topography.

Different spatial methods have been analyzed for SD, up to now, the most relevant are:

- Inverse Distance Weight (IDW),
- Radial Basis Function (RBF),
- Kriging (ordinary, simple, universal and disjuncted),

The first two are deterministic interpolation methods creating surfaces from measured points, based on either the extent of similarity (e.g., Inverse Distance Weighted) or the degree of smoothing (e.g., Radial Basis Functions). They use a sample of control points in estimating an unknown value, so a change in an input value only affects the result within the neighbour points. The advantage of these methods is that the values of the known points stay unchanged in the process of interpolation so it can display the spatial anomalies of a phenomenon. The main disadvantage is that even if the spatial anomalies of a phenomenon are exhibited causal factors cannot be represented. It needs a dense network of points with known values.
The used formula for precipitation evaluation is:

For IDW:

$$rain\hat{}(s_0) = \sum_{i=1}^{N} \lambda_i rain(s_i) \quad \textbf{Eq 12}$$

where:

N is the number of measured sample points within the neighbourhood defined for s_0

λ_i are the distance-dependent weights associated with each sample point.

$rain(s_i)$ is the observed value at location s_i

Weights are calculated using:

$$\lambda_i = \frac{d_{i0}^{-p}}{\sum_{i=1}^{N} d_{i0}^{-p}} \quad \textbf{Eq 13}$$

$$\sum_{i=1}^{N} \lambda_i = 1 \quad \textbf{Eq 14}$$

where:

d_{i0} is the distance between the prediction location s_0 and the measured location s_i

p is the power parameter that defines the rate of reduction of the weights as distance increases.

IDW is forced to be an exact interpolator to avoid the division by zero that occurs when $d_{i0} = 0$ at the sampled points. IDW is an extremely fast interpolation method, though it is very sensitive to the presence of outliers and data clustering. In addition, this method does not provide an implicit evaluation of the quality of the predictions (Burrough and McDonnell 1998, Johnston et al. 2001).

RBFs are a series of exact deterministic interpolation techniques that include different basis functions like thin-plate spline, spline with tension, completely regularized spline, multiquadric function, and inverse multiquadric spline (ArcGis Desktop help). RBFs can be seen as the process of fitting a flexible membrane to the data points so the total curvature of the surface is minimized. Being also an exact interpolator, RBFs are different from IDW because they allow the prediction of points above the maximum measured value and below the minimum measured value. In other words if IDW is based either on the extent of similarity the RBFs is based on the degree of smoothing. The predictor defined by a RBF is a linear combination of N basis functions (one for each data point in the neighbourhood) of the form:

$$rain(s_0) = \sum_{i=1}^{N} \omega_i \cdot \Phi(\|s_i - s_0\|) + \omega_{n=1} \quad \textbf{Eq 15}$$

φI is a radial basis function.

$R = ||s_i - s_0||$ is the distance between the prediction location s_0 and the measured location s_i.

$\{\omega_i: i = 1, 2, \ldots, n + 1\}$ are the weights to be estimated.

The vector of weights $w = (\omega_1, \omega_2, \ldots \omega_n)$ is calculated by solving the following system of equations:

$$\begin{pmatrix} \Phi & 1 \\ 1' & 0 \end{pmatrix} \begin{pmatrix} w \\ \omega_{n+1} \end{pmatrix} = \begin{pmatrix} rain \\ 0 \end{pmatrix} \quad \textbf{Eq 16}$$

where:

Φ is a matrix with i,j-th elements corresponding to $\Phi(||s_i - s_0||)$ for each pair of data points.

1 is a column vector of 1.

rain is a column vector containing the data points.

ω_{n+1} is a bias parameter.

The Kriging method is a geostatistical interpolation technique utilizing the statistical properties of the measured points. Geostatistical techniques quantify the spatial autocorrelation among measured points and account for the spatial configuration of the sample points around the prediction location. Kriging is a stochastic method because it assigns weights based not only on the distance between surrounding points but also on the spatial autocorrelation among the measured points, which is determined by modelling the variability between points as a function of separation distance.

There were not significant differences among the different interpolations methods used but the Radial Basis Function was overall the best one and, therefore, with the highest capability to accurately reproduce the independent data. Furthermore evaluations based on statistical basis (correlations between observed and forecast values) and the comparison with observations for selected test cases indicates that a better correlation between observations and forecast could be obtained incorporating topographic information in the downscaling.

Taking into account this possibility a downscaling technique utilizing the Multiple Regression Interpolation (MRI) method (physical disaggregation of precipitation with topographical variables) (http://iahs.info/redbooks/a248/iahs_248_0033.pdf) has been analyzed. We have studied various topographic variables as:

- Slope
- Aspect
- Mean elevation
- Geographic coordinate (separately longitude and latitude)
- Euclidian distance to the nearest coast
- Direction to the nearest coast (8 compass points classes)

The topographic variables most promising for MRI disaggregation in our study regions are the elevation, aspect and slope.

$$\textbf{\textit{Rain = a0 + a1 X1 + a2 X2 + a3 X3 + residual}} \quad \textbf{Eq 17}$$

where: Rain is the rainfall variable, X1, X2, X3 represent the set of topographic variables selected in the regression equation for Rain (elevation, aspect and slope), a0 through a3 are the calculated regression coefficients and *residual* is the error.

For multivariate linear regression (Baillargeon 1989; Vigier 1981), the stepwise upward regression method is used to link a rainfall variable P and a set of topographic variables X1, X2, X3.

The topographic variables for the domain of interest are precomputed for the desired resolution (i.e. 100m) and are saved as rasters. They are derived from a high resolution DEM raster of the studied area domain. Each COSMO LM grid point with geographic coordinates *i,j* is used to build a single linear equation:

$$Rain_{i,j} = a0 + a1\ Elevation_{i,j} + a2\ Aspect_{i,j} + a3\ Slope_{i,j} \qquad \textbf{Eq 18}$$

Values of Elevation/Aspect/Slope at geographic coordinates *i,j* are determined from the precomputed rasters. Such a collection of equations is then solved to determine the regression coefficients and the error terms. The constant coefficient *a0* for simplification is "incorporated" in the error terms. Since the regression coefficients are invariant over the domain area but the error terms are not, the error terms are interpolated to cover the whole area of study (domain). The chosen interpolation method for the residual is the RBF method. Having the coefficients a1, a2, a3, rasters of Elevation, Aspect and Slope and raster of the residual we can easily compute the MRI interpolated value of precipitation in any point of the domain.

Results show that only a little part of precipitation can be disaggregated with the physical method, MRI; the bigger part is disaggregated with the residual. In a way it is an expected result since we have observed that very little correlation exists between the precipitation and the underlying topography. Anyway it has been observed that the use of MRI (respect to purely spatial interpolation) is still able to give a better overall output when put in cascade with the stability models simply because it does take into account the features of the topography.

A GIS tool for downscaling implementing the Multiple Regression Interpolation has been developed by CMCC and is called: MRI module. It is implemented as a plug-in module for ArcGIS that automatically elaborates fine resolution downscaled precipitation data (rasters) based on a given COSMO LM 24h/48h precipitation forecast. The calculated ArcGIS raster data is directly read by the numerical code which constitutes the following step in stability model cascade. User interaction with this module is very minimal and consists of a selection of the directory where the precomputed topographic variables (rasters) are stored and also where the results will be saved and selecting from a dropdown list of layers the feature set of the COSMO LM data to be downscaled.

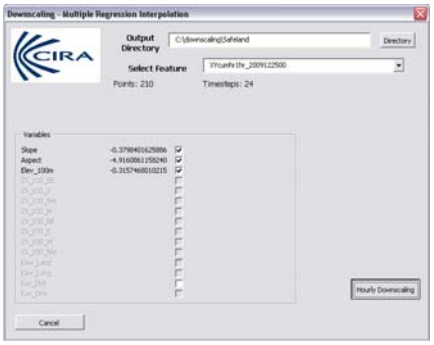

Figure 12: ArcGIS MRI module user interface

The downscaling procedures are equal for both the numerical stability models: regional or slope scale. The simulation chain could be used in the range time in which the forecast of local area model is available. COSMO LM 7km model has as typical forecast time range 72 hours while COSMO LM 2.8 km model has 24 hours. For this application the COSMO-LM 7 km run has had a forecast time range of 24 or 36 hours and for the configuration with 2.8 km a forecast range of 24 hours. The choice of these forecast time ranges is due to the to the necessity to reduce the computational time and due to the big number of test cases performed (more then 40 days have been simulated and others have been obtained changing the horizontal resolution but also testing different physical parameterization). This high number of test cases allowed an evaluation of the system performances and to capture advantages and deficiencies. The configuration with 7 km of horizontal resolution uses the nudging technique. The nudging technique is a standard part of the LM COSMO package; this is a method for the observation data assimilation in the numerical model. The choice of this data assimilation system for the operational LM is mainly determined by the high resolution of the model and by the task to employ it also for nowcasting purposes in the future. Hence, detailed high-resolution analyses have to be able to be produced frequently and quickly, and this requires a thorough use of asynoptic and high-frequency observations such as aircraft data and remote sensing data.

Table 3: list of the test cases performed and some features of them

Studied Area	*Event (From)*	*Event (to)*	*Number of simulation performed*	*Features of COSMO LM simulation*	*Downscaling*	*Stability analysis*
Tuscany	20 Dec 2009	6 Jan 2010	17	Hor. Res. = 7km Forecast Time Range = 24 hours (36 hours for 23th and 24th Dic 2009)	From 7 km to 10 m	Regional level
Tuscany	30 Oct 2003	1 Nov 2002	3	Hor. Res. = 7km Forecast Time Range = 36 hours	From 7 km to 10 m	Regional level
Ischia	29 Apr 2006	1 May 2006	9	Hor. Res. = 7km ; Forecast Time Range = 24 hours Hor. Res. = 2.8 km (no convection); Forecast Time Range = 24 hours Hor. Res. = 2.8 km (with convection); Forecast Time Range = 24 hours	From 7km to 5 meters From 2.8 km to 5 meters	Regional level
Cervinara	3 Apr 2007	4 Apr 2007	8	Hor. Res. = 7km Forecast Time Range = 24 hours Hor. Res. = 2.8 km Forecast Time Range = 24 hours (no convection) Hor. Res. = 2.8 km (shallow convection); Forecast Time Range = 24 hours	From 2.8 km to 100 meters	Slope level
Cervinara	6 Mar2007	7 Mar 2007	7	Hor. Res. = 7km Forecast Time Range = 24 hours Hor. Res. = 2.8 km Forecast Time Range = 24 hours (no convection) Hor. Res. = 2.8 km (shallow convection); Forecast Time Range = 24 hours	From 2.8 km to 100 meters	Slope level
Cervinara	6 Feb 2007	10 Feb 2007	13	Hor. Res. = 7km Forecast Time Range = 36 hours Hor. Res. = 2.8 km Forecast Time Range = 24 hours (no convection) Hor. Res. = 2.8 km (shallow convection); Forecast Time Range = 24 hours	From 7 km to 100 meters From 2.8 km to 100 meters	Slope level

4 TEST CASE DESCRIPTION AND RESULTS

4.1 CERVINARA

In the last decades a number of catastrophic debris slides took place in Campania region. Events since 1580 have been mapped and are illustrated in Figure 13. It shows that the slopes impacted by soil movements are mainly located in the Apennine chain surrounding the Mt. Somma-Vesuvius where pyroclastic soils (mainly ashes and pumices) accumulated essentially by air-fall deposition in the last tens of thousands of years as a result of volcanic activity.

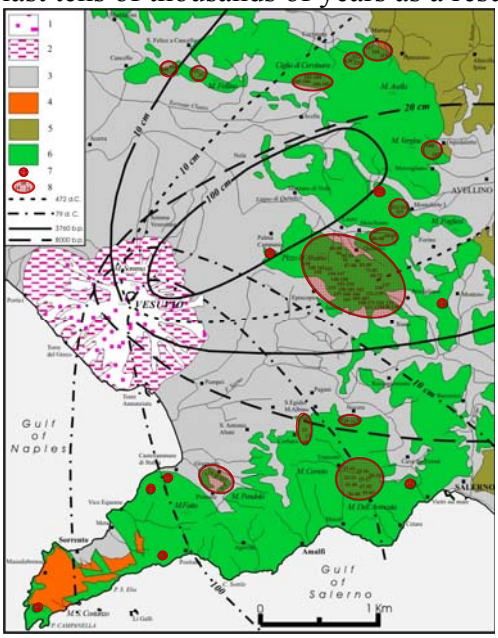

Figure 13: Distribution of flowslides in the air-fall pyroclastic deposits of Campania (modified after Di Crescenzo e Santo, 2005). 1) lavas; 2) pyroclastic flows; 3) alluvial deposits; 4) marly arenaceous terrigenous deposits; 5) terrigenous deposits with clay interbeds; 6) carbonate rocks; 7) landslide; 8) groups of landslides.

The Avella and Partenio Mountains, Sarno Mt. and Lattari Mt. in the Peninsula Sorrentina are areas susceptible to landsliding: among these the Partenio Mountains located north-eastern of Naples have been selected for the evaluation of the simulation chain since they represent a typical geomorphological context for region. It is characterized by alternating layers of pumices and volcanic ashes resting on fractured limestone. The soil stratigraphic sequence in this area is illustrated in Figure 14. From top to bottom, there is a first ashy layer rich in roots and humus (layer V), a layer of pumices of centimetre dimensions (layer A) (not always present), another ashy layer (B) followed by a stratum of finest pumices (C) and, at the end of sequence, a layer of weathered ashes (D).

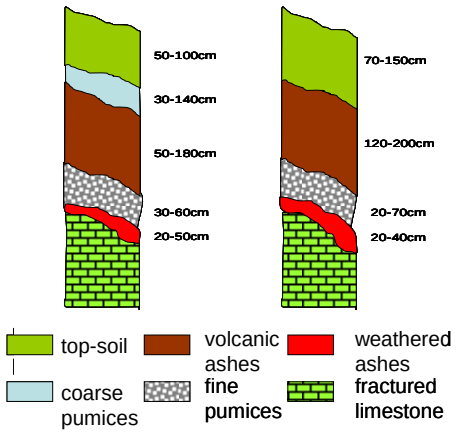

Figure 14: Typical sequences of Mt. Partenio

The test cases are focused on Cervinara slope which in 1999 has been involved in a catastrophic flowslide and which has been well investigated in the past. The selected area is characterised by fairly regular steep slopes consisting of layered unsaturated air-fall pyroclastic soils overlying fractured limestone. Many in-situ and laboratory investigations have been carried out providing detailed data on soil properties (Picarelli et al., 2006).

Figure 15 presents a plan-view and a cross-section of the slope in the vicinity of the 1999 landslide. The slope angle is around 40° and the average thickness of the pyroclastic cover which has been investigated through a number of pits and boreholes, is slightly higher than 2m. The cover includes alternating layers of pumices and loose non–plastic volcanic ashes; the lowermost layer, just above the limestone, is altered, denser than the others and slightly plastic.

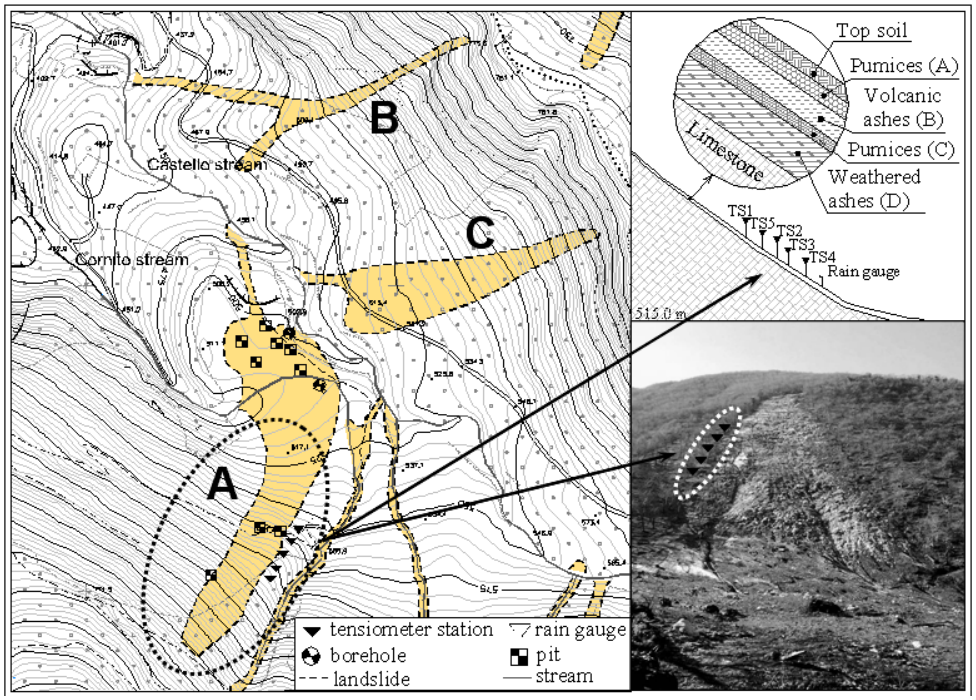

Figure 15: Cervinara site: plan-view, monitoring station and schematic cross-section

In particular, in situ investigations and monitoring of suction and rainfall are available (Damiano, 2004) as well as mechanical and hydraulic properties of the soils (Olivares and Picarelli, 2003; Olivares and Damiano, 2007). Thanks to the high number of observations, also atmospheric, it has been decided to test the chain on this site running different test cases. The test cases have been selected choosing days in which are present a cumulated rain amount quite high (recorded by pluviometers). The test cases have the scope to evaluate the performances of the simulation chain, comparing observed and simulated suction at different soil depths, even if during these days no landslide has been recorded. In particular, the test cases concern the period 2006 and 2007.
In the Cervinara test cases, stability analyses at slope levels have been performed using downscaled rainfall by COSMO LM 7 and 2.8km as input for the IMOD-3D. A description of the two used configuration is reported in the following table.

Table 4: comparison of the two COSMO LM configurations for the Cervinara test case

COSMO LM configurations	LM 7 km	LM 2.8 km
Domain Size (grid points)	200 x 140	360 x 266
Grid Spacing (horizontal)	0.0625° (7 km)	0.025° (2.8 km)
Number of vertical Layers	40	40
Time Step	40 sec	24 sec
Forecast Range	24 hrs	24 hrs
Initial Time of Model Runs	00 UTC	00 UTC
Lateral Boundary Conditions	ECMWF	LM 7 km
LBC Update Frequency	3 hrs	1 hr
Initial State	Nudging Scheme	NO
Dynamics	3 TL Leapfrog scheme; split-explicit	3 TL Leapfrog scheme; split-explicit
Physics	TKE; multi-layer soil model	multi-layer soil model; different convection schemes
COSMO LM Version	4_11	4_11

The simulations are performed using the COSMO model version 4.11 (for the 7 km and for the 2.8 km configuration). Initial and boundary data are taken from ECMWF forecasts data (with ca. 28 km of horizontal resolution).The assimilation is used for the configuration of the 7 km COSMO LM. The simulations are initialized at 00:00 UTC and they run for 24 hours or

33 hours. The number of vertical levels is 40 and the number of levels in the soil are seven. Sub grid scale convection (Tiedtke scheme) is used for the simulation at 7km but for the simulation at 2.8 km two different configurations have been used:

- Shallow convection: Only a parameterization for the shallow convection is used while the deep convection is evaluated explicitly due to the high resolution.
- No convection: Due to the characteristic of the rainfall event no parameterization is used neither for deep nor for shallow convection.

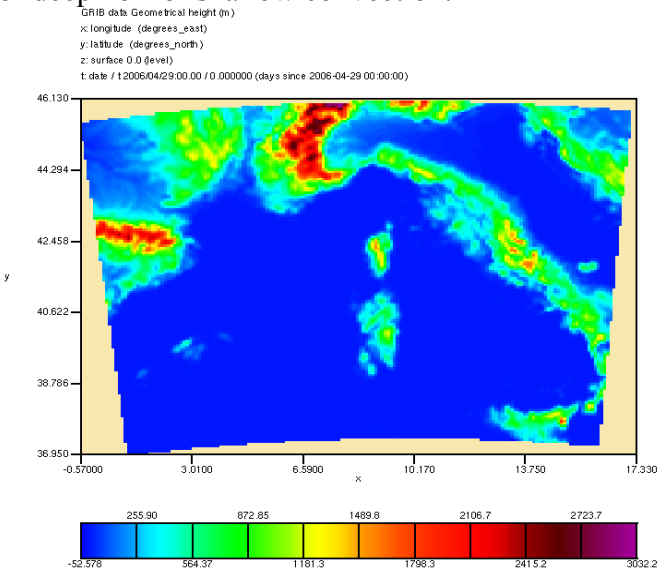

Figure 16: domain of COSMO LM 7km for Cervinara and Ischia test case. In the Figure is represented the geometrical height (orography) of the domain.

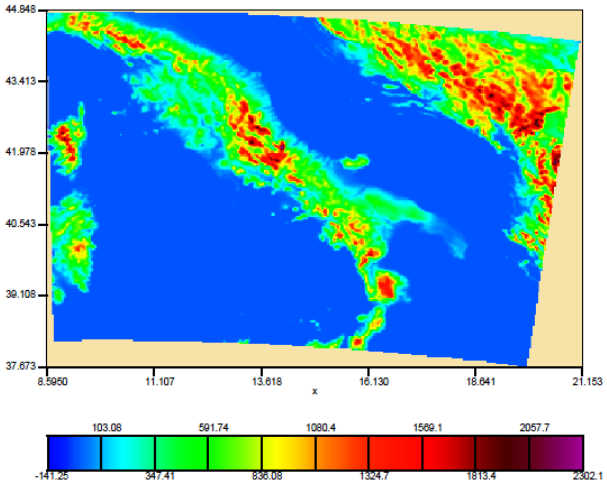

Figure 17: domain of COSMO LM 2.8 km for Cervinara test case. In the figure is represented the geometrical height (orography) of the domain.

Table 5: Comparison of the cumulated precipitation observed (in situ station of Cervinara) and forecasted (3 different COSMO LM configurations).

Date	*Observed (lat=41°;long= 14.7°)*	*COSMO 7km*	*COSMO 2.8km Shallow convection*	*COSMO 2.8km*
6 February 2007	3 mm	3 mm	n.a.	n.a.
7 February 2007	54.4 mm	10 mm	16 mm	n.a.
8 February 2007	19.2 mm	0.7 mm	2 mm	n.a.
9 February 2007	10.2 mm	2 mm	2 mm	n.a.
10 February 2007	2.8 mm	12 mm	n.a.	n.a.
6 March 2007	0 mm	0 mm	n.a.	0 mm
7 March 2007	68.4 mm	27 mm	33 mm	46 mm
3 April 2007	7 mm	0.3 mm	0.4 mm	0.5 mm
4 April 2007	34.4 mm	7 mm	5 mm	14 mm

Table 6: Comparison of the cumulated mean 24h precipitation observed and COSMO 2.8 km forecasted (configuration named "shallow convection") in the bounding area of eight weather monitoring stations.

Date	*Mean observed from 8 weather stations*	*Areal COSMO 2.8km Shallow convection*
7 February 2007	48mm	11.9 mm
8 February 2007	14.4mm	2.1 mm
9 February 2007	8mm	2.7 mm
7 March 2007	50mm	37.1 mm
3 April 2007	4mm	0.1 mm
4 April 2007	29.4mm	3.5 mm

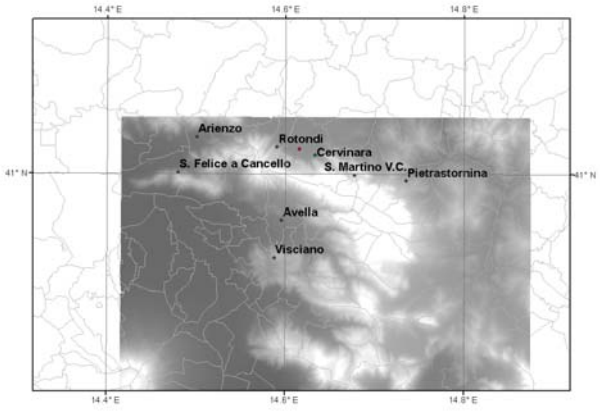

Figure 18: Cervinara – neighbouring weather stations used for statistically validating the test case forecast.

Table 7: Statistic validation of COSMO LM rainfall forecast (COSMO 2.8km shallow convection) for the threshold 5 mm for the Cervinara event.

Threshold 5 mm	THREAT SCORE	BIAS	FALSE ALARM RATE	HIT RATE RAIN
2007-02-07	**0.6**	**0.9**	**0.2**	**0.7**
2007-02-08	**0**	**0**	**0**	**0**
2007-02-09	**0**	**0**	**n.a.**	**0**
2007-03-07	**1**	**1**	**0**	**1**

2007-04-03	0	0	n.a.	0
2007-04-04	0	0	n.a	0

Table 8: Statistic validation of COSMO LM rainfall forecast (COSMO 2.8km shallow convection) for the threshold 20 mm for the Cervinara event.

Threshold 20 mm	THREAT SCORE	BIAS	FALSE ALARM RATE	HIT RATE RAIN
2007-02-07	0	0	n.a.	0
2007-02-08	0	0	0	0
2007-02-09	0	0	n.a.	0
2007-03-07	0.9	1.1	0.1	1
2007-04-03	0	0	n.a.	0
2007-04-04	0	0	n.a	0

In order to evaluate the model performance in the domain under observations some statistical indices are available, such as BIAS, THREAT SCORE, and FALSE ALARM RATE AND HIT RAIN RATE, which are listed in the Table 7 and Table 8. Details on the meaning of these indices can be found on http://www.cawcr.gov.au/projects/verification/.

- BIAS: Measures the ratio of the frequency of forecast events to the frequency of observed events. Indicates whether the forecast system has a tendency to under forecast (BIAS<1) or over forecast (BIAS>1) events. Does not measure how well the forecast corresponds to the observations, only measures relative frequencies. Range: 0 to ∞. Perfect score: 1. The Bias represents also the correspondence between the mean forecast and mean observation.
- THREAT SCORE: Measures the fraction of observed and/or forecast events that were correctly predicted. It can be thought of as the accuracy when correct negatives have been removed from consideration, that is, TS is only concerned with forecasts that count. Sensitive to hits, penalizes both misses and false alarms. Does not distinguish source of forecast error. Depends on climatological frequency of events (poorer scores for rarer events) since some hits can occur purely due to random chance. Range: 0 to 1, 0 indicates no skill. Perfect score: 1.
- FALSE ALARM RATE: Sensitive to false alarms, but ignores misses. Very sensitive to the climatological frequency of the event. Range: 0 to 1. Perfect score: 0.
- HIT RATE RAIN: Sensitive to hits, but ignores false alarms. Very sensitive to the climatological frequency of the event. Good for rare events. Range: 0 to 1. Perfect score: 1.

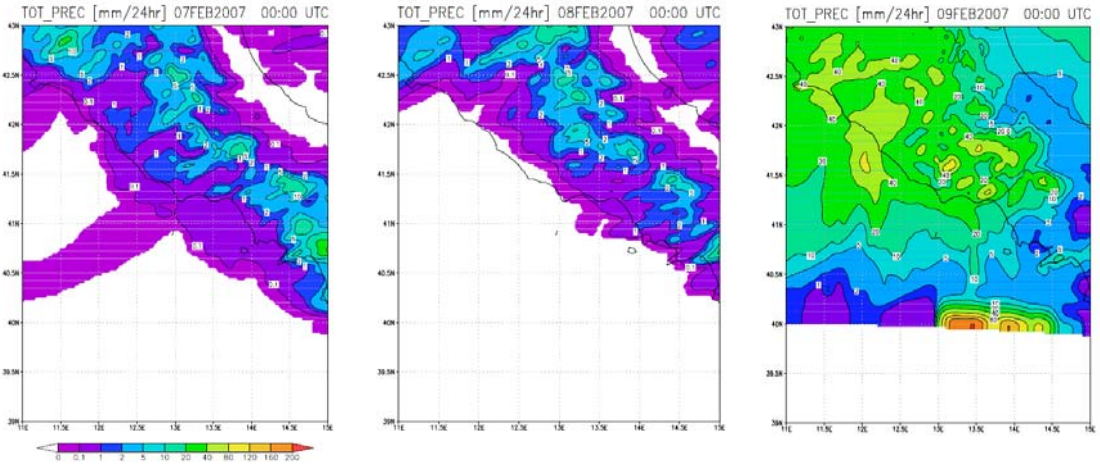

Figure 19: cumulated daily rainfall from COSMO LM 2.8 km (named "shallow convection") on 24 hours starting from 00UTC. On the left the simulated rain for 20070207, in the centre for 2007020800 and on the right side 2007020900.

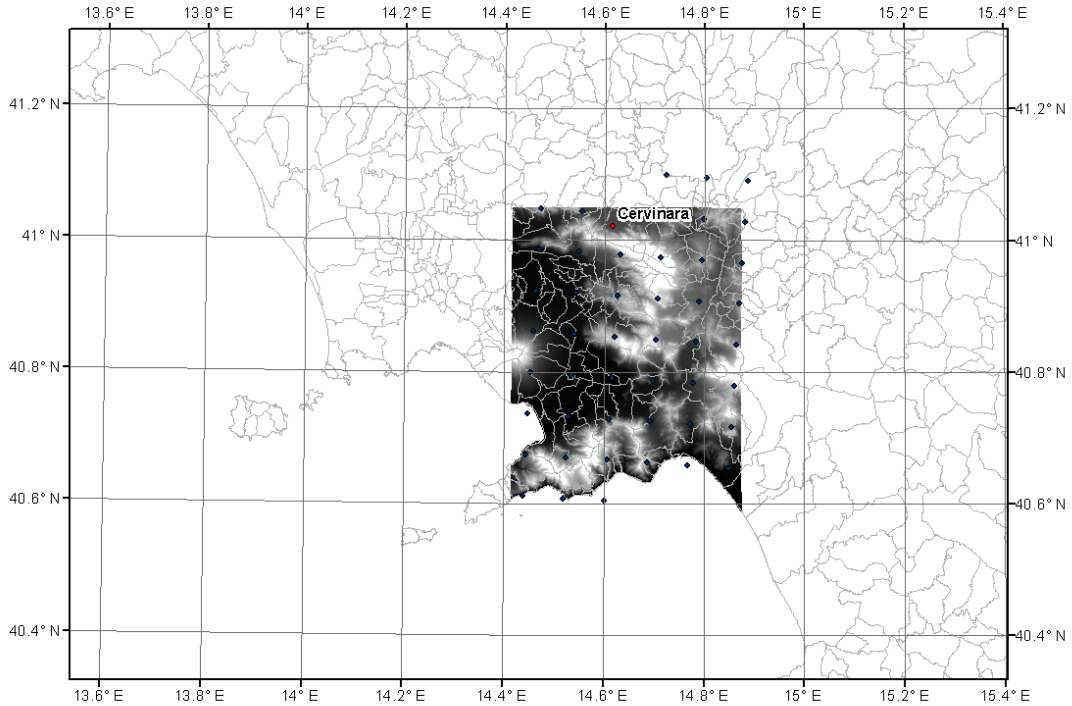

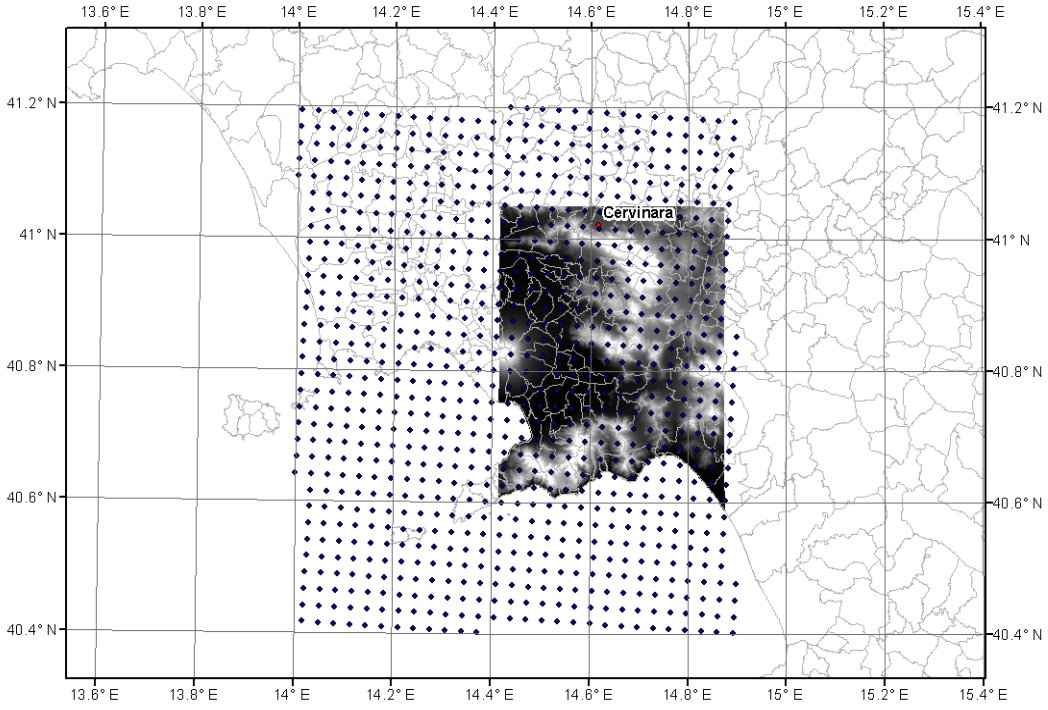

Figure 20: The blue points represent the COSMO LM model grid point (on the upper part the grid point of COSMO LM 7 km and on the lower part the grid point of COSMO 2.8 km), in black there is the digital elevation model (DEM) of the area used for the downscaling and in red there is the in situ station reported for the validation.

The validation reported in Table 6, Table 7 and Table 8 is only a rough way to evaluate the performance of the COSMO-LM model in the test cases. In fact the simulated rainfall, representing the input for the slope stability model, is evaluated with a downscaling algorithms using simulated rainfall on a big area covered by a digital elevation model (see Figure 21). Unfortunately for this test case observed precipitations are only available in 8 in situ station (see figure 18), covering a small area with respect to one used for downscaling. From a theoretical point of view it is not adequate to evaluate the model performances using statistical approach. Furthermore the COSMO LM model exhibits a systematic underestimation of the precipitation amount. A slight improvement is represented by the configuration with a higher resolution: 2.8 km instead of 7 km.

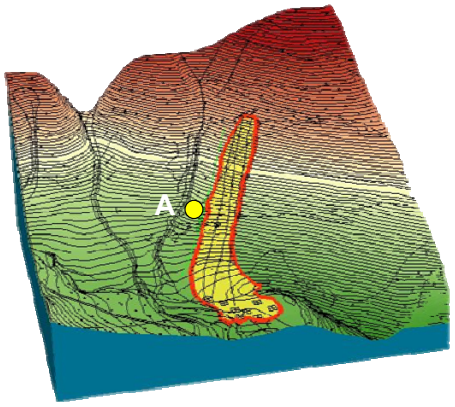

Figure 21: Cervinara case: Digital Elevation Model (DEM) used for numerical simulation.

The "simulation chain" has hence been validated initializing the infiltration model in the period between January 2006 and May 2007. The numerical simulations have been performed using the rainfall data from monitoring as upper boundary condition for the meteorological simulations. Results of in-situ and laboratory investigations of geotechnical properties (Picarelli et al., 2006) were used as input for the slope stability simulations. In particular, the boundary conditions at the ground surface is given by: i) the average daily rainfall intensity as indicated from monitoring in wet seasons or ii) the evaporation flux obtained from the relation suggested by Wilson et al. (1991) or alternatively indirectly determined from monitoring, during the dry seasons. For the lateral and base surfaces a condition of free flow has been adopted.
For the Cervinara case the geotechnical model has been calibrated through numerical simulations of infiltration aimed at reproducing the values of suction measured in 2006.
Figure 21 shows the digital elevation model (Scale 1:2000) used for numerical simulation. The slope has been schematized in the IMOD-3D module with a 3D mesh derived from the DEM (with dx=dy=0.5 m, dz=0.12m).

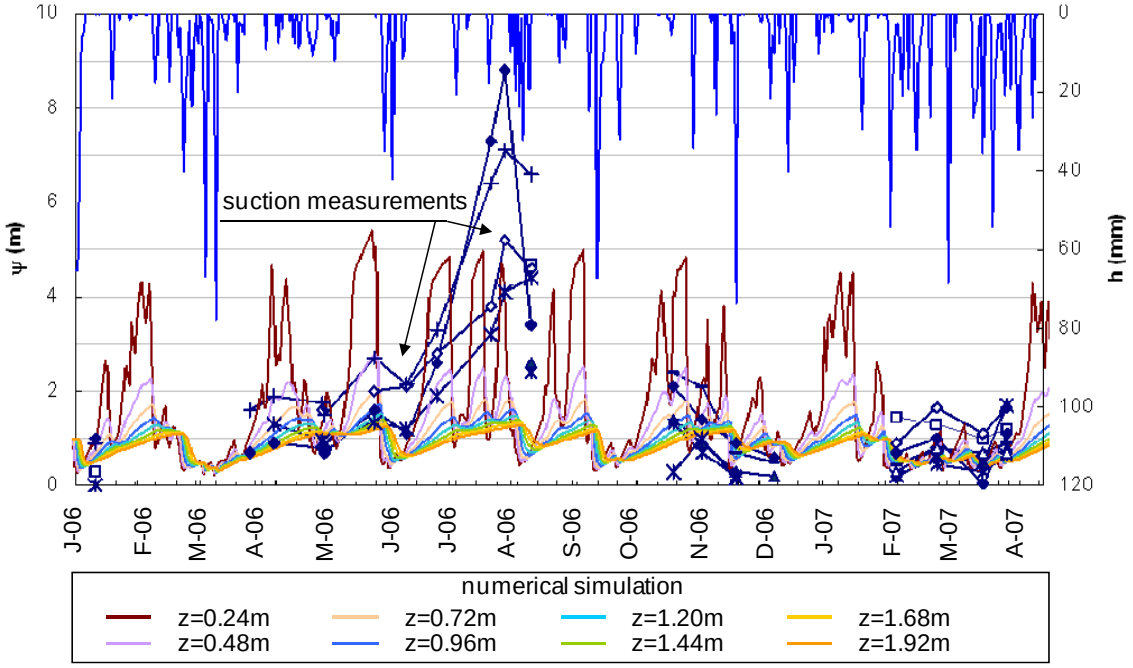

Figure 22: Numerical calibration for Cervinara case: best fitting obtained of suction measurement through numerical simulation.

Figure 22 shows the best fitting of suction measurement obtained through numerical simulation. For this calibration the results of numerical simulations between the depth of 0.2m and 1.5 m are reported (one curve each 22cm of depth for the point (A) located along the slope) together with the experimental data obtained by tensiometer readings (blue points in figure 22).
The comparison between the suction measurements and numerical data shows a good agreement between simulation and measurements. Obviously, the in situ measurements are discontinuous and the lines between the measurements do not represent the real values of suction.
During the wet periods fair agreement was obtained. During the dry periods the predicted trend is qualitatively in agreement with measurements in the topsoil, albeit at lower values. This is probably due to the simplified assumptions on evaporation flux applied in the model at the ground surface that do not take into account the presence of vegetation.

The "simulation chain" has been "closed" by three tests. The tests consist of numerical simulations of the effects of the rainfall in the 48/120 hours after the three selected dates by substituting downscaled forecast rainfalls to the measured rainfall.
The selected dates are:

1. 3 – 4 April 2007.
2. 6 – 7 March 2007.
3. 6 – 10 February 2007.

In the first and second case the period of simulation is of 48 hours; in the third case the period of simulation is of 120 hours. For Cervinara case, the Figures 23, 24 and 25 show the forecasted rainfalls in terms of intensity and cumulated height.

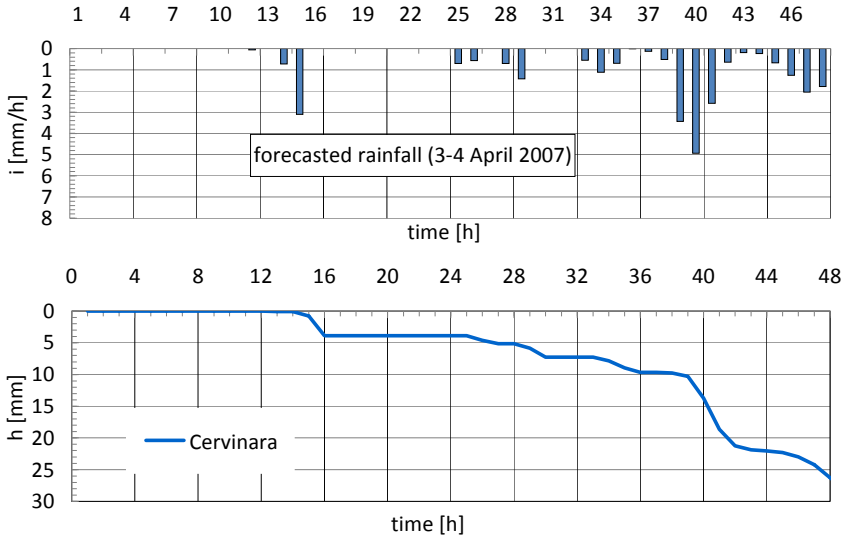

Figure 23: The forecast rainfall of 3-4 April 2007; a) intensity, b) cumulated height.

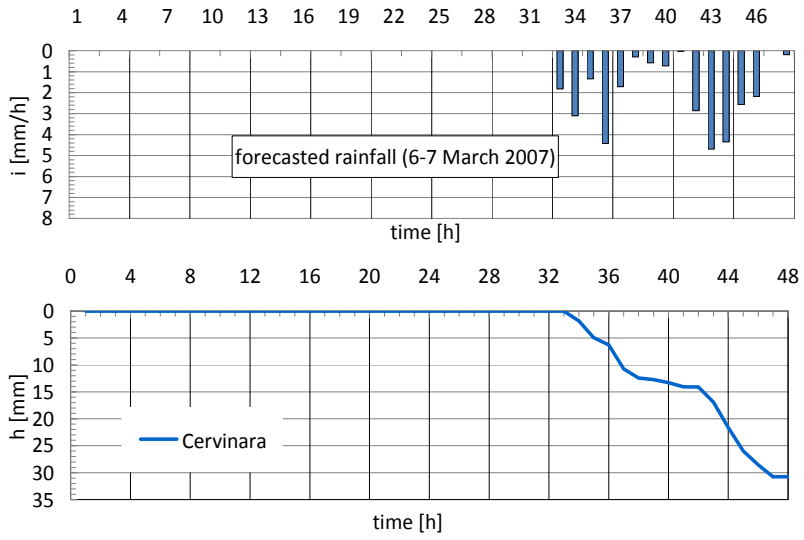

Figure 24: The forecast rainfall of 6-7 March 2007; a) intensity, b) cumulated height.

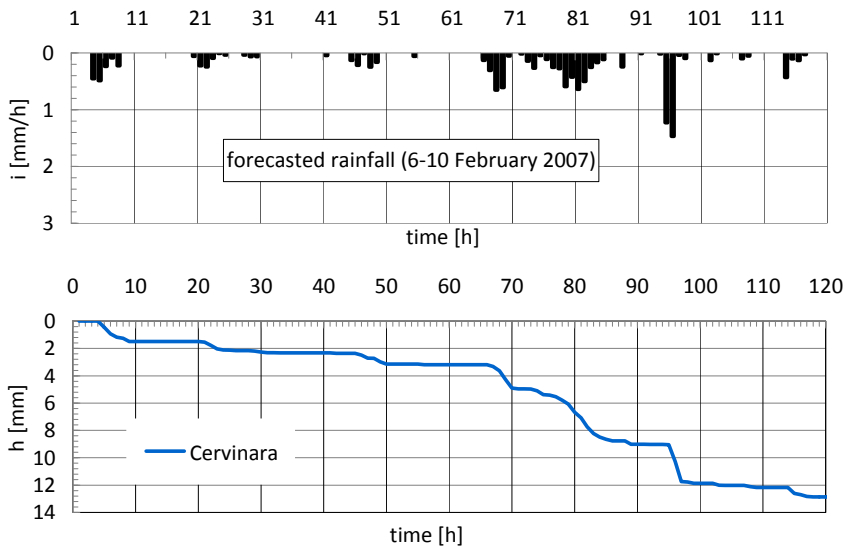

Figure 25: The forecast rainfall of 6-10 February 2007; a) intensity, b) cumulated height.

In the first and second tests (fig 23 and 24) the cumulated rainfall is of about 30mm but, in the first case the rain is distributed over 34 hours while in the second case within a very shorter period (15 hours). Moreover, in the third case not only the forecasted rainfall is characterised by a lower cumulated height (12 mm) but the rain is even distributed over a longer period (120 hours). The comparison between the measured rainfall (from pluviometric measurements in the point A; see table 5) and forecasted rainfall in terms of intensity and height reveals not a so good agreement between them; the forecasted cumulated height is about half the measured.

The slope response predicted by IMOD-3D module is reported in the following Figures (Fig. 26, 27, 28, 29, 30 and 31).

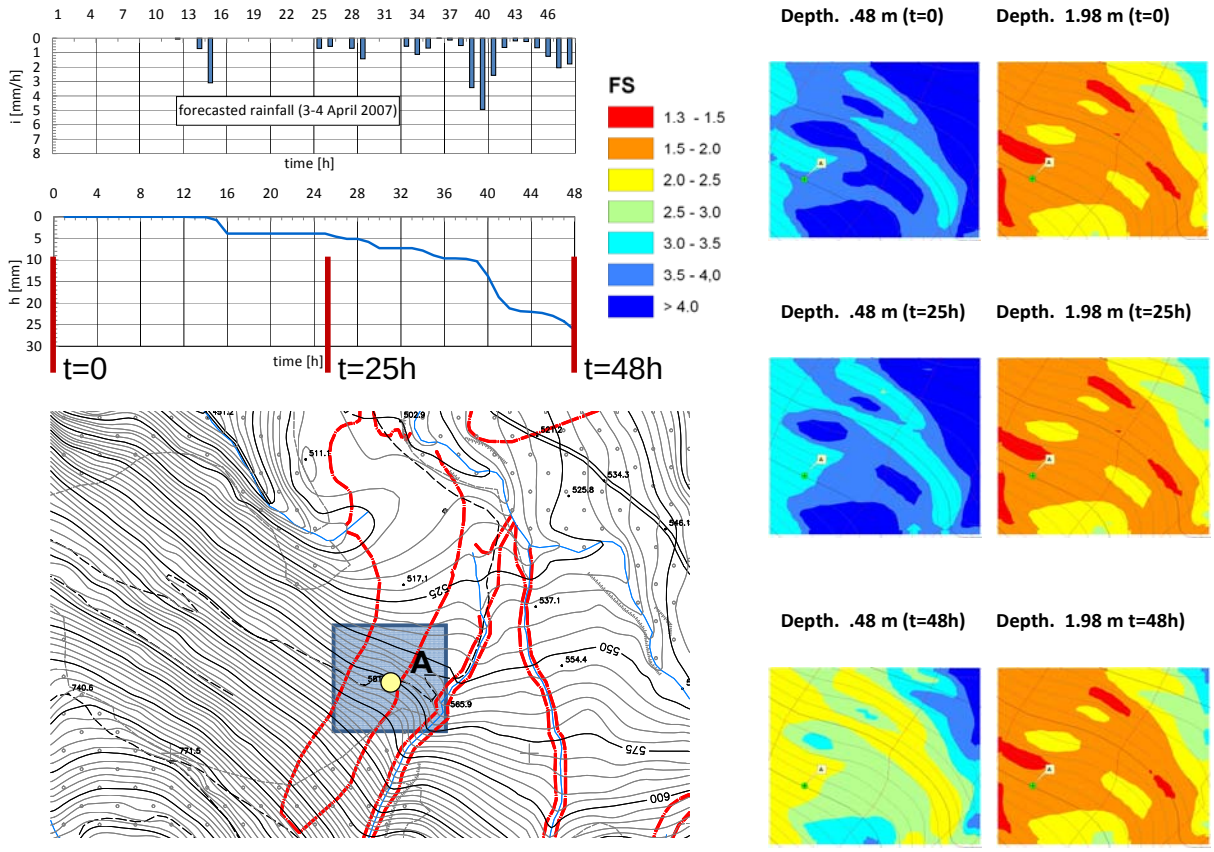

Figure 26: Safety factor contour maps for Cervinara test case 1 [3-4 April 2007].

The Figure 26 shows the results of the numerical simulation of the infiltration process in terms of safety factor FS using the output of downscaling module as boundary condition at the ground surface (Figure 23) and the results of numerical simulation (calibration step) reported in Figure 21 as initial condition. As expected, a strong reduction of safety factor occurs only in the shallower portion of the deposit (from the ground surface up to about 60 cm). The effects are negligible at greater depths.
Similar information can be obtained from the Figure 27 where, for the point A located along the slope, the same simulations are analysed in terms of capillary height profiles, volumetric water content profiles and safety factor (FS) profiles.

Comparing the three tests it is possible to observe what follows:

1. the wetting front depth is influenced by the duration of the event. In fact, in the third case (DT=120 hours) there is a strong reduction of volumetric water content up to 60cm while in the second case (DT= 12hours) the maximum depth reached by the infiltration process is of about 36 cm. This clearly influences the depth where the reduction of safety factor is significant.
2. For rain of higher intensity and for initial condition characterised by higher volumetric water content (lower capillary height) the reduction of safety factor assumes the maximum values (Test case 1).

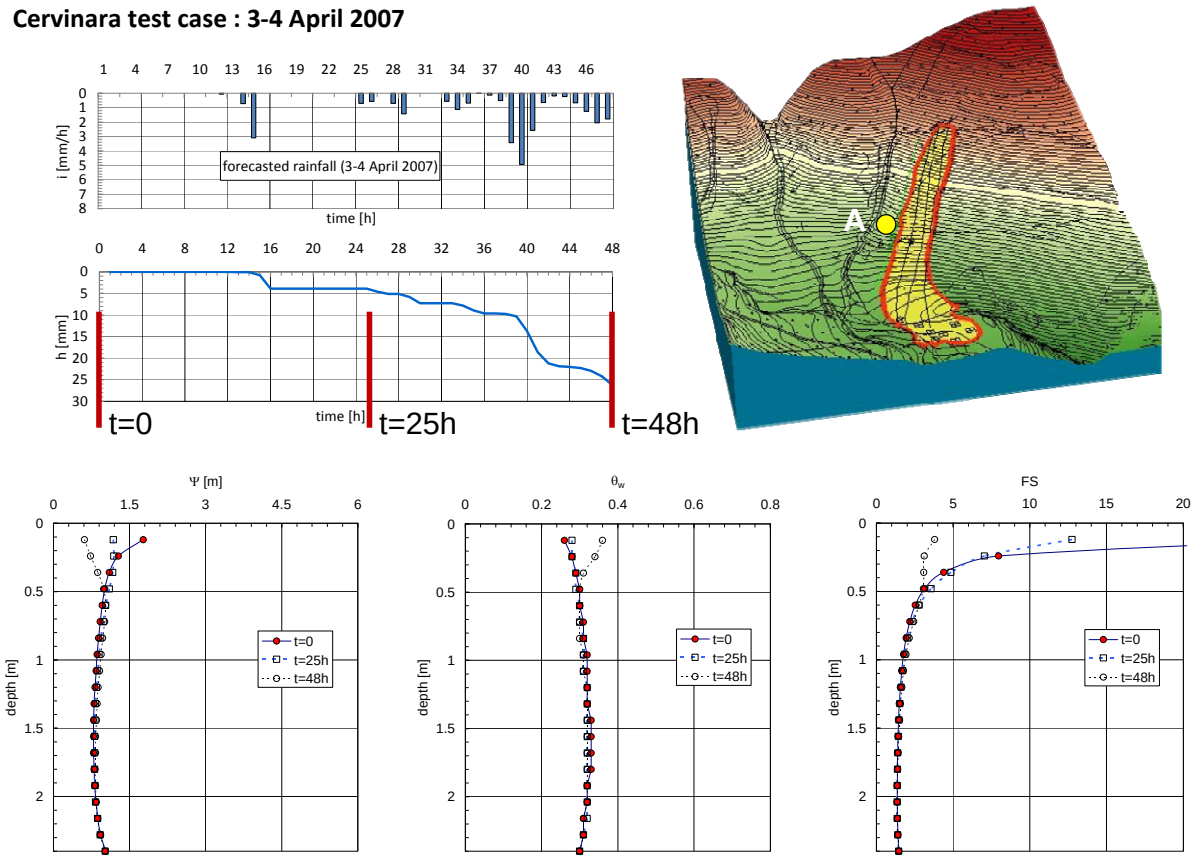

Figure 27: Cervinara test case 1 [3-4 April 2007]; results (point A) in terms of a) capillary height profile, b) volumetric water content profile, c) safety factor profile.

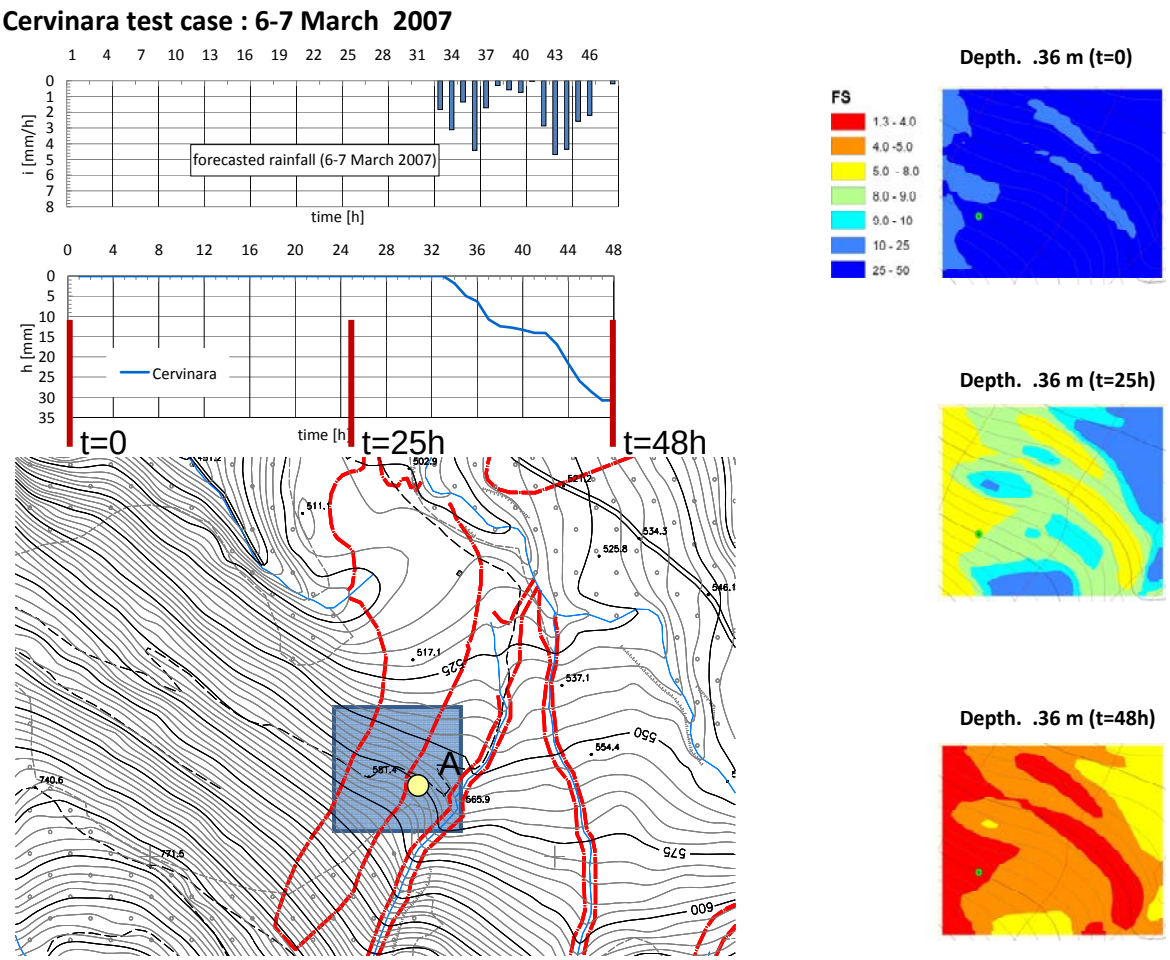

Figure 28: Safety factor contour maps for Cervinara test case 2 [3-4 April 2007].

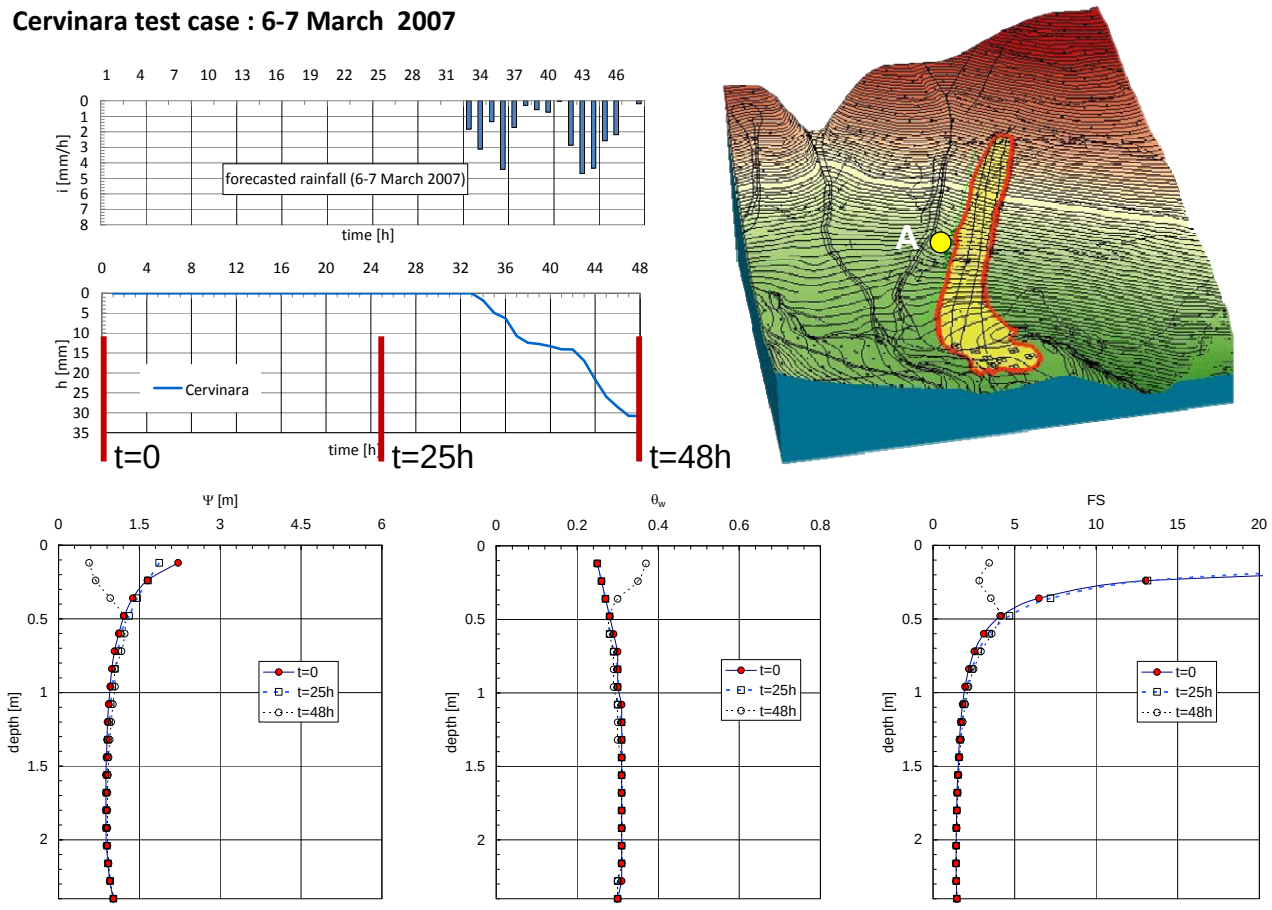

Figure 29: Cervinara test case 2 [3-4 April 2007]; results (point A) in terms of a) capillary height profile, b) volumetric water content profile, c) safety factor profile.

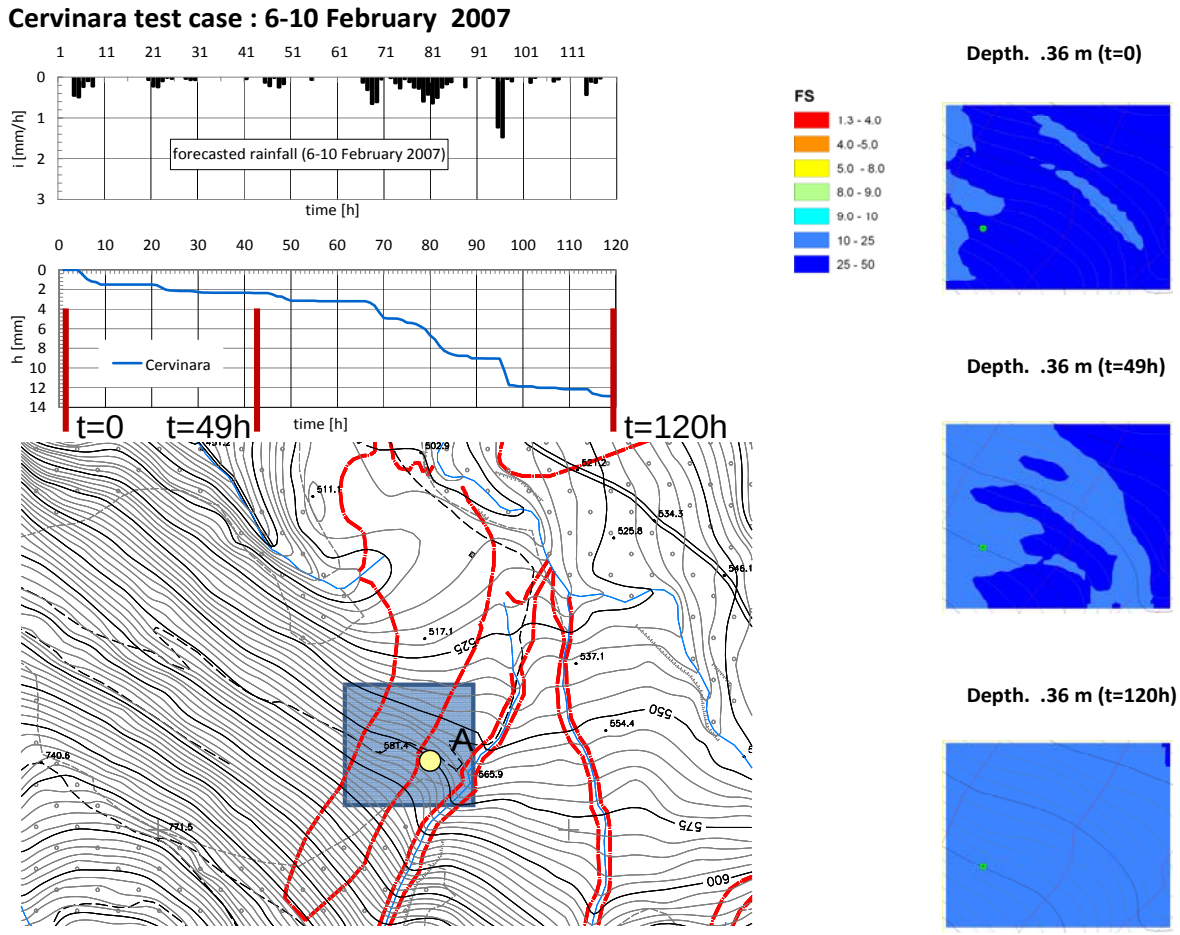

Figure 30: Safety factor contour maps for Cervinara test case 2 [3-4 April 2007].

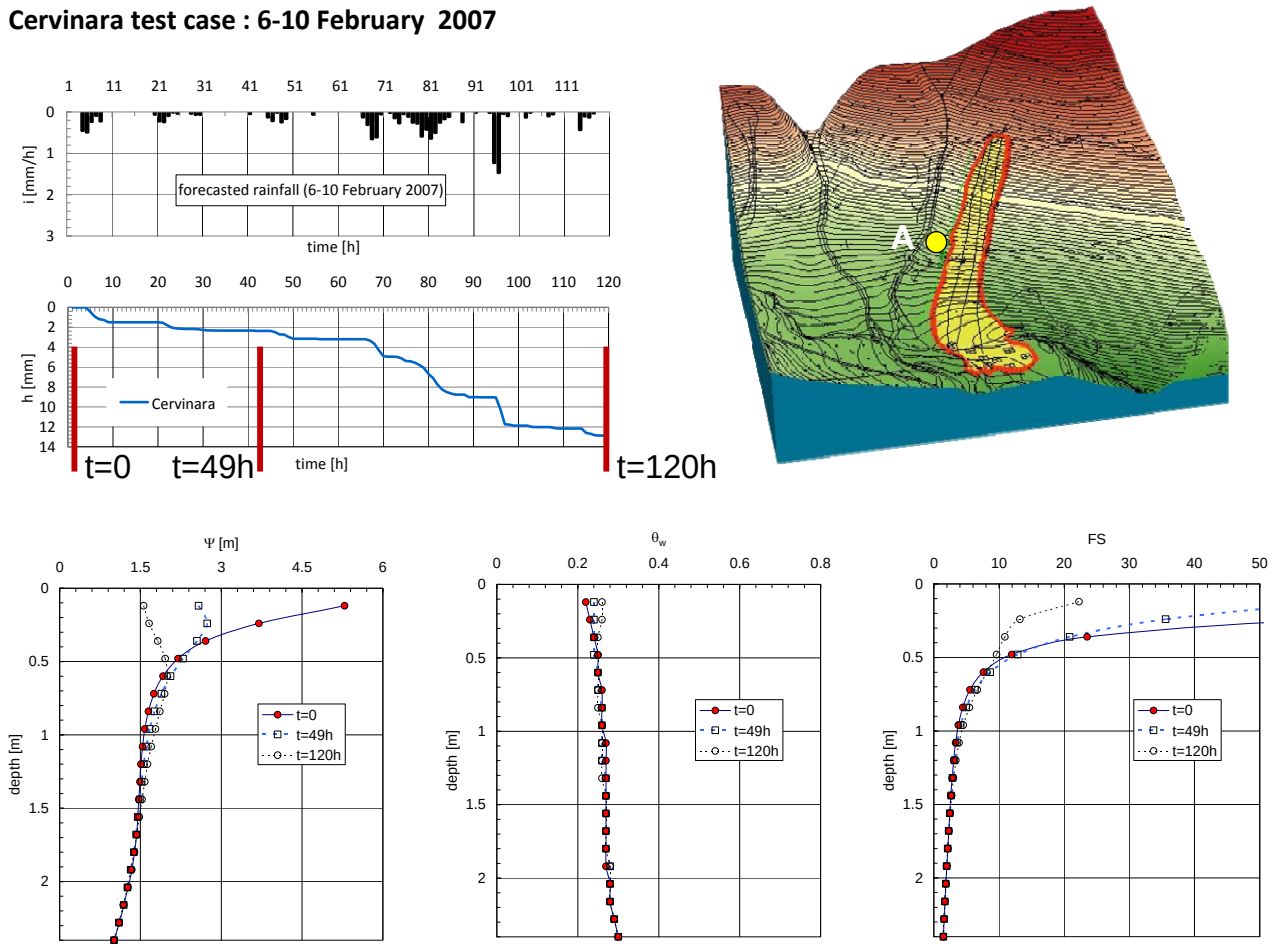

Figure 31: Cervinara test case 2 [3-4 April 2007]; results (point A) in terms of a) capillary height profile, b) volumetric water content profile, c) safety factor profile.

In all three tests our "simulation chain" was successful in providing reliable quantitative information about the link between forecasted rainfall and slope response (at slope scale) as it considered the spatial and temporal distribution of forecasted rainfall, the properties of soils (in saturated and unsaturated conditions) and the initial conditions (provided by numerical simulation initialized from monitoring).

4.2 ISCHIA

The island of Ischia is located in the southern part of the Tyrrhenian Sea, between 40°44' North latitude and 13°56' East longitude, 33 km from Naples. This island is 7 km wide from North to South and 10 km from East to West. The coastline is 39 km long and the total surface is 46 km^2.

The geomorphological evolution of the island of Ischia is strictly related to its tectonic and volcanic activity and in particular to the development of the Monte Epomeo structural horst. The uplifting of this horst started about 30.000 years ago with an asymmetric movement that led to the development of different morphology in different areas of island.

From the island of Ischia little information on shallow landslides, very few is available prior to 2006. Some events certainly have occurred in the past, as the geologic and geomorphologic settings of the territory are very similar to other areas in Campania. Namely volcanic soils overlying steep massifs where landslides have occurred frequently and often with catastrophic results. Moreover, many debris flows deposits have been found within the volcanic succession on the island. There is also geomorphologic evidence of deep landslide especially in the western side of the island and near Monte Vezzi (De Vita et al., 2006) (Figure 32). However, as no precise documentation exists regarding earlier events it is not possible to create a comprehensive landslide inventory.

The chosen test case concerns a convective rainfall event that occurred on April 30, 2006. The precipitation triggered four small soil slips on the slopes of Mt. Vezzi (about 400 m on the sea level), in the SE portion of the island (Figure 33).

The soil slips changed quickly into debris flows that reached the floodplain at the base of the hill. The landslides caused 4 victims and destroyed several buildings, forcing the evacuation of 250 inhabitants.

Figure 32: Monte Vezzi landslides triggered by a heavy rainstorm in the morning of April 30, 2006.

Figure 33: Google image of the Ischia's flow slide.

4.2.1 Meteorological event description and forecasting simulation

The Bracknell analysis map of sea level pressure (www.wetterzentrale.de/topkarten/fsfaxbra.html) show on April 29th and 30th April 2006 the persistence of a low pressure area on the Tyrrhenian Sea centred on the North Corsica isle (Figure 34). This configuration shows that the Ischia isle was affected by a weak cyclonic circulation at soil level moving humidity and wind from the Tyrrhenian Sea to the close Italian coast.

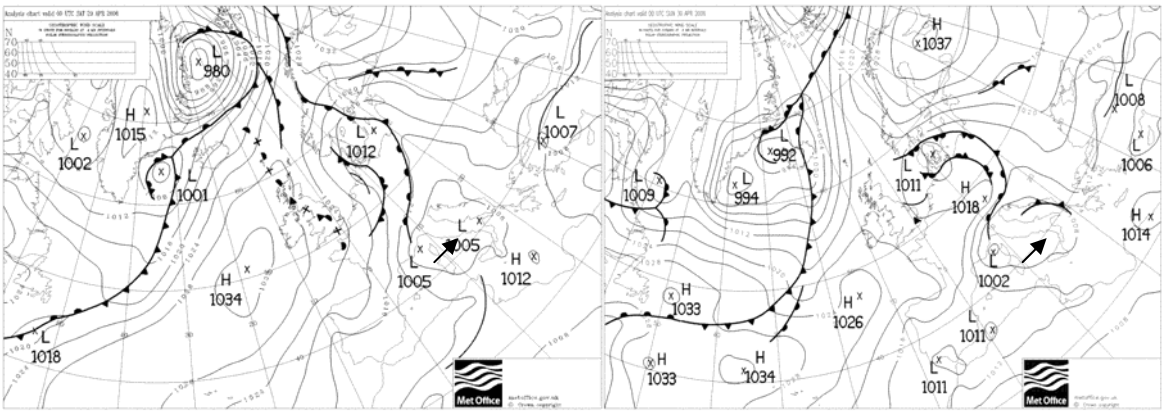

Figure 34: fronts and sea level pressure charts (Bracknell analysis) for 29/04/2006 00UTC and 29/04/2006 00UTC. The black arrows indicates Ischia isle.

The ECMWF analysis geopotential at 500 hPa shows the presence of a minimum located on the eastern coast of Sardinia on the April 29th at 00 UTC moving along east and, then, located on Campania region on the April 30th at 00 UTC. In the same map there is also shown a big low pressure area on the North Europe moving slowly on the Mediterranean area. This movement determines the entry of a cold area on the Mediterranean area that met the low

pressure area already persistent. This situation produces unstable conditions with high probability of convective activity on the Italian area (Figure 35).

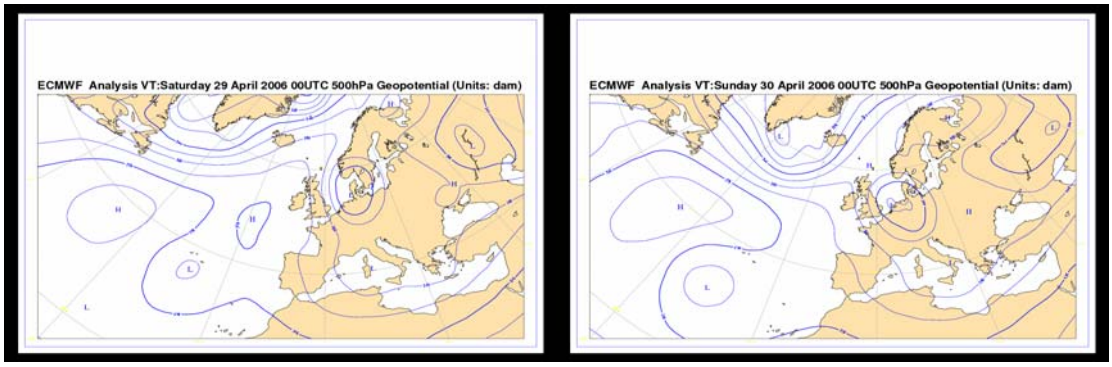

Figure 35: ECMWF analysis map for the 500 hPa geopotential on 29th and 30th April 2006 at 00UTC.

Correct forecasts are difficult to obtain during convective precipitation especially for low resolution models. In fact the deterministic configuration of the ECMWF model completely misses the forecast of strong precipitation on the Ischia isle during the night between April 29th and 30th (Figure 35). Neither the probabilistic configuration of ECMWF model shows a probability to have precipitation up to 20 mm in the area (Figure 36).

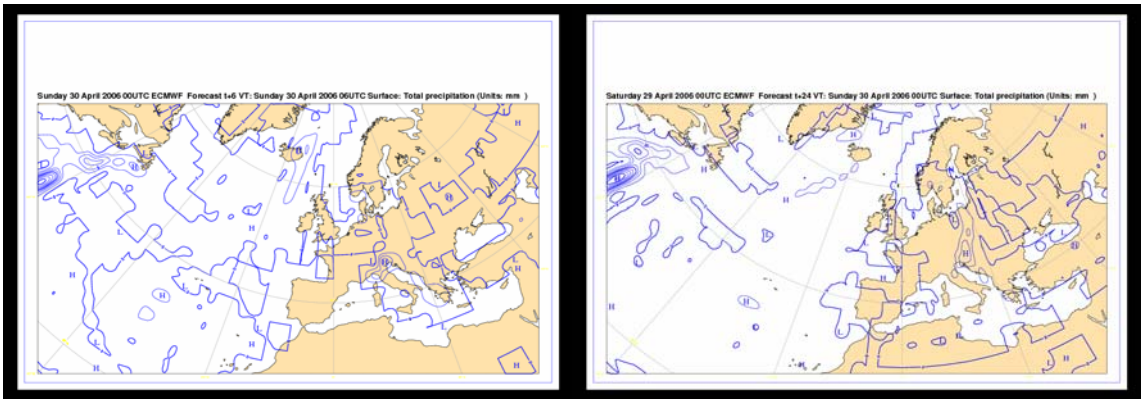

Figure 36: ECMWF deterministic configuration (+ 6 and + 24 time forecast for the simulation with analysis on 30th April 2006 at 00UTC).

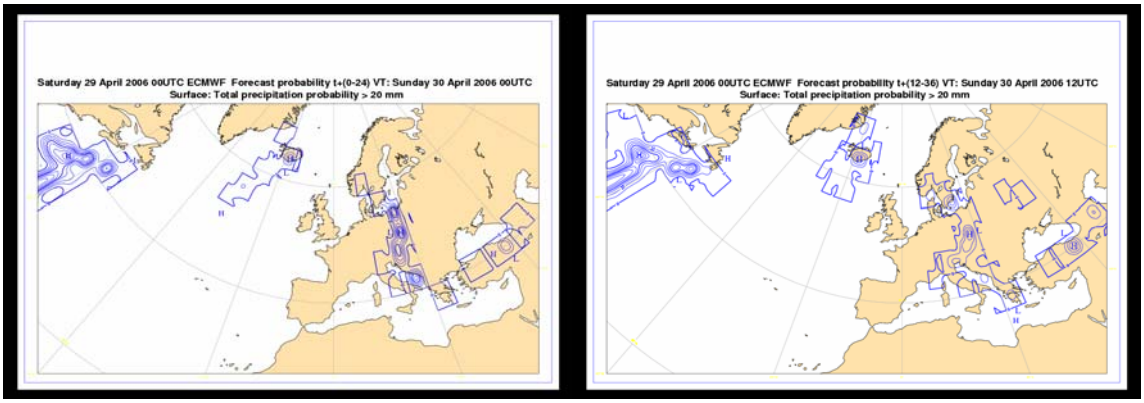

Figure 37: ECMWF probabilistic configuration (+ 24 and + 36 time forecast for the simulation with analysis on 29th April 2006 at 00UTC).

Measurements by a local station on the island confirm the convective features of the rainfall (intense and very localized storm).

In order to simulate the rain events that triggered the landslide different simulations with COSMO LM model have been performed.

The simulations are performed using COSMO model version 4.11 (for the 7 km and for the 2.8 km configuration). Initial and boundary data are taken from ECMWF forecasts data (with about 28 km of horizontal resolution).The assimilation is used for the configuration at 7 km if COSMO LM. The simulations are initialized at 00:00 UTC and they run for 24 hours. The number of vertical levels is 40 and the number of levels in the soil is 7.

The sub grid scale convection is used for the simulation at 7km and also for the simulation at 2.8 km (also if also a simulation without convection parameterization has been performed in order to evaluate the effect of this parameterization in this convective test case). Different moist convection parameterizations are available in the model. During the test cases the Tiedtke scheme (Tiedtke, 1989) is used. This scheme computes the effect of moist convection on temperature, horizontal wind in the atmosphere, and the precipitation rates of rain and snow at the ground. Usually with the configuration of 2.8 km this parameterization is not used, but for this particular test case in which the convective cells are very small the best results are obtained taking into account this parameterization. Is also available a convection scheme including only the shallow convection based on the Tiedtke scheme, this scheme is often used for the 2.8 km configuration, but this was not tested for this application.
Some characteristics of the two different COSMO LM configurations are reported in the following table:

Table 9: Brief comparison of the two COSMO LM configurations.

COSMO LM configurations	LM 7 km	LM 2.8 km
Domain Size (grid points)	200 x 140	275 x 230
Grid Spacing (horizontal)	0.0625° (7 km)	0.025° (2.8 km)
Number of vertical Layers	40	40
Time Step	40 sec	24 sec
Forecast Range	24 hrs	24 hrs
Initial Time of Model Runs	00 UTC	00 UTC
Lateral Boundary Conditions	ECMWF	LM 7 km
LBC Update Frequency	3 hrs	1 hr
Initial State	Nudging Scheme	NO

Dynamics	3 TL Leapfrog scheme; split-explicit	3 TL Leapfrog scheme; split-explicit
Physics	TKE; multi-layer soil model	multi-layer soil model; different convection schemes
COSMO LM Version	4_11	4_11

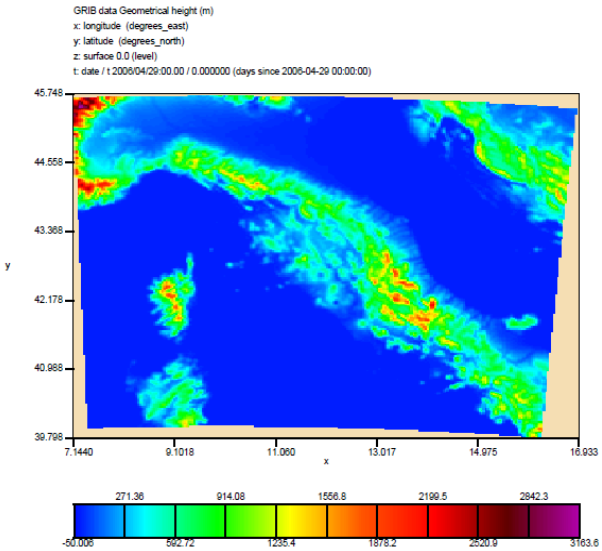

Figure 38: domain of COSMO LM 2.8 km for Ischia test case. In the Figure is represented the geometrical height (orography) of the domain.

A validation comparing the cumulated precipitation observed situate the meteorological station with the numerical forecast has been performed. In the following table (Table 10) the cumulated observed and the forecasted values using the 3 different COSMO LM configurations are presented. The forecast values are obtained by weighting the distance average from the grid points most closely to the observation point. A figure with the position of the COSMO LM model grid point, the Digital elevation model (DEM) of the area and the location of the in situ station is shown in the Figure 39.

Table 10: Comparison of the cumulated precipitation observed by in situ stations and forecasted using the 3 different COSMO LM configurations. The COSMO LM 2.8km simulation with moist convection parameterization is called COSMO 2.8km. The other without this parameterization is called COSMO 2.8km no conv.

	Ischia Porto				**Monte Epomeo (Ischia)**			
DATA	*Obs (mm)*	*COSMO 7km (mm)*	*COSMO 2.8km no conv (mm)*	*COSMO 2.8km (mm)*	*Obs (mm)*	*COSMO 7km (mm)*	*COSMO 2.8km no conv (mm)*	*COSMO 2.8km (mm)*
Cumulated rain from (29/4/06 08.00 UTC to 4/30/06 09:00) UTC	113	9	16	29	27	9	9	23

	Napoli Capodimonte				Pozzuoli (Naples)				Ercolano (Naples)			
DATA	*Obs(mm)*	*COSMO 7km(mm)*	*COSMO 2.8km no conv (mm)*	*COSMO 2.8km(mm)*	*Obs(mm)*	*COSMO 7km(mm)*	*COSMO 2.8km no conv (mm)*	*COSMO 2.8km(mm)*	*Obs(mm)*	*COSMO 7km(mm)*	*COSMO 2.8km no conv (mm)*	*COSMO 2.8km(mm)*
Cumulated rain from (29/4/06 08.00 UTC to 4/30/06 09:00 UTC)	11	4	9	4	12	7	11	11	4	5	13	12

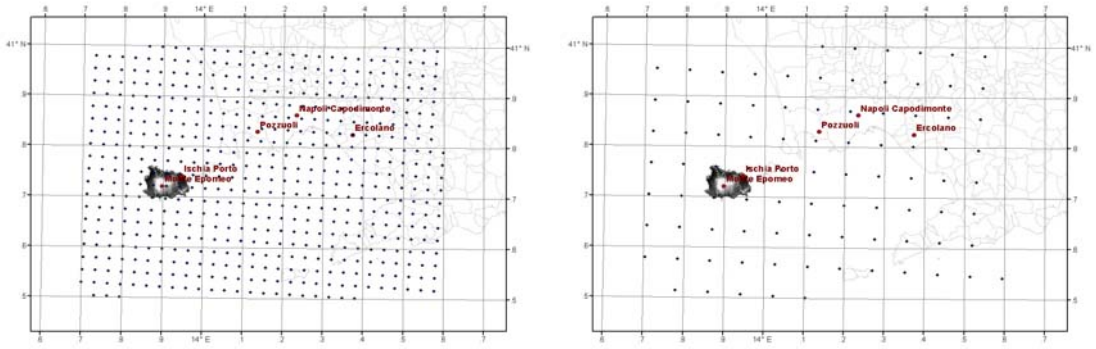

Figure 39: The blue points represents the COSMO LM model grid point (on the left side the grid point of COSMO LM 7 km and on the right side the grid point of COSMO 2.8 km), in black there is the digital elevation model (DEM) of the area used for the downscaling and in red there are the in situ station used for the validation.

There is a good agreement between the 3 configuration of COSMO LM model and the situ station located in the area of the landslide. Looking at the results on the Ischia isle it is clear that the configuration called COSMO LM 2.8 km captures the convective feature of the event, with respect to the other configurations, but it is not adequate to capture the real intensity of the event.

This application shows a deficiency of the numerical model in the forecast of much localized rainfall events; this feature could be improved in the future using more resolute atmospherical model and improving the physical scheme implemented in the model. Rainfall events caused by intensive convective cells ask for a different early warning scheme not based on numerical weather forecasts.

4.2.2 Measured rainfall intensity data

This test case offers a great opportunity for comparison between the typical operating dataset discussed in this deliverable of the SafeLand project and a high temporal and spatial resolution of a measured rainfall dataset. The measured rainfall data is estimated from ground based radar measurements at the Grazzanise station near Naples which is operated by the Italian Air Force,. The radar rainfall intensity map has a temporal resolution of 30 minutes and a spatial resolution of 500 meters. The rainfall cumulative map of radar measured data in show in Figure 40 the cumulated period is from the 29th and 30th of April 2006.
The cumulated value reaches 480 mm of rain in two days, even if this peak does not coincide with the Monte Vezzi Area (Figure 40).

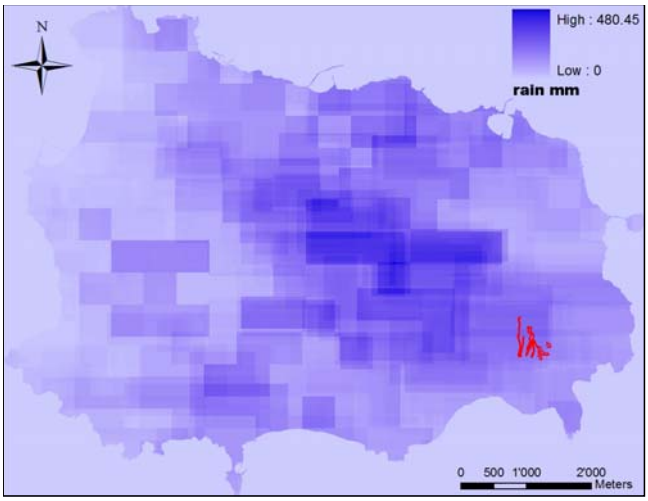

Figure 40: the cumulative map of the ground based radar measurement related to the 29th and 30th of April 2006. The Monte Vezzi landslides are traced in red.

4.2.3 Geotechnical input data preparation

For the Island of Ischia the stationary data needed to perform the simulation with HIRESSS (see chapter 3.1.2) was obtained from in situ test sand laboratory analysis of samples found in the literature (Mattiangeli, 2007; Cattoni et al., 2007; Crosta & Dal Negro, 2003; Casagli et al., 2007; Apuani et al., 2005; Calcaterra et al., 2003; Frattini et al., 2004).

The lithological map in Figure 41 was the base map used to individuate the litho technical area and prepare the input data map needed by HIRESSS. The geotechnical parameters assigned to every litho technical areas and each relative variation, needed in the Monte Carlo simulation, are reported in Table 11 and Table 12.

The DEM used to obtain the slope parameters is a high resolution 5 meter map: the spatial resolution of the DEM lock the spatial resolution of the HIRESSS output. Each map with the results of the stability analysis in this area has more than 3 million pixels.

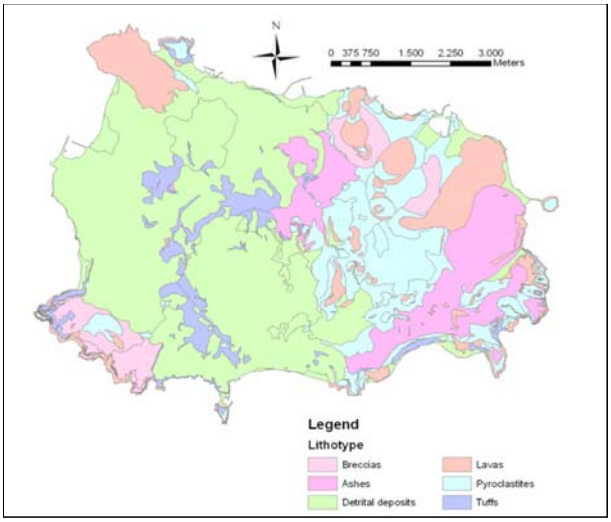

Figure 41: Schematic lithological map of the Island of Ischia.

Table 11: Parameters from in-situ measurements of the litho technical areas individuated on Ischia Island.

Litho technical area	Dry soil unit weight (N/m³)	Friction angle (Degrees)	Hydraulic conductivity (m/s)
Pyroclastites	14000	19	$3 \cdot 10^{-4}$
Lavas	14000	37	$2 \cdot 10^{-6}$
Detrital deposits	14000	28	$2 \cdot 10^{-4}$
Tuffs	18000	26	$6 \cdot 10^{-4}$
Ashes	15000	36	$1 \cdot 10^{-6}$
Breccias	18000	25	$2 \cdot 10^{-4}$

Table 12: Relative variations of all parameters considered in the Montecarlo simulation. The probability distribution of each parameters, used in the simulation of this test case is a uniform probability distribution.

Parameters	Relative error
Cohesion	40%
Friction angle	20%
Slope	20%
Dry soil unit weight	21%
Soil depth	20%
Hydraulic conductivity	60%
Pore size index distribution	30%
Bubbling pressure	20%
Porosity	20%
Residual water content	30%

4.2.4 Slope stability analysis

Slope stability analyses were performed using two different sets of rainfall data on the Ischia test area: one using a combination of radar measured rainfall data and COSMO-LM forecasted rainfall data, the second using only the radar data of the entire event. The combined rainfall data set, as stated, is a realistic application of the slope analysis chain. The first 24-hour slope stability analysis is produced from the measured radar data to prepare the initial condition for the queued next 24 hours of forecasted rainfall provided by COSMO-LM. The output results of the HIRESSS slope stability analysis are maps of probability of failure with a spatial resolution of 5 meters and a temporal resolution of 1h.

The pixel by pixel analysis is most demanding because it compares the pixel instability with the pixel that was actually involved in a landslide. It is difficult to have good results because a landslide must be located with a precision within 5 meters; the georeferencing error can be comparable and this is the most evident problem connected with this type of validation. However, it can be an indicator of the general behaviour of the model. Instead, a basin aggregation result analysis method is used. The high resolution analysis map is then elaborated and the result is aggregated in a basin. Aggregation by basin is a more reasonable method of analyzing the results than the deterministic approach and, basically, consists of aggregating the results in a larger area and then comparing basin to basin. The method is reasonable because it provides a stability evaluation of an area that will be quite homogeneous; moreover, the physical model does not take into account the parameters that can be determinant to trigger a landslide in a particular point and not in another only a few meters away having the same apparent characteristics. Therefore, the aggregation allows taking into account partially the chaotic components of real soil. Moreover, shallow landslides are very dangerous when they flow and merge in channels, so it can be useful to understand the stability situation of an entire micro-basin.

The basins are defined by regrouping the cells that belong to the upslope contributing area of a same flow node. Nodes that regroup are considered to have contributions of more than 3000 pixels. The individuated basin allows a good spatial resolution even after re-aggregation.

The resulting analysis is focused on Monte Vezzi, because it is the only landslide with a precise date and location.

In Figure 42 the average probability of slope instability is shown, computed between 13:00 and 16:00 of the day before the landslide was triggered.

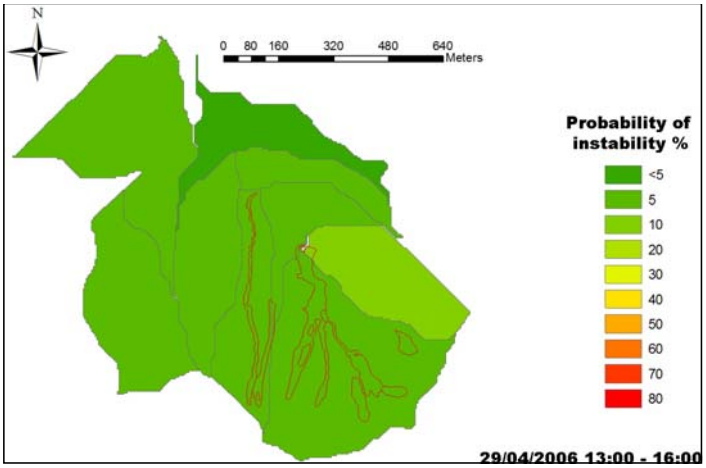

Figure 42: The average probability of slope instability of Monte Vezzi area computed between 13:00 and 16:00 on 29 April 2006. The landslides contours are drawn in red.

The analysis is performed, as stated earlier, from the radar measurement until the end of the 29th of April, and it shows a normal situation, with some peaks having less than 10% of instability probability. The Monte Vezzi area maintains the same conditions in the hours immediately after midnight (Figure 43).

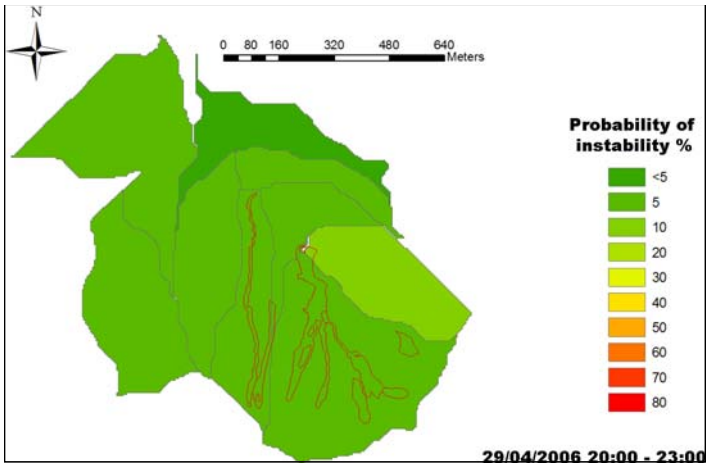

Figure 43: The average probability of slope instability of Monte Vezzi area computed between 20:00 and 23:00 on 29 April 2006. The landslides contours are drawn in red.

After 24:00 on 29 April, HIRESSS processes the forecasted rainfall data. The result during the time frame when the landslides occurred is shown in Figure 44: between 6:00 and 9:00 on 30 April there is not any evidence of changes in stability conditions. The forecasted instability probability remains under 10% without any indication of exceeding thresholds of the warning system. The low instability condition continues during all hours of 30 April (Figure 45).

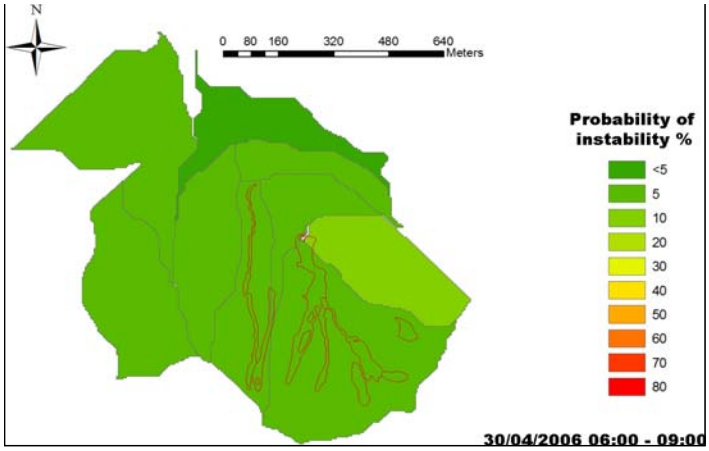

Figure 44: The average probability of slope instability computed between 6:00 and 9:00 on 30 April 2006, the period when the Monte Vezzi landslides occurred. The analysis is performed using forecasted rainfall data. The landslides contours are drawn in red.

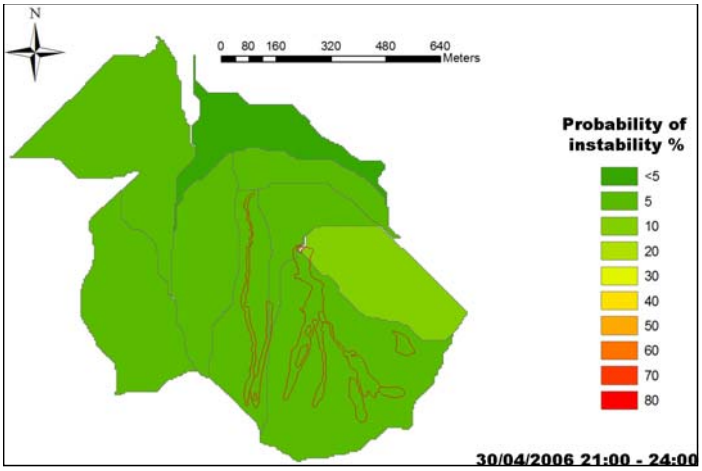

Figure 45: The average probability of slope instability of the Monte Vezzi area computed between 21:00 and 24:00 of 30 April 2006 using forecasted rainfall data. The landslides contours are drawn in red.

The results of the HIRESSS simulation performed using the radar measurements are shown in Figure 46 and Figure 47. The area involving landslides increased the average probability of instability. Between 2:00 and 5:00 the area where landslides occur reaches almost 40% of probability of slope failure.

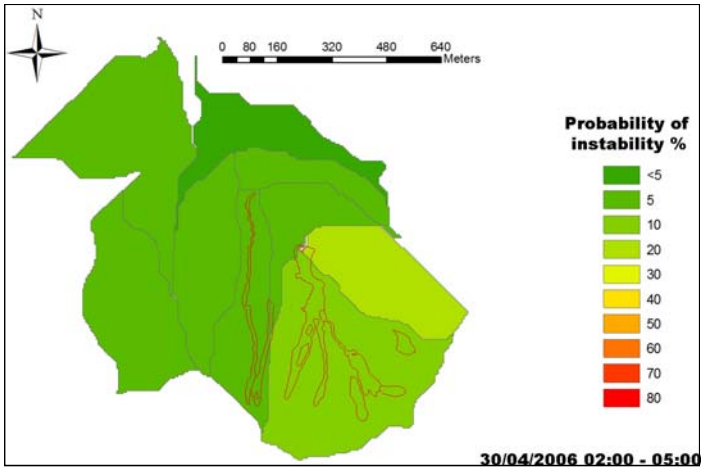

Figure 46: The average probability of slope instability of the Monte Vezzi area computed between 2:00 and 5:00 on the morning of 30 April 2006 using radar measurements. The landslides contours are drawn in red.

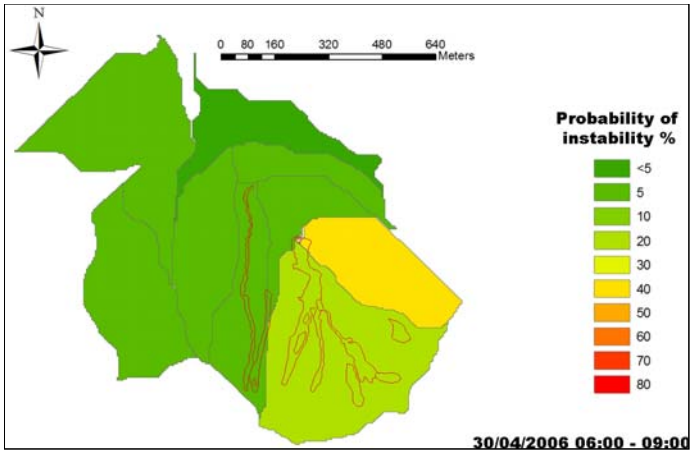

Figure 47: The average probability of slope instability of Monte Vezzi area computed between 6:00 and 9:00 the morning of 30 April 2006 using radar measurements. Monte Vezzi landslides occurred between 6:30 and 8:00. The landslides contours are drawn in red.

The simulation reaches a failure probability percentage between 40% and 50% when the landslides occurred (Figure 47). The failure probability jumps up between 50% and 60% if the hourly computed map is analyzed in this critical time frame. After the 6:00 to 9:00 time frame the instability probability of the area decreases progressively to non critical values also using the full radar rainfall dataset (Figure 48).

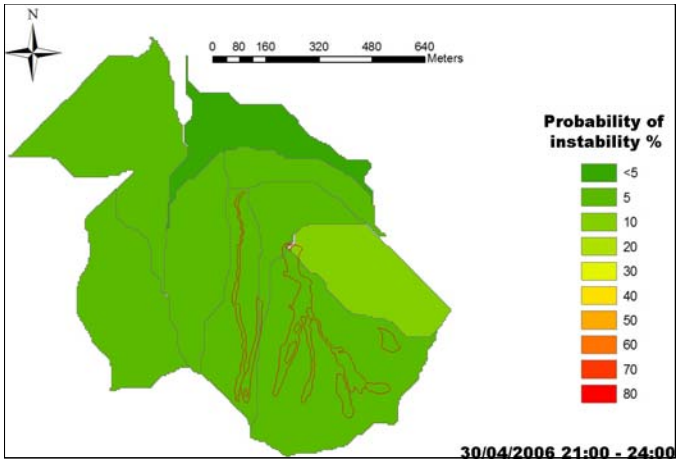

Figure 48: The average probability of slope instability of the Monte Vezzi area at the end of the day on 30 April 2006. The map refers to the timeframe between 21:00 and 24:00. The landslides contours are drawn in red.

The non aggregated full resolution results are shown in Figure 49 and Figure 50. The two maps show the average of slope failure probability and the progressive behaviour that leads to landslide triggering. The map in Figure 51, obtained from the forecasted dataset, instead shows non critical conditions during the rest of the day.

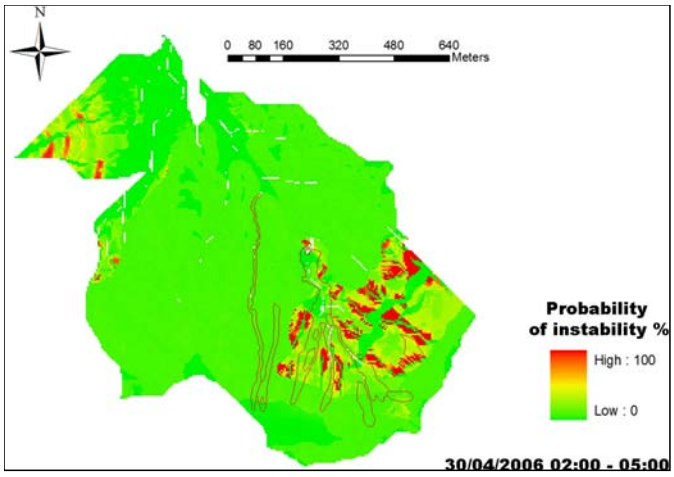

Figure 49: Full resolution map of average slope failure probability of the Monte Vezzi area from 2:00-5:00 on 30 April 2006. The map is computed from the full radar rainfall dataset. The landslides contours are drawn in red.

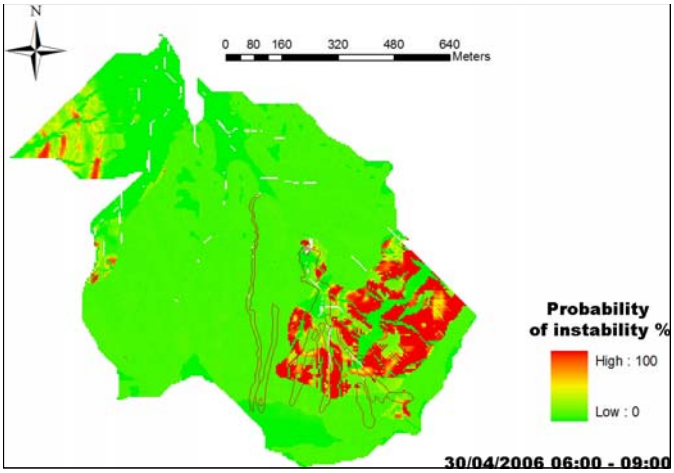

Figure 50: full resolution map of average slope failure probability of the Monte Vezzi area from 2:00-5:00 on 30 April 2006. The map is computed using the full radar rainfall dataset. The landslides contours are drawn in red.

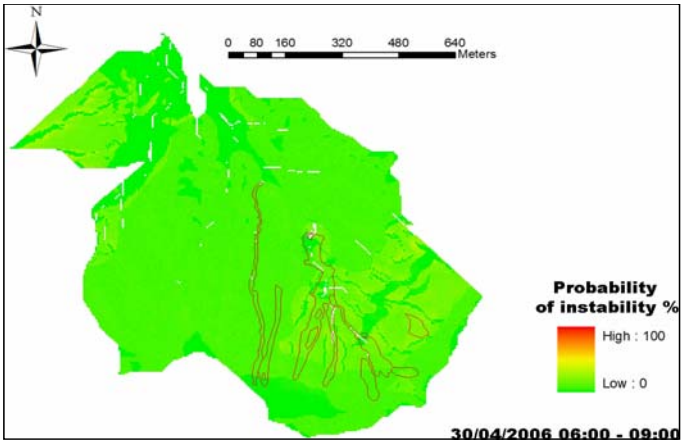

Figure 51: full resolution map of average slope failure probability of the Monte Vezzi area from 2:00-5:00 on 30 April 2006. The map is computed using the COSMO-LM rainfall dataset. The landslides contours are drawn in red.

4.2.5 Discussion of results

The slope stability analysis performed with HIRESSS using the measured radar rainfall dataset shows a progressive increase of slope failure probability that peaks in the time slot when the landslides were triggered. Throughout the 30 April, the area recovers stability and returns to a normalized condition before the end of the day. The HIRESSS simulation provides realistic and satisfying results in this area coupled with radar measurement, but there is not a complete landslide inventory of that period to perform a complete validation. The simulation performed with the hybrid measured-forecasted dataset, that will be the typical operative method proposed in this deliverable, shows unsurprisingly incorrect results. As mentioned, the meteorological event is recognized by the COSMO-LM simulation, but the real intensity of the phenomena is not reproduced. Summarizing, this case study suggests focalizing future efforts on improving the forecasting of the much localized convective event.

4.3 APENNINE AREA: TUSCANY REGION

The Northern Apennines is a complex thrust-belt system made up by the juxtaposition of several tectonic units, piled during the Tertiary under a compressive regime that was followed by extensional tectonics from the Upper Tortonian. The latter phase produced a sequence of horst-graben structures with an alignment NW-SE that resulted in the emplacement of Neogene sedimentary basins, mainly of marine (to the West) and fluvio-lacustrine (to the East) origin (Martini and Vai, 2001). Today, the morphology is dictated by the presence of NW-SE trending ridges where Mesozoic and Tertiary flysch and calcareous units outcrop, separated by Pliocene-Quaternary basins.

The inter-mountain basins formed from the Upper Tortonian (in the South-West) to the Upper Pliocene and Pleistocene (in the North-East). While the former experienced several episodes of marine regression and transgression during the Miocene and Pliocene, the latter were characterized by a fluvio-lacustrine depositional environment and gave rise to the present typical Tuscan smooth landscape.

These geological settings clearly affect the typology and occurrence of surface processes, primarily through the differences in the mechanical properties linked to the various prevalent lithologies. On this basis six main litho technical categories can be distinguished, such as cohesive soils, granular soils, hard rocks, weak rocks, complex units with predominance of rock material and complex units with predominance of argillaceous material.
In particular the study area which is located in Northern Tuscany and includes the provinces of Pistoia, Prato and Lucca shows two different geological settings in the east and west sectors respectively.

In the west sector the ridges that divide the basins are usually made up of carbonaceous rocks with slope gradients of even greater than 60°, often sub vertical or vertical. These slopes are usually rocky and with discontinuous vegetation, without forest. The carbonaceous rock faces are connected to the lower parts of the slopes, composed of metamorphic sandstone and phyllitic–schist, by talus and scree deposits. These slopes are usually moderately steep, especially in the intermediate areas (values ranging from 25° to 40°). There is, however, an increase in gradient in the lower slopes, as a consequence of the accentuation of erosive processes resulting from the Olocenic–Pleistocenic uplift of the Apuan metamorphic core.

The slopes are largely characterized by soils which typically cover the slopes underlain by predominantly phyllitic–schist and metamorphic–arenaceous rocks and are also mantled by dense forest (mainly chestnut). On the contrary, the calcareous and dolomitic slopes are usually rocky or with very thin soil cover. As shown below, the soils covering metamorphic sandstone and phyllite are usually the most involved in landsliding; these soils are rather thin (0.5–2 m thick).
The east sector shows a more uniform geological condition with the prevalence of flysch formation rock-type (Macigno) which is composed of quartz and feldspar sandstone alternated with layers of siltstone. The slope gradients varying from 0° in the plain and 55°. In the mid and upper sections of the valley, where most landslides usually occur, the stratigraphy consists of a 1.5 to 5 m thick layer of colluvial soil overlying the bedrock.

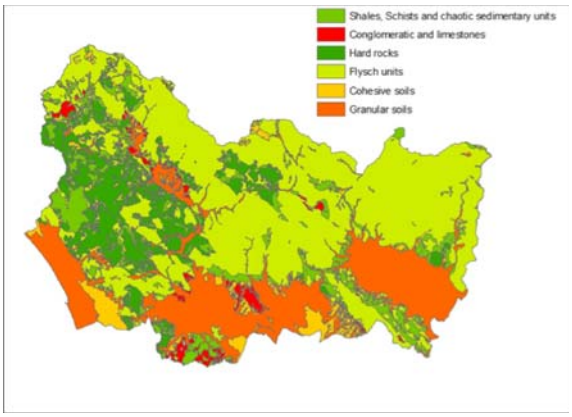

Figure 52: Schematic lithological map of the Prato, Pistoia and Lucca province area.

In Figure 52 the lithological map of the area is shown. In the south portion one can find mainly flat areas with cohesive and granular soils outcrop. In the East sector, there is the predominance of flysh units, mainly complex units with predominance of rock material and complex units with predominance of argillaceous material. In the West sector, there is the predominance of hard rocks, mainly phyllitic–schist and metamorphic–arenaceous rocks and secondarily shales, limestones and conglomerates.

4.3.1 Geotechnical input data preparation

The provinces area of Pistoia, Lucca and Prato has been elected for a large fieldwork campaign of measurements specifically planned for the SafeLand project.

There are two main problems in managing a large area with HIRESSS: the uncertainty in the parameters and the amount of measurements to be taken.

HIRESSS has the instruments to manage uncertainties in data but does not completely eliminate the need for field and laboratory measurements. The variation of the input data must be evaluated in order to provide the Monte Carlo parameters that allow reducing computational time. If the range of parameters uncertainty is not too large, it is possible to obtain more accurate results employing a less heavy Monte Carlo simulation. Moreover, the quantification of the field measurements needed to run the simulation on a large scale is very important to plan a large scale fieldwork.

The measurements campaign proposed and carried out is oriented to solve these two questions. After the identification of the soil litho technical classes from an analysis of lithological and geological 1:100000 maps, a large scale sampling was planned to estimate the parameters and their range of variation within the same litho technical area. The campaign comprised 34 field measurements (Figure 53).

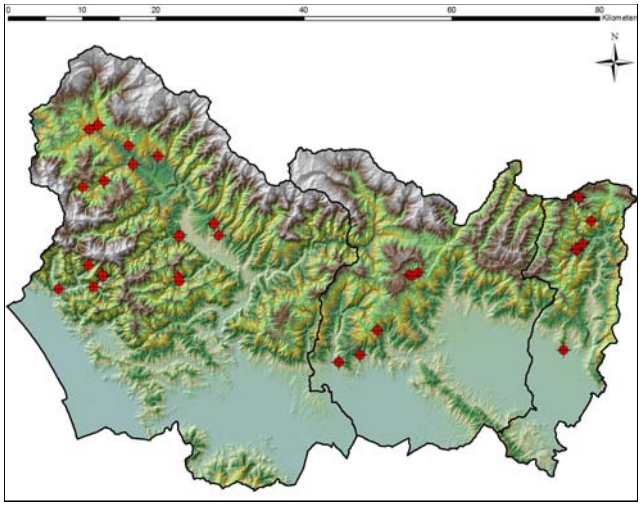

Figure 53: Distribution of field measurements over Lucca, Pistoia and Prato province area.

The Shear strength parameters were evaluated in situ by using the Borehole Shear Test (BST, Figure 54), obtaining values under natural conditions without disturbing the soil samples.

At the same depth as the BST, matric suction values were measured with tensiometers (Figure 56). Saturated hydraulic conductivity within the unsaturated zone was measured in-situ using the Amoozemeter or Compact Constant Head Permeameter (CCHP) (Figure 55).

The procedure used for measuring the hydraulic conductivity in the field is termed constant-head well permeameter technique (Philip, 1985). Results were then entered into the Glover solution, which computes the saturated permeability of the soils.

Figure 54: BST in situ measurements setup.

Figure 55: Amoozemeter measurements setup.

Figure 56: Tensiometer setup for matric suction measurements.

The measurements operated in situ were:

- Saturated hydraulic conductivity
- Friction angle
- Matric suction
- Soil water content

A sample of soil was taken at each location to perform laboratory analysis and then to define the value of the other parameters used in the stability simulator, such as bulk density, porosity and grain size curve.

At least two complete sets of measurements were executed for each litho technical typology. The average and the maximum deviation were evaluated for all litho technical classes (Table 14). In Table 13 the geotechnical input parameter values are reported of each litho technical area.

The DEM used to obtain the slope parameters is a high resolution 10 meter map: the spatial resolution of the DEM controls the spatial resolution of HIRESSS output. Each map resulting from the stability analysis in this area has more than 50 million pixels.

Table 13: Input parameters from in-situ measurements of the litho technical areas identified in the Pistoia, Prato and Lucca province area.

Litho technical area	Dry soil unit weight (N/m^3)	Friction angle (Degrees)	Hydraulic conductivity (m/s)
Shales, schists and chaotic sedimentary units	14000	35	$1 \cdot 10^{-6}$
Conglomerate and limestone	14000	30	$1 \cdot 10^{-6}$
Hard rocks	14000	32	$1 \cdot 10^{-7}$
Flysch units	18000	34	$1 \cdot 10^{-6}$
Cohesive soils	15000	29	$1 \cdot 10^{-6}$
Granular soils	18000	32	$6 \cdot 10^{-6}$

Table 14: Relative variations of each parameter considered in the Monte Carlo simulation of the Lucca, Pistoia and Prato province area. The probability distribution used in this test case simulation is a uniform probability distribution.

Parameters	Relative error
Cohesion	40%
Friction angle	20%
Slope	20%
Dry soil unit weight	21%
Soil depth	20%
Hydraulic conductivity	60%
Pore size index distribution	30%
Bubbling pressure	20%
Porosity	20%
Residual water content	30%

4.3.2 First test case: from 20th December 2009 to 6th January 2010

This test case interests the Northern Apennine chain and it includes three provinces; Pistoia, Prato and Lucca with a general extension of 3103 km^2 (Figure 58). This area, due to its geological and physiographic setting is strongly susceptible to mass movements, in particular shallow rapid landslides. In December 2009, during Christmas, the area was hit by a severe rainstorm which triggered around 300 shallow landslides (Figure 57).

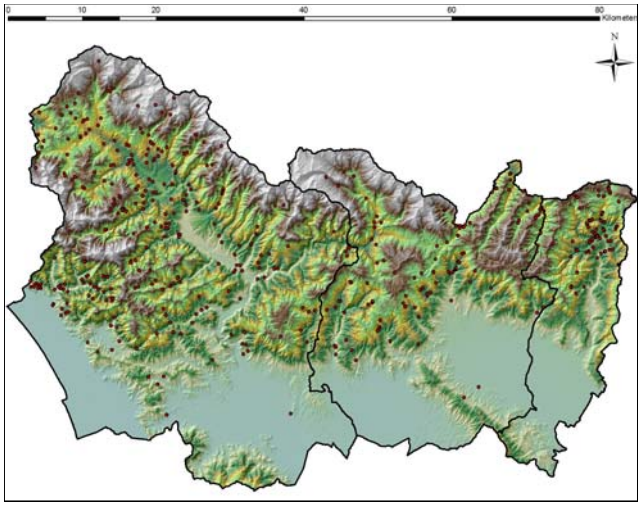

Figure 57: the landslides spatial distribution reported after the meteorological events of December 2009 on the Lucca, Pistoia and Prato province area.

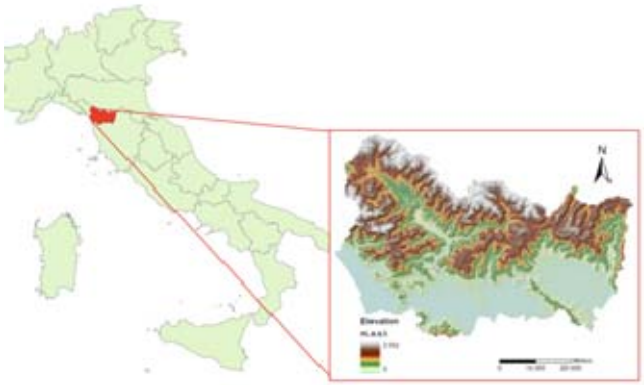

Figure 58: Location map of one of the case study for the application of the coupled hydrological stability model.

4.3.3 Meteorological event description and forecasting simulation

In order to simulate the different rain events that triggered a high number of landslides in the area during this period, different simulations have been performed with the COSMO LM model. The very long simulated period of 10 days, has required a high computational time (more than 100 hours on the on the CMCC supercomputer a NEC-SX8R).
On December 21 a flow of mild and humid air coming from Atlantic Ocean affected the Tuscany region. During the 22 and 23 of December the movement of the Atlantic high pressure area towards East, associated with the downhill of a low pressure from the France Northwest area, caused an intense moist southerly flow, with very intense rainfall, on the northern Apennine zones. On December 24th and 25th the presence of another pressure minimum centred on the Leoni Golf causes a westerly humid flow on the Tuscany region with intense rainfall and also convective thunderstorms. On the December 26 the perturbation leaves the Italian area and an increasing of the pressure values are visible from the Bracknell analysis map (Figure 59).

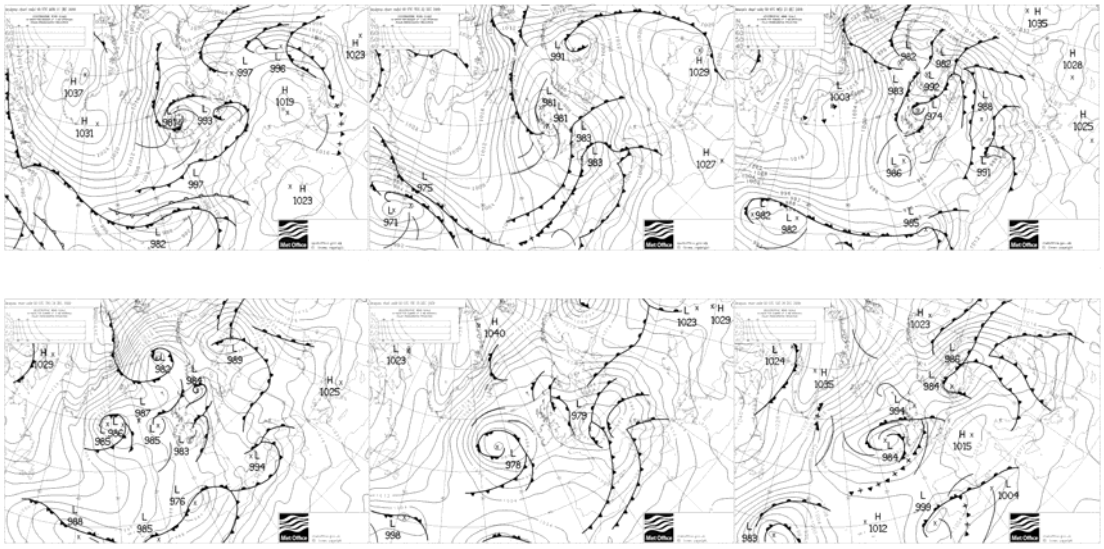

Figure 59: fronts and sea level pressure charts (Bracknell analysis) for 21/12/2009 00UTC to 26/12/2009 00UTC.

From 31 of December until the night of 2 January 2010 a new westerly humid flow gives a new impulse to the precipitation on the Tuscany region. This is caused by a trough which moved from south-eastern France towards the centre of Italy,. After that phase the minimum pressure area leaves Italy and moves eastwards giving a stop to the precipitation on the area.

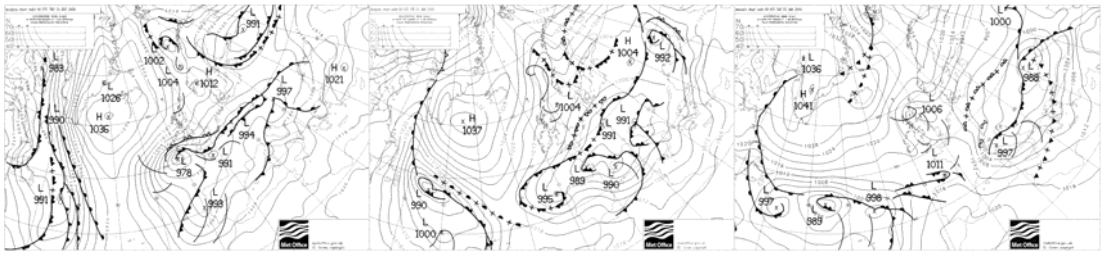

Figure 60: fronts and sea level pressure charts (Bracknell analysis) for 31/12/2009 00UTC to 2/1/2010 00UTC.

On the 5 and 6 of January a new perturbation affects the Tuscany region due to another low pressure area coming from the Atlantic Ocean which causes a humid southerly flow over the area.

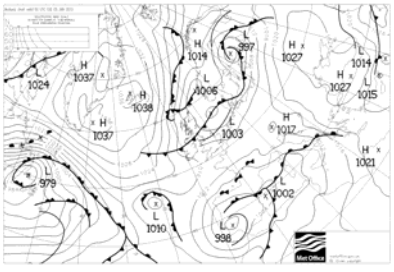

Figure 61: fronts and sea level pressure charts (Bracknell analysis) for 05/01/2010

The simulations of the complete period are performed using COSMO 7 km model version 4.11. Initial and boundary data are taken from ECMWF forecasts data (with about 14 km of horizontal resolution).The assimilation is used for the configuration at 7 km. The simulations are initialized at 00:00 UTC and they run for 24 or 36 hours. The number of vertical levels is 40 and the number of levels in the soil is 7.

The sub grid scale convection parameterization used for the simulation at 7km the Tiedtke scheme (Tiedtke, 1989). The 7km configuration has a domain with: 200 grid points for the longitude and 140 grid points for the latitude (Figure 62). The field of downscaling rainfall has been evaluated using all the information in the Digital Elevation Model, reported in the Figure 63, and the COSMO LM grid points represented in the same figure.

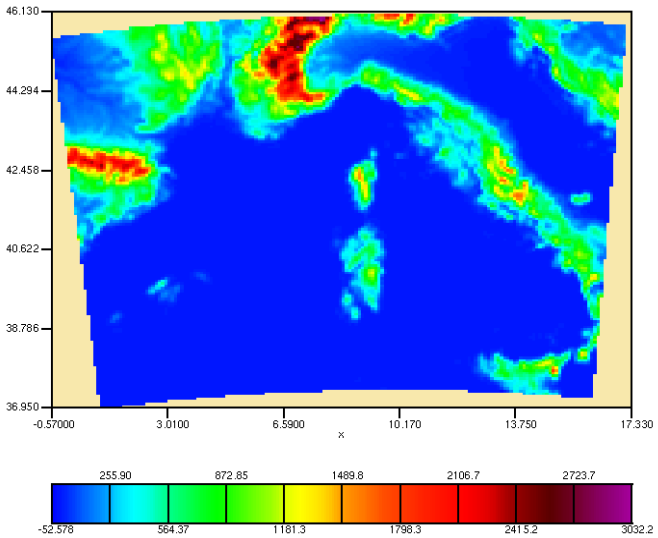

Figure 62: domain of COSMO LM 7 km for Ischia test case. In the Figure is represented the geometrical height (orography) of the domain.

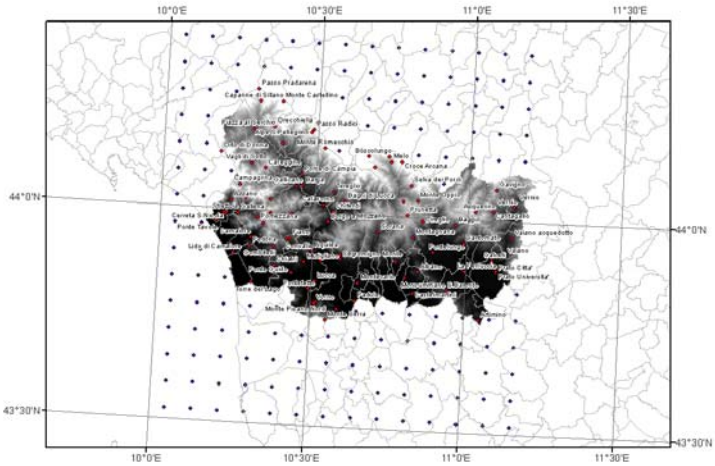

Figure 63: The blue points represents the COSMO LM model grid point(on the left side the grid point of COSMO LM 7 km , in black there is the digital elevation model (DEM) of the area used for the downscaling and in red there are the in situ station reported for the validation.

Table 15: Observed and forecasted daily rainfall. An average has been performed on the DEM area reported in the Figure 63. No observed values are available from 2009-12-30 to 2010-01-05.

	Mean observed (mm/24 hrs)	**Mean forecast** (mm/24 hrs)
2009-12 -20	3	0
2009-12 -21	13	21
2009-12 -22	58	55
2009-12 -23	30	27
2009-12-24	61	60
2009-12-25	28	19
2009-12-26	0.7	3.5
2009-12-27	0	0.5
2009-12-28	12.	8
2009-12-29	4	0
2009-12-30	21	7
2009-12-31	28	30
2010-01-01	39	22
2010-01-02	0.3	0.1
2010-01-03	0	1
2010-01-04	4	11
2010-01-05	9	18

Table 16: Statistic validation of COSMO LM rainfall forecast (from .20 December 2009 to 29 December) for the threshold 5 mm.

Threshold 5 mm	**THREAT SCORE**	**BIAS**	**FALSE ALARM RATE**	**HIT RATE RAIN**
2009-12 -20	**n.a.**	**n.a.**	**n.a.**	**n.a.**
2009-12 -21	**0.8**	**1.2**	**0.2**	**1**
2009-12 -22	**1**	**1**	**0**	**1**
2009-12 -23	**1**	**1**	**0.1**	**1**
2009-12-24	**0.9**	**1**	**0**	**1**
2009-12-25	**0.8**	**0.8**	**0**	**0.8**
2009-12-26	**0**	**n.a.**	**1**	**n.a**
2009-12-27	**n.a.**	**n.a.**	**n.a.**	**n.a.**
2009-12-28	**0.7**	**0.8**	**0**	**0.8**
2009-12-29	**n.a.**	**n.a**	**n.a**	**n.a**
2009-12-30	**0.8**	**0.9**	**0**	**0.9**
2009-12-31	**1**	**1**	**0**	**1**
2010-01-01	**0.9**	**1**	**0**	**1**
2010-01-02	**0**	**0**	**n.a.**	**n.a.**
2010-01-03	**n.a.**	**n.a.**	**n.a.**	**n.a.**
2010-01-04	**0.3**	**3.6**	**0.7**	**1**
2010-01-05	**0.8**	**1.3**	**0.2**	**1**

Table 17: Statistic validation of COSMO LM rainfall forecast (from .20 December 2009 to 29 December) for the threshold 20 mm.

Threshold 20 mm	**THREAT SCORE**	**BIAS**	**FALSE ALARM RATE**	**HIT RATE RAIN**
2009-12 -20	**n.a.**	**n.a.**	**n.a.**	**n.a.**
2009-12 -21	**0.2**	**3.4**	**0.8**	**0.6**
2009-12 -22	**1**	**1**	**0.1**	**1**
2009-12 -23	**0.7**	**1.3**	**0.3**	**0.9**
2009-12-24	**0.8**	**1.3**	**0.2**	**1**
2009-12-25	**0.2**	**0.7**	**0.5**	**0.3**
2009-12-26	**n.a.**	**n.a.**	**n.a.**	**n.a.**
2009-12-27	**n.a.**	**n.a.**	**n.a.**	**n.a.**

2009-12-28	**0**	**0**	**n.a**	**n.a**
2009-12-29	**n.a.**	**n.a**	**n.a**	**n.a**
2009-12-30	**0**	**0**	**n.a.**	**0**
2009-12-31	**0.6**	**0.7**	**0.1**	**0.6**
2010-01-01	**0.5**	**0.5**	**0.1**	**0.5**
2010-01-02	**n.a.**	**n.a.**	**n.a.**	**n.a.**
2010-01-03	**n.a.**	**n.a.**	**n.a.**	**n.a.**
2010-01-04	**n.a.**	**n.a.**	**n.a.**	**n.a.**
2010-01-05	**0**	**7.4**	**0.9**	**0.6**

Looking the results listed in the above tables is possible to see that there is a quite good agreement between forecast and observation especially during the days with more rainfall. Unfortunately other observations on the period from 31 December 2009 to 6 January 2010 are not available.

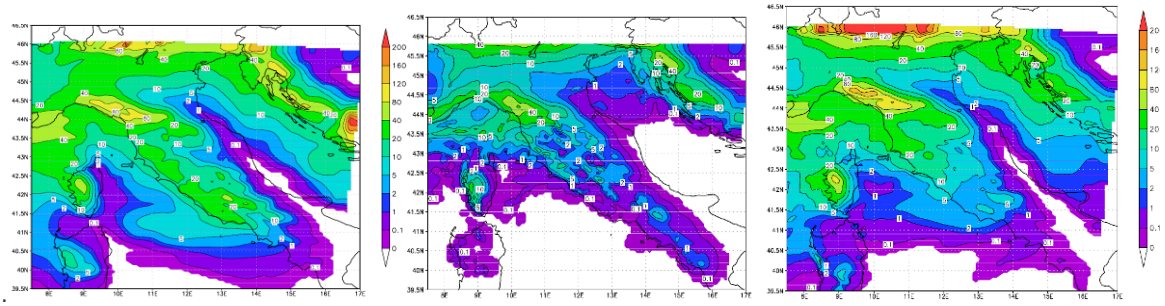

Figure 64: Cumulated daily rainfall from COSMO LM 7 km. On the left the simulated rain for 20091222, in the centre for 20091223 and on the right side 20091224.

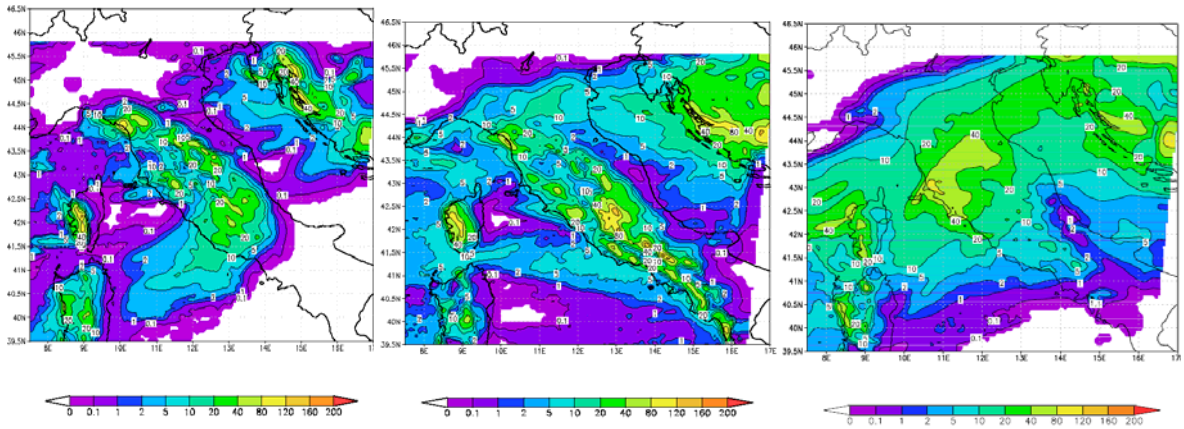

Figure 65: Cumulated daily rainfall from COSMO LM 7 km. On the left the simulated rain for 20091230, in the centre for 20091231 and on the right side 20100105.

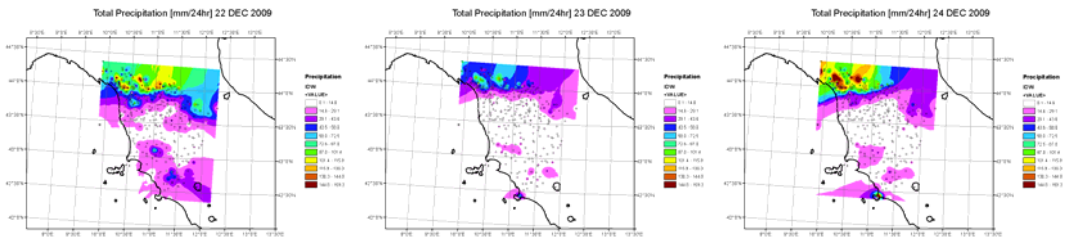

Figure 66: Interpolated observed daily rainfall. The algorithm used for interpolation is IDW (inverse distance weight). The black points are the in situ pluviometer.

In this test case it is also important to consider the effect of the extended snowfall recorded in the region on 18 and 19 December .During this period, which lasted up to 20 December, the minima temperatures in the mountain areas were -10 °C or lower. Starting the day on December 21 the cold flow was replaced by milder air with more elevated temperatures with a range between minima and maxima from 13° to 17 °C. The COSMO LM model well forecast the behaviour of temperature in this period, and also the fast change of the temperature regime (Figure 67). The Autorità di Bacino – Fiume Serchia reports (Regione Toscana, 2010) that the amount of rainfall among the 22 and the 25 December2009 and the values of temperatures was sufficient, with high probability, to melt all the cumulated snowfall. The snow melting has the effect to increase the water available at the soil level. This effect has to be taken it into account in the stability analysis.

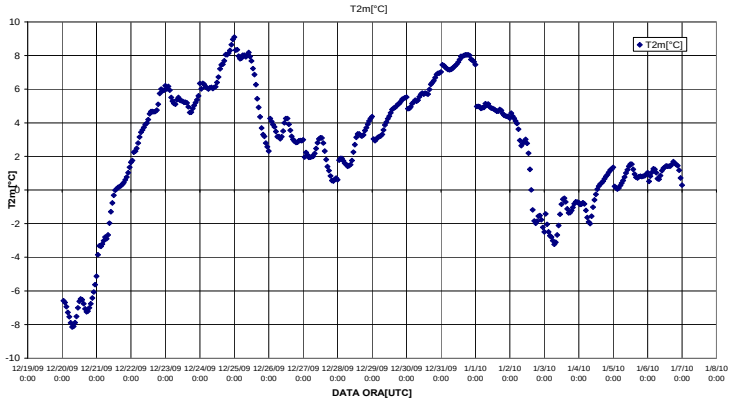

Figure 67: Mean areal temperature from 20 December 2009 to 6 December 2010. The area is the one represented with blue points in the Figure 63.

4.3.4 Slope stability analysis

The slope stability analysis on the Tuscan test area was performed with two rainfall datasets that simulate the operational functioning of the system chain. First dataset regarding 24 December 2009 and a second one regarding 25 December. Each dataset was composed of 2 days of rain gauges hourly measurement data followed by a day of COSMO-LM hourly forecasted data. Each dataset has an initial condition that takes into account the antecedent rain measured by the rain gauges.

The rainfall data came from the Tuscan civil protection database that collects measurements of a network of hundreds of automated rain gauges. The measurements are collected every hour and contribute to consolidating an almost continuous database from 2003.

As stated in the meteorological description, the events of December 2009 were characterized by sudden snow melting that adds a huge complication to the stability simulation. COSMO-LM model does not take into account in the rainfall map output possible snow melting phenomena. Even HIRESSS does not implement in its internal physics engine the snow

melting effect so the simulation's result basically shows a slope stability overestimation.

In order to compensate roughly for the effect of the snow melting, a constant quantity of rain was added at each time step of the simulation. Basically, it is estimated a water value that was stored in the snow from measurements taken by regional authority and we spread the total amount of water over every rainfall intensity input map like a constant hourly addition. According to a regional authority report the snow melting started on 22 December and consequently we add this hypothetic contribution at every pixel of the rainfall input map. This is a very rough management of the snow melting phenomena and the simulation confirmed that it is an incorrect and insufficient method.

The results are aggregated in the defined basin, as explained in section 4.2, by regrouping the cells that belong to the upslope contributing area of a same flow node. Even in this area we selected the nodes that regroup more than 3000 pixel contribution but the basins are larger on average because of the lower pixel resolution (every cell is 10-meter size).

The slope stability simulation results for 24 December 2006 are shown in Figure 68 and Figure 69. The maps represent the average of probability of slope failure for two 12-hour intervals. Most of the reported landslides occurred during the night hours between 23 December and 24 December, but the simulation does not show any critical conditions.

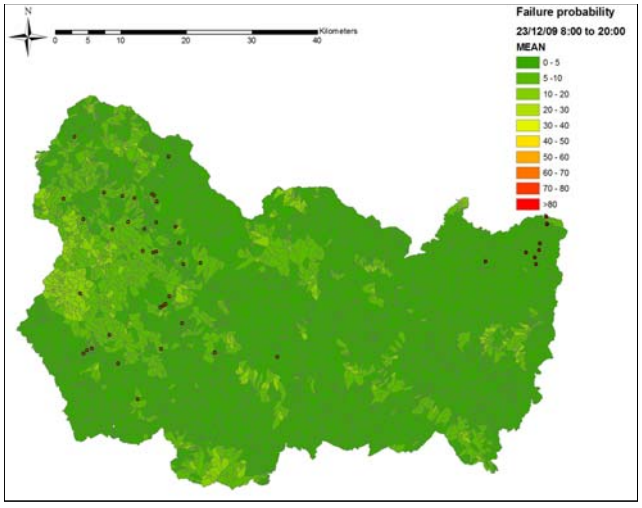

Figure 68: Simulated probability of slope failure at the Lucca, Pistoia and Prato province area during 23 December 2009. The reported landslides that mostly occurred during the night between 23 and 24 December 2009 are traced in red. The failure probability is the average of a 12 hour time slot (8:00 to 20:00 24/12/2009).

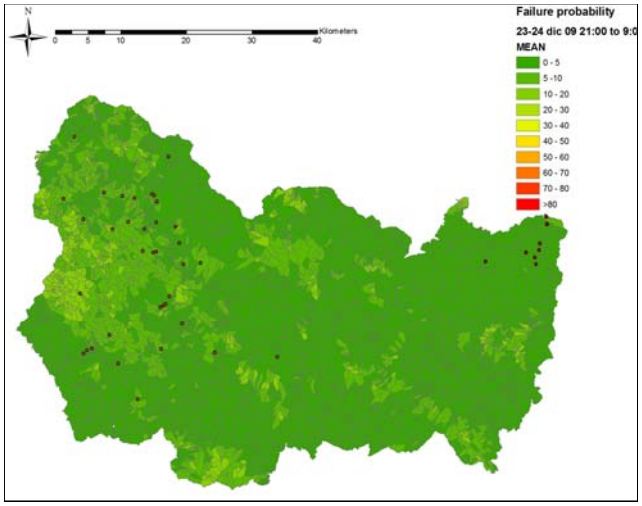

Figure 69: Simulated probability of slope failure at the Lucca, Pistoia and Prato province area during the night of 23-24 December 2009 events. The reported landslides that mostly occurred during the night between 23 and 24 December 2009 are traced in red. The failure probability is the average of 12 hour time slot (21:00 23/12/2009 to 9:00 24/12/2009).

The simulation during the 25 December shows a more critical and variable condition of the area, reaching a higher value of slope failure probability. The average maximum instability peaks in the night between the two days. The simulation results are shown in Figure 70 to Figure 75.

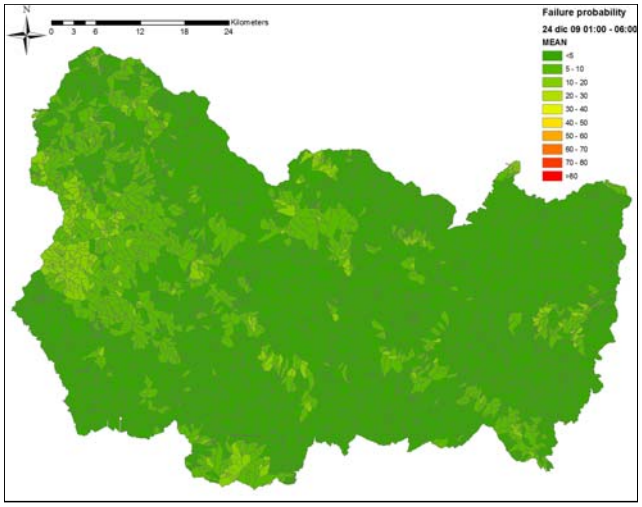

Figure 70: The simulated slope failure probability of the Lucca, Pistoia and Prato province area during the night of the December 2009 event. The failure probability is the average from 1:00 to 6:00 of 24th December. The largest part of landslides reported was actually triggered during the night between the 24th and 25th.

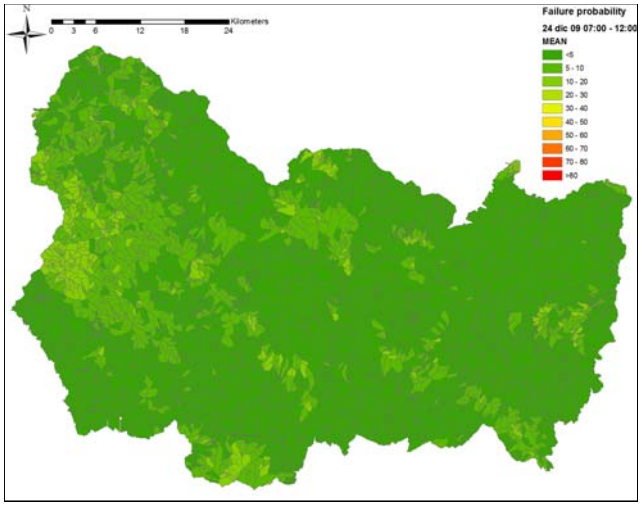

Figure 71: The simulated slope failure probability of the Lucca, Pistoia and Prato province area during the night of the December 2009 event. The failure probability is the average from 7:00 to 12:00 of 24th December. The largest part of landslides reported was actually triggered during the night between the 24th and 25th.

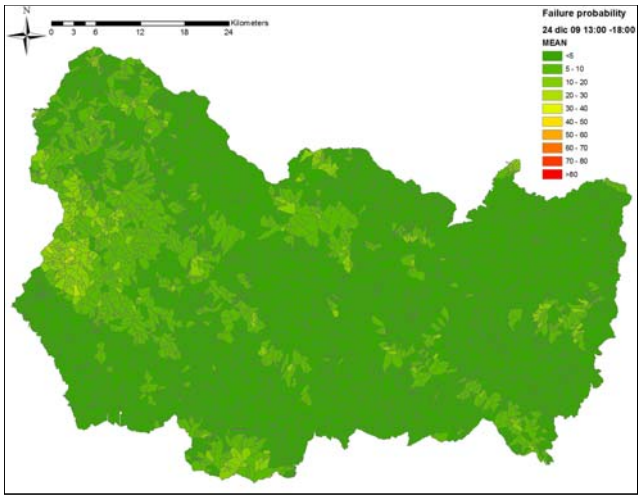

Figure 72: The simulated slope failure probability of the Lucca, Pistoia and Prato province area during the night of the December 2009 event. The failure probability is the average from 13:00 to 18:00 of 24th December. The largest part of landslides reported was actually triggered during the night between the 24th and 25th.

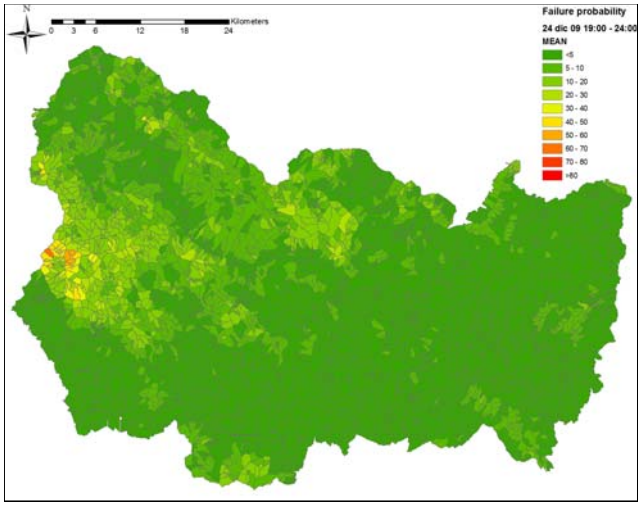

Figure 73: The simulated slope failure probability of the Lucca, Pistoia and Prato province area during the night of the December 2009 event. The failure probability is the average from 19:00 to 24:00 of 24th December. The largest part of landslides reported was actually triggered during the night between the 24th and 25th.

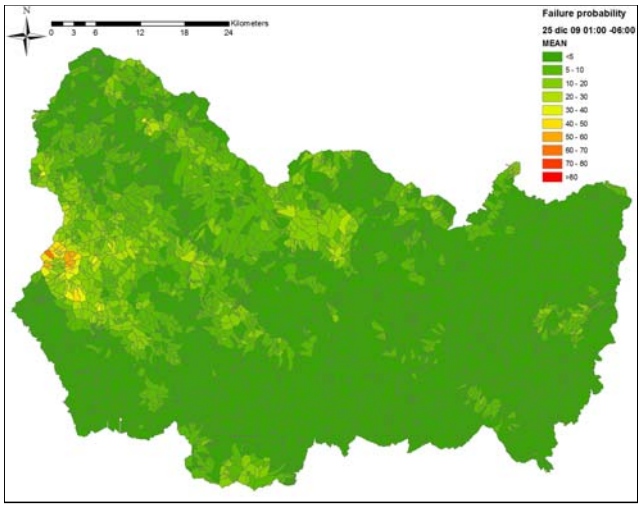

Figure 74: The simulated slope failure probability of the Lucca, Pistoia and Prato province area during the night of the December 2009 event. The failure probability is the average from 1:00 to 6:00 of 25th December. The largest part of landslides reported was actually triggered during the night between the 24th and 25th.

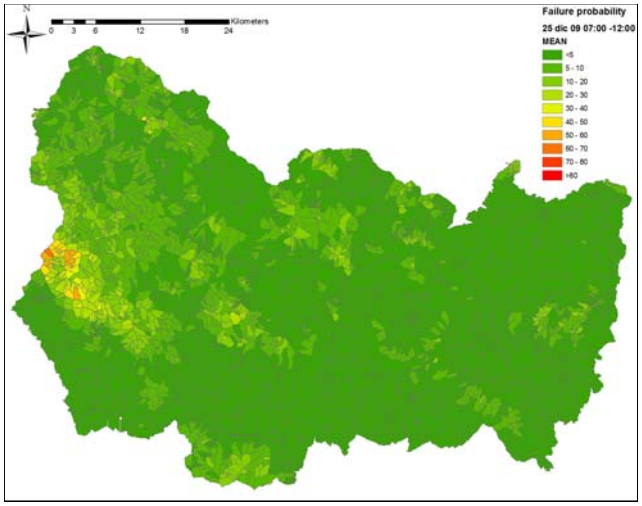

Figure 75: The simulated slope failure probability of the Lucca, Pistoia and Prato province area during the night of the December 2009 event. The failure probability is the average from 7:00 to 12:00 of 25th December. The largest part of landslides reported was actually triggered during the night between the 24th and 25th.

4.3.5 Discussion of results

The results of the slope stability analysis were deeply affected by the errors due to snow melting phenomena. Both simulations performed largely underestimate the slope failure probability of events that triggered hundreds of landslides, even if not all of them were shallow failures. The HIRESSS physics engine contains approximations that allow analyzing only shallow landslide triggering. The dataset comprising the 24-25 December shows some critical areas diffused mainly over the Lucca province but the simulation does not allow a clear spatial identification of initiation of possible slope movements. We can conclude that the simulating chain was able to catch a generalized state of instability probability, at least in the 25 December simulation and in Lucca province, which is confirmed by the large number of landslides reported and almost spatially distributed over all the area. The east part of that area does not show any critical situation despite the large number of landslides reported in that area. This test case has shown a weakness of the simulation chain that is not to able to manage the contribution of the snow at the slope instability mechanism, even if the general critical condition can be detected. To overcome this limitation the next step can be to link the atmospherical model COSMO LM and HIRESS also using forecast of temperature as well as precipitation. Furthermore it is also necessary to introduce a subroutine for the assimilation of snow depth measurement in the HRESSS software in order to know the height of the snow fall. These two data, forecast of temperature at soil level and measurement of snow depth can be used to forecast the contribute of the snow melting in terms of water availability at soil level. .

4.3.6 Second test case: from 30th October 2003 to 1st November 2003

This test case addresses the same region as the first test case (Figure 58) but covers an intense rainfall event that occurred between the 30th of October 2003 up until the 1st of November 2003.

4.3.7 Meteorological event description and forecasting simulation

From the October 24 to the 1 November 2003 an intensive rainfall event affected the Tuscany region (see Figure 58) and triggered some landslide in this area. The last part of the intense rainfall event was due to the coming of a very deep low pressure from the Atlantic sea on the West Mediterranean area. The effect of this configuration on the area of interest was the presence of diffused rain due, firstly, to a westerly humid flow and, therefore, to humid southern winds.

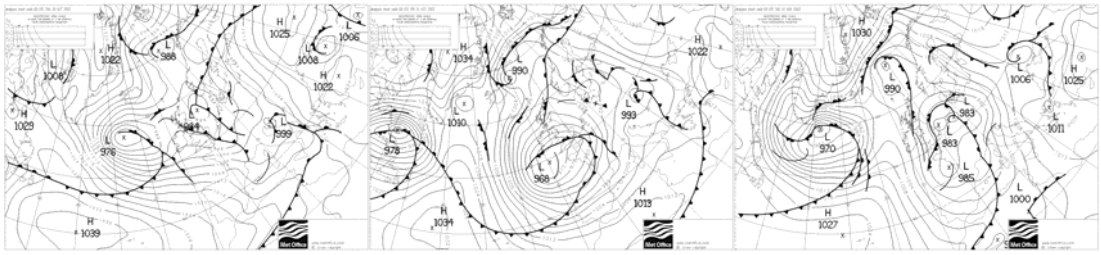

Figure 76: fronts and sea level pressure charts (Bracknell analysis) for 30/10/2003 to 01/11/2003.

Simulations with COSMO LM 7km model were performed in order to simulate the rain event that triggered the landslide in the area during this period. Initial and boundary data are taken from ECMWF forecasts data (with about 40 km of horizontal resolution).The assimilation is used for the configuration at 7 km. The simulations are initialized at 00:00 UTC and they run for 33 hours. The number of vertical levels is 40 and the number of levels in the soil is 7.The Tiedtke scheme is used to parameterize the sub grid convection. The field of downscaling rainfall has been evaluated using all the information in the Digital Elevation Model, reported in the Figure 39, and the COSMO LM grid points represented in the same figure. The COSMO LM model domain has the same features reported in the paragraph 4.3 for the first case on the Tuscany region.

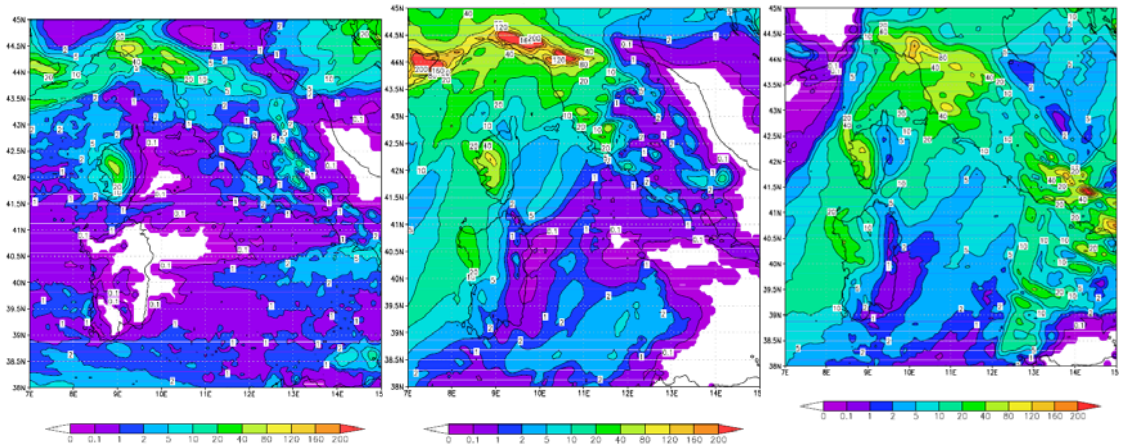

Figure 77: cumulated rainfall on 33 forecast hours from COSMO LM 7 km. On the left the simulated rain for 20031030, in the centre for 20031031 and on the right side 20031101.

Table 18: observed and forecasted daily rainfall. An average has been performed on the DEM area reported in the Figure 39. No observed values are available for this test case.

	Mean observed (mm/24 hrs)	**Mean forecast** (mm/24 hrs)

2009-10-30	19	15
2003-10-31	57	23.5
2003-11-01	64	54

Table 19: statistic validation of COSMO LM rainfall forecast for the threshold 5 mm.

Threshold 5 mm	THREAT SCORE	BIAS	FALSE ALARM RATE	HIT RATE RAIN
2003-10-30	**0.7**	**1.1**	**0.2**	**0.9**
2009-10-31	**0.6**	**1.6**	**0.4**	**1**
2009-11-01	**0.8**	**1.2**	**0.2**	**1**

Table 20: statistic validation of COSMO LM rainfall forecast for the threshold 20 mm.

Threshold 20 mm	THREAT SCORE	BIAS	FALSE ALARM RATE	HIT RATE RAIN
2003-10-30	**0.1**	**0.6**	**0.7**	**0.2**
2009-10-31	**0.4**	**1.8**	**0.5**	**0.8**
2009-11-01	**0.8**	**1.2**	**0.2**	**1**

The intense rainfall of the 3 days has been well captured by the COSMO LM model with 7 km of horizontal resolution.

4.3.8 Slope stability analysis

The event at the end of October 2003 was not affected by snow melting phenomena like those of December 2009 and was characterized by heavy rainfall.

The rainfall input dataset is composed of three days of rain gauge hourly measured rainfall intensity that precedes a 33 hours COSMO-LM forecasted dataset on 31 October 2003. The initial saturation condition was computed taking into account the rainfall data from the 24 October. Most of the landslides, according to historic reports, were triggered during the 31 October and the first hours of the next day.

The simulation results are shown from Figure 78 to Figure 81 where the average of slope failure probability in a period of 12 hours is reported. This large timeframe permits to identify the most critical period over the simulation. As it can be seen in Figure 80 and Figure 81, critical conditions are approached within the first hours of the 31 October, and reach a peak in the second half of the day. Analyzing the period starting from 13:00 of 31 October using an average computed over a period of 3 hours (Figure 82 to Figure 86), it is possible to see the evolution of slope failure probability over the night between the 31 October and 1 November. The simulation indicates the west part of the region as the most probable for landslide triggering, followed by the central north area.

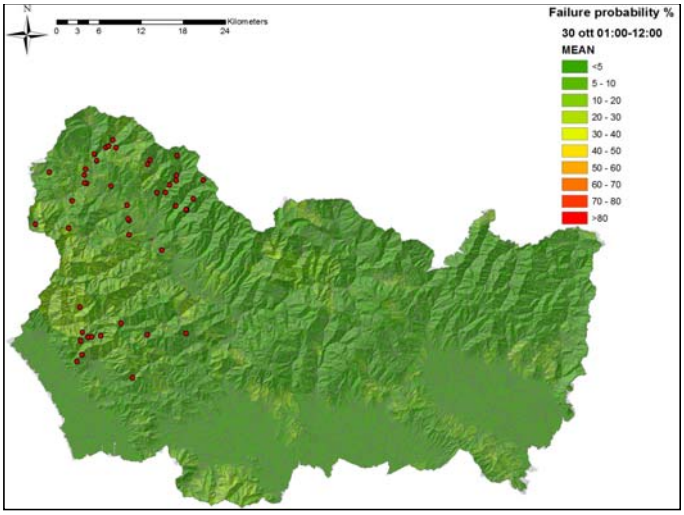

Figure 78: The simulated slope failure probability of the Lucca, Pistoia and Prato province area during the 30 October 2003 event. Map shows the average of 12 hour timeframe (1:00-12:00). Landslides reported in the 2003 event are represented by red dots.

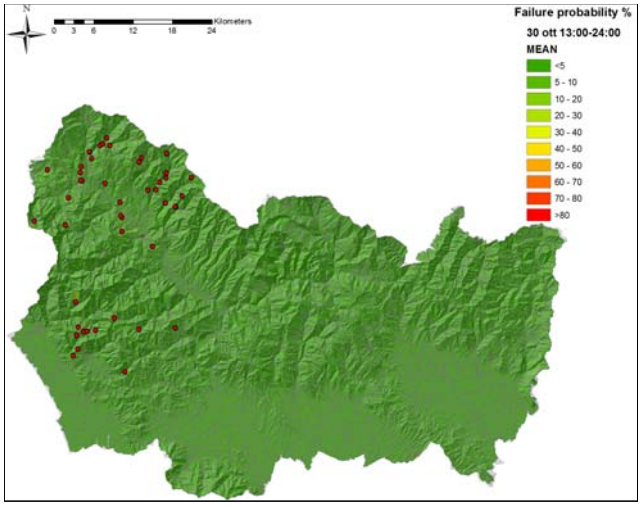

Figure 79: The simulated slope failure probability of the Lucca, Pistoia and Prato province area during the 30 October 2003 event. Map shows the average of 12 hour timeframe (13:00-24:00). Landslides reported in the 2003 event are represented by red dots.

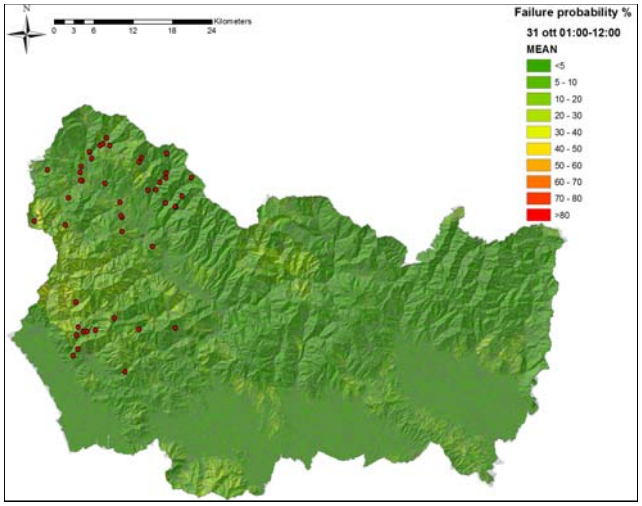

Figure 80: The simulated slope failure probability of the Lucca, Pistoia and Prato province area during the 31 October 2003 event. Map shows the average of 12 hour timeframe (1:00-12:00). Landslides reported in the 2003 event are represented by red dots.

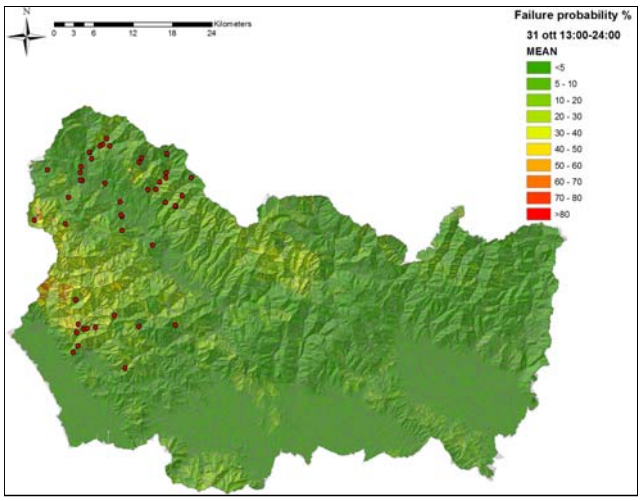

Figure 81: The simulated slope failure probability of the Lucca, Pistoia and Prato province area during the 31 October 2003 event. Map shows the average of 12 hour timeframe (13:00-24:00). Landslides reported in the 2003 event are represented by red dots.

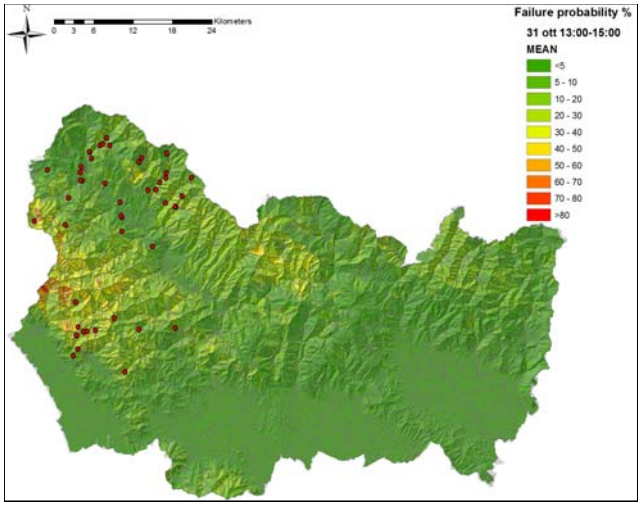

Figure 82: The simulated slope failure probability of the Lucca, Pistoia and Prato province area during the 31 October 2003 event in a shorter timeframe analysis. Map shows the average of 3 hour timeframe (13:00-15:00). Landslides reported in the 2003 event are represented by red dots.

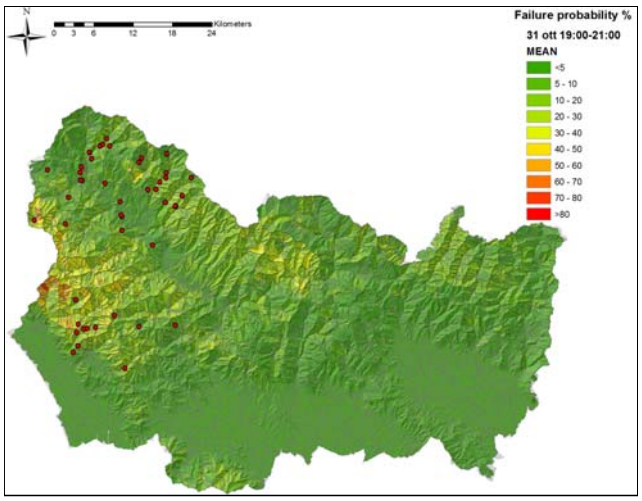

Figure 83: The simulated slope failure probability of the Lucca, Pistoia and Prato province area during the 31 October 2003 event in a shorter timeframe analysis. Map shows the average of 3 hour timeframe (19:00-21:00). Landslides reported in the 2003 event are represented by red dots.

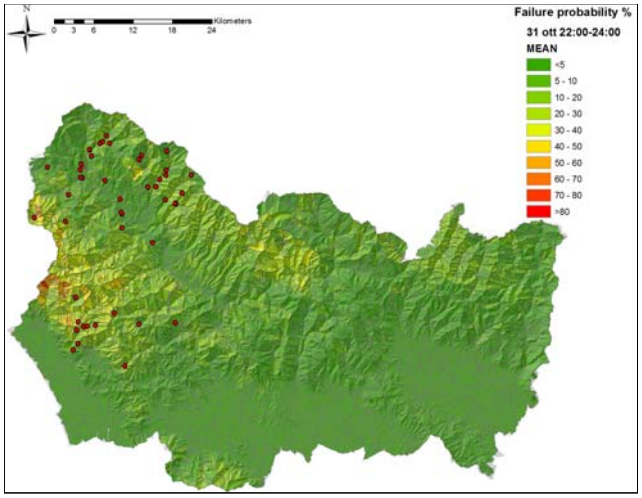

Figure 84: The simulated slope failure probability of the Lucca, Pistoia and Prato province area during the 31 October 2003 event in a shorter timeframe analysis. Map shows the average of 3 hour timeframe (22:00-24:00). Landslides reported in the 2003 event are represented by red dots.

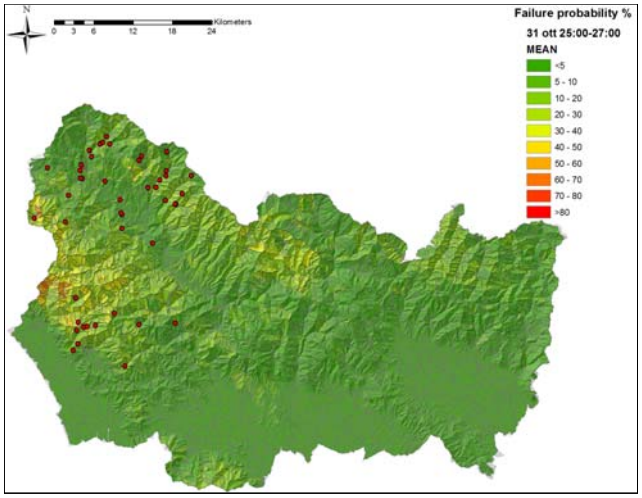

Figure 85: The simulated slope failure probability of the Lucca, Pistoia and Prato province area during the 1thNovember 2003 event in a shorter timeframe analysis. Map shows the average of 3 hour timeframe (1:00-3:00). Landslides reported in the 2003 event are represented by red dots.

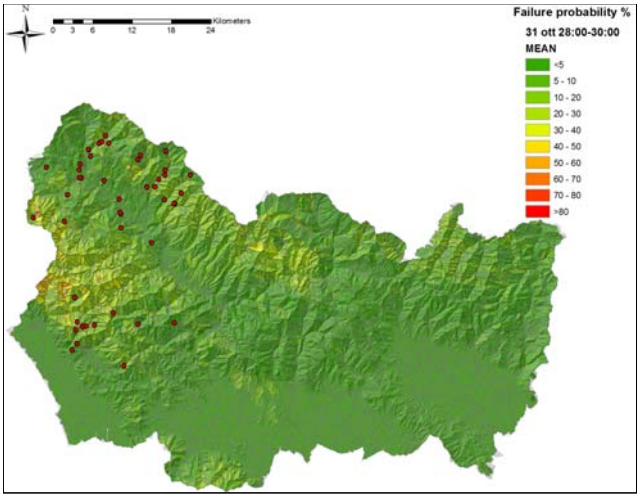

Figure 86: The simulated slope failure probability of the Lucca, Pistoia and Prato province area during the 1st November 2003 event in a shorter timeframe analysis. Map shows the average of 3 hour timeframe (4:00-6:00). Landslides reported in the 2003 event are represented by red dots.

4.3.9 Discussion of results

The stability analysis simulation of the 2003 event shows a better coupling between HIRESSS and the COSMO-LM forecasted rainfall intensity. The event is not affected by meteorological phenomena not implemented in the simulating chain, like snow melting encountered in the 2009 event simulation, and the results have a better agreement with the historic landslides reports.

The simulations do not detect a widespread critical slope condition at the North West of the area but only some localized spots. The landslides reports are numerous in this area but we cannot discriminate between shallow landslides or other soil movement types due to lack of descriptions. Obviously the slope stability simulator cannot recognize other type of landslides due to its physics engine that can detect only conditions for triggering shallow landslides.

The east part of test area appears affected by an overestimation of the slope failure probability considering the number and the position of triggered landslides. Even in the 2009 event simulation this zone was identified as the most unstable but even in this event there is a small number of reported soil movements. A possible partial explanation is a lack of reporting because the area is a non populated mountainous region: usually most of reported landslides involve infrastructure and water stream. The results of the two simulations suggest a more accurate investigation of this area to verify a possible inaccuracy of geotechnical and morphometric parameters. Moreover the physical engine will be revised and improved to take into account the different land use, not yet implemented, which can be another explication to overestimation of failure probability in that area.

5 IMPLEMENTATION OF THE SIMULATION CHAIN WITHIN EARLY WARNING SYSTEMS

Severe rainfall may produce severe impact on slope stability with a potential for loss of life and property in the most vulnerable areas. Extreme rainfall events are expected to be more frequent in the future due to the effects of the climate change as the rise of the temperatures. All these modifications can reduce slope stability. The awareness of these changes indicates the needs to develop some appropriate tools to realize monitoring and prevention of landslides and, in particular, of shallow soil slides which can transform in rapid flows. Furthermore, the developments in the recent years of the simulation tools either for weather forecasting either for the assessment of slope stability, together with a better understanding of soil characteristics, through measurement campaigns and accurate laboratory experiments, allowed a large improvement of the predictive capabilities through simulation models. The challenge of this work is to integrate all this knowledge in a complex model for systematic prediction of shallow landslides, triggered by intense rainfalls. The tools will allow having a warning map on a large area or detailed stability analysis on a particular test site, with the possibility of fast upgrade. The model output will provide a failure probability on a regional/national area and also accurate values of the safety factor at slope level. This last product can be available only where well documented data about soil structure, properties, and initial conditions are available (possibly through geotechnical investigations and monitoring). The simulation chain that has been showed in this report is mainly based on a non hydrostatic limited area model for numerical weather prediction (NWP), operating in the short range time (that means less than 72 hours). Downscaled rainfall forecasts represent the input for the two soil stability models (at regional and slope scale).
The simulation chain developed in this research activity has some very important features:

- The time required for producing regional warning maps is 2-3 hours (from the time when the output of the atmospherical model is available). This is possible because the HIRESSS software can run on supercomputer. The HIRESSS code can produce probabilistic slope failure maps with a spatial resolution up to 10 m at any regional extension.
- The time required for producing safety factor maps at slope level, using the software IMOD-3D, is less then five minutes using a laptop.
- The RMI module (for downscaling of precipitation forecast) manages the output of COSMO LM in automatic way.

It is important to underline that the software COSMO LM, used for this application, is operative in many European countries. This features permit to have daily the availability of the atmospherical data and, in particular, of the rainfall forecast in all the European area. This is a very important issue because allows the daily use of the simulation chain and, therefore, its validation. The daily running of the implemented simulation chain is the first step to decide about its operative implementation. In parallel way, the systematic validation of the tool allow knowing and managing the forecast uncertainty; for example to resolve the presence of some systematic errors and, then, to realize an upgrade of the system.

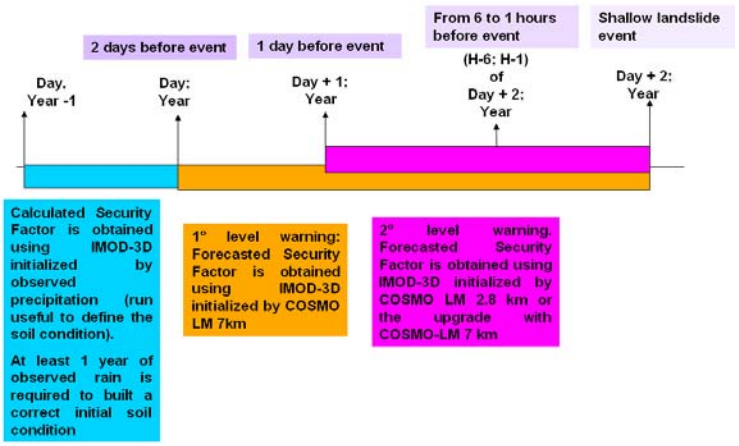

Figure 87: Suggested time windows for producing forecast maps at regional scale.

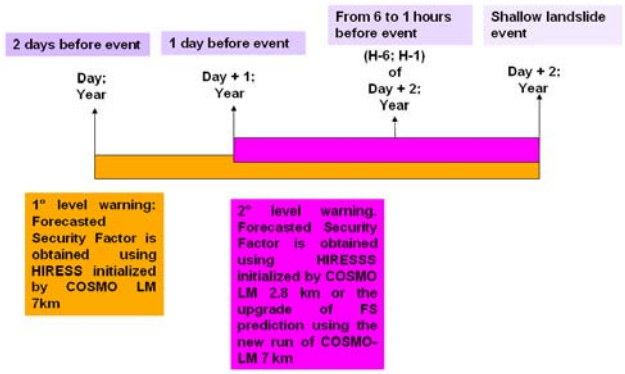

Figure 88: Suggested time windows for producing forecast maps for specific sites..

Figure 87and Figure 88 show a description of suggested time windows using the tools developed in this research activity. The two different versions of COSMO-LM will provide the input for:

- A first level warning: available with 48 hours in advance using precipitation forecast from COSMO LM 7 km (on a bigger area but with less detailed precipitation forecast).
- A second level of warning: available 24 hours in advance using precipitation forecast from COSMO LM 2.8 km (on a smaller area then COSMO LM 7 km but with more detailed precipitation forecast). This new set of forecast allows an upgrade of the previous regional warning map and slope stability evaluation on some particular sites. The new sets of forecast are provided by the new run of COSMO LM 7 km and from the COSMO LM 2.8 km.

The second level warning is more precise but is available only 24 hours in advance using data from COSMO LM 2.8 km characterized from a typical forecast range time of 24 hours or less.

6 ACKNOWLEDGEMENT

Thanks ARPA Emilia Romagna for the support and data furniture and to COSMO Consortium. Thanks to Centro funzionale per la previsione meteorologica e il Monitoraggio meteo-Pluvio-IDrometrico e delle frane, Settore Programmazione Interventi di Protezione Civile sul Territorio-Regione Campania for providing precipitation gauge observations.

7 REFERENCES

[1] Anthes, R. A. 1974. Data assimilation and initialization of hurricane prediction models. J. Atmos. Sci. 31 :702-719.Anthes

[2] Antofie T.E. (2009) Research Activity on Statistical Dowscaling for Precipitation, Research Paper RP0057, Centro Euro-Mediterraneo per i Cambiamenti Climatici (CMCC). http://www.cmcc.it/publications-meetings/publications/research-papers/rp0057-isc-02-2009

[3] Baillargeon, G. (1989) Probabilité´s Statistiques et Techniques de Régression (Statistical Probabilities and Regression Techniques), Editions SMG, 631 pp.

[4] Bell V.A., Moore R.J. (2000) Short period forecasting of catchment-scale precipitation. Part II: a water-balance storm model for short-term rainfall and flood forecasting, Hydrology And Earth System Sciences, 4(4), pp 635-651

[5] Burrough P.A., McDonnell R.A. (1998). Principles of Geographical Information Systems. Oxford: Oxford University Press.

[6] Burton A. O'Connell P.E. (2003a) Algorithms for the identification and estimation of rainband and raincell features, MUSIC Project Report, Deliverable 5.1, 27pp

[7] Burton A.; O'Connell PE (2003b) Algorithms for estimating the properties of rainband and raincell features, MUSIC Project Report, Deliverable 5.2, 33pp

[8] Ciccione M., Pircher V. (1984) A preliminary assessment of very-short-term forecasting of rain from single radar data, Proc, Nowcasting II, ESA, pp 241-246

[9] Cluckie I.D., Xuan Y. (2006) An experiment of rainfall prediction over the Odra catchment by combining weather radar and numerical weather model, 7th International Conference on Hydroinformatics

[10] Damiano E. (2004). Meccanismi d'innesco di colate di fango in terreni piroclastici. Ph.D. Thesis, Roma, 2004

[11] Damiano E., Olivares L. (2010). The role of infiltration processes in steep slopes stability of pyroclastic granular soils: laboratory and numerical investigation. Natural Hazards, Journal of the Inter. Society for the Prevention and Mitigation of Natural Hazards, 52(2), 329-350.

[12] Davis, H. C., and R. E. Turner, 1977: Updating predic-tion models by dynamical relaxation: An exami-nation of the technique. J. Appl. Meteor., 17, 998-1013.

[13] Dierer, S., Arpagaus, M., Seifert, A., Avgoustoglou, E., Dumitrache, R., Grazzini, F., Mercogliano, P. & Starosta, K. 2009 "Deficiencies in quantitative precipitation forecasts: sensitivity studies using the COSMO model" Meteorologische Zeitschrift

[14] Doms, G. & Schattler, U. 1998: The non-hydrostatic limited area model LM (Lokal Model) of DWD. Part I. Scientific documentation. Deutscher Wetterdienst, 160 pp. [Available online at http://cosmo-model.cscs.ch]

[15] Doms G. and Schattler U. (2003). A description of the Nonhydrostatic Regional Model LM, Part 1-Dynamics and numerics, available on www.cosmo-model.org

[16] Doms, G., J. F□orstner, E. Heise, H.-J. Herzog, M. Raschendorfer, R. Schrodin, Th. Reinhardt, and G. Vogel, 2005: A description of the Nonhydrostatic Regional Model LM, Part II: Physical parameterization. Available at: http://www.cosmo-model.org.

[17] ECMWF, Part VII: ECMWF Wave-model documentation, in IFS documentation CY28r1, available at http://www.ecmwf.int/research/ifsdocs/CY28r1/index.html, edited 2004

[18] Ferraris, L., Rudari, R. & Siccardi, F. 2002 The uncertainty in the prediction of flash floods in the northern mediterranean environment, J. Hydrometeorol., 3, 714–727

[19] Fredlund D.G. (1979). Second Canadian Geotechnical Colloquium: appropriate concepts and technology for unsaturated soils. Canadian Geotechnical Journal, 16: 121-139.

[20] Fredlund D.G. and Rahardjo H. (1993). Soil Mechanics for Unsaturated Soils. In Wiley-Interscience Publication, John Wiley & Sons, Inc.

[21] Heise, E., M. Lange, B. Ritter, and R. Schrodin, 2003: Improvement and Validation of the Multi-Layer Soil Model. COSMO Newsletter, No. 3, February 2003, pp. 198-203.

[22] Heise, E., B. Ritter, R. Schrodin, 2006: Operational Implementation of the Multilayer Soil Model. – Technical Report No. 9, Consortium for Small-Scale Modelling, July 2006

[23] (COSMO)Holton, J.R. 2004. An introduction to Dynamic Meteorology, Elsevier Academic Press

[24] Itasca Ltd. (2008). FLAC 2D, Version 6.0, Finite Difference Code and User Manual.

[25] Johnston K., Ver Hoef J.M., Krivoruchko K., Lucas N., 2001: Using ArcGIS Geostatistical Analyst, ESRI Inc., Redlands, CA

[26] Kenney T.C., Lau K.C. (1977). Temporal changes of groundwater pressure in a natural slope of non fissured clay. Canadian Geotechnical Journal, 21, 138-146

[27] Krahn J. (2004). Seepage modelling with SEEP/W; Vadose Zone Modeling with VADOSE/W; Stability Modelling with SLOPE/W - An Engineering Methodology. GEO-SLOPE International Ltd., Calgary, Canada

[28] Mazzarella, E. De Luise (2007) L'evento meteorico del 30 Aprile 2006 a Ischia. ID:317812]http://www.ijege.uniroma1.it/rivista/ijege-07/ijege-07-volume-02/l2019evento-meteorico-del-30-aprile-2006-a-ischia/

[29] Mecikalski J.R. (2007) Satellite-based Convective Initiation Nowcasting System Improvements Expected from the MTG FCI Meteosat Third Generation Capability, Technical Report EUM/CO/07/4600000405/JKG, University of Alabama in Huntsville

[30] Olivares L., Picarelli L. (2003). Shallow flowslides triggered by intense rainfalls on natural slopes covered by loose unsaturated pyroclastic soils. Géotechnique 53(2), pp. 283-288.

[31] Olivares L., Damiano E. (2007). Post-failure mechanics of landslides: laboratory investigation of flowslides in pyroclastic soils. Journal of Geotechnical and Geoenvironmental Engineering, ASCE, 133(1), pp. 51-62.

[32] Picarelli L., Evangelista A., Rolandi G., Paone A., Nicotera M.V., Olivares L., Scotto di Santolo A., Lampitiello S., Rolandi M. (2006). Mechanical properties of pyroclastic soils in Campania Region. Invited paper, 2nd Int. Workshop on Characterisation and Engineering Properties of Natural Soils, Singapore

[33] Persson, A., 2001: User guide to ECMWF forecast products. ECMWF Meteorological Bulletin M3.2, 153 pp

[34] Pielke, R.A. 1984. Mesoscale Meteorological Modeling. 2nd ed. Academic Press, 750 pp.

[35] Philip, J. R. (1985). Approximate analysis of the borehole permeameter in unsaturated soil. *Water Resour. Res. 21,* 1025-33.

[36] Regione Toscana– Servizio Idrologico Regionale - CENTRO FUNZIONALE DELLA REGIONE TOSCANA (2010), "REPORT sull'evento alluvionale registrato nei giorni 24-25 dic. 2009 nel Bacino del Fiume Serchio"

http://www.cfr.toscana.it/supporto/documentazione/report_evento_alluvionale_serchio_2009-12-25.pdf

[37] Rossi, G. ,2010, "A physically based distributed slope stability simulator to analyze shallow landslides triggering in real time and on a large scale", PHD Thesis.

[38] Settore programmazione interventi di protezione civile sul territorio – centro funzionale per la previsione meteorologica e il monitoraggio MeteoPluvioIdrometrico e delle frane- Rapporto di evento 29-30 Aprile 2006- http://issuu.com/protezionecivilecampania/docs/rapporto_evento_ischia

[39] Schrodin, E., and E. Heise, 2002: A New Multi-Layer Soil Model. COSMO Newsletter, No.2, February 2002, pp. 149-151

[40] Stauffer, D. R., and N. L. Seaman, 1990: Use of four-dimensional data assimilation in a limited-area mesoscale model. Part I: Experiments with synoptic-scale data. Mon. Wea. Rev., 118, 1250-1277.

[41] Tiedtke, M., 1989: A comprehensive mass flux scheme for cumulus parameterization in large-scale models. Mon. Wea. Rev., 117, 1779-1800.

[42] Trentmann, J.; Keil, C.; Salzmann, M.; Barthlott, C.; Bauer, H. S.; Schwitalla, T.; Lawrence, M. G.; Leuenberger, D.; Wulfmeyer, V.; Corsmeier, U.; Kottmeier, C.; Wernli, H. (2009). Multi-model simulations of a convective situation in low-mountain terrain in central Europe. Meteorology and Atmospheric Physics, Vol. 103, p. 95-103.

[43] Van Genuchten, M. Th. (1980). A closed-form equation for predicting the hydraulic conductivity of unsaturated soils, Soil Sci. Soc. Am. J. 44:892-898

[44] Vigier, M. (1981) Mèthodes d'Assurance Qualité—Fiabilité et d'Expérimentation (Quality Insurance Methods—Reliability and Experiments). Collection Universite´ de Compiègne, 398 pp.

[45] Wilson, JW. 2004. Precipitation nowcasting: past, present and future. Sixth International Symposium on Hydrological Applications of Weather Radar

[46] Zace Ltd. (2003). Z_Soil.PC_3D, Finite Element Code and User Manual.